INFORMATION TO USERS

This manuscript has been reproduced from the microfilm master. UMI films the text directly from the original or copy submitted. Thus, some thesis and dissertation copies are in typewriter face, while others may be from any type of computer printer.

The quality of this reproduction is dependent upon the quality of the copy submitted. Broken or indistinct print, colored or poor quality illustrations and photographs, print bleedthrough, substandard margins, and improper alignment can adversely affect reproduction.

In the unlikely event that the author did not send UMI a complete manuscript and there are missing pages, these will be noted. Also, if unauthorized copyright material had to be removed, a note will indicate the deletion.

Oversize materials (e.g., maps, drawings, charts) are reproduced by sectioning the original, beginning at the upper left-hand corner and continuing from left to right in equal sections with small overlaps.

Photographs included in the original manuscript have been reproduced xerographically in this copy. Higher quality 6" x 9" black and white photographic prints are available for any photographs or illustrations appearing in this copy for an additional charge. Contact UMI directly to order.

ProQuest Information and Learning
300 North Zeeb Road, Ann Arbor, MI 48106-1346 USA
800-521-0600

UMI®

DISSERTATION

STRUCTURE-FUNCTION RELATIONSHIPS OF THE RYANODINE RECEPTOR

Submitted by

Jennifer J. O'Brien

Department of Anatomy and Neurobiology

In partial fulfillment of the requirements

For the Degree of Doctor of Philosophy

Colorado State University

Fort Collins, Colorado

Spring 2002

ProQuest Information and Learning Company
300 North Zeeb Road
P.O. Box 1346
Ann Arbor, MI 48106-1346

COLORADO STATE UNIVERSITY

March 22, 2002

WE HEREBY RECOMMEND THAT THE DISSERTATION PREPARED UNDER OUR SUPERVISION BY JENNIFER J. O'BRIEN ENTITLED STRUCTURE-FUNCTION RELATIONSHIPS OF THE RYANODINE RECEPTOR BE ACCEPTED AS FULFILLING IN PART REQUIREMENTS FOR THE DEGREE OF DOCTOR OF PHILOSOPHY.

Committee on Graduate Work

Sue C Kinnamon

Kathryn M Partin

Adviser

Co-Adviser (if applicable)

Department Head/Director

ABSTRACT OF DISSERTATION

STRUCTURE-FUNCTION RELATIONSHIPS OF THE RYANODINE RECEPTOR

Ryanodine receptors form a family of Ca^{2+} activated Ca^{2+} release channels localized to the membrane of the endo/sarcoplasmic reticulum. During excitation-contraction coupling in muscle, depolarization of the plasma membrane activates dihydropyridine receptors (DHPRs), which in turn trigger ryanodine receptors to release the Ca^{2+} necessary to elicit a contraction. In cardiac muscle, Ca^{2+} influx via the cardiac DHPR is thought to activate the cardiac ryanodine receptor, RyR2, while in contrast, Ca^{2+} influx in skeletal muscle is not required to activate the skeletal isoform, RyR1. However, it is possible that the skeletal DHPR allosterically causes an increased Ca^{2+} sensitivity of RyR1 such that resting levels of cytoplasmic Ca^{2+} are sufficient to activate RyR1. In the first part of my dissertation, I used whole-cell patch clamp and photometric measurement of cytoplasmic Ca^{2+} in dysgenic myotubes expressing E4032A-RyR1 to examine the role of Ca^{2+} activation in skeletal-type excitation-contraction coupling, because the point mutation, E4032A, was shown in lipid bilayers to drastically reduce the Ca^{2+} activation of RyR1. I found that Ca^{2+} activation is not required for the initiation of excitation-contraction coupling. Because amino acids 720–765 of the DHPR II-III loop and 1837–2168 (sR16) of RyR1 were shown to physically interact in yeast two-hybrid assays, I studied, in the second part of my dissertation, both a chimera in which sR16 was substituted into RyR2 and that chimera's inverse to test the functional importance of this

interaction. My results suggest that sR16 participates in, but is not necessary for, skeletal-type excitation-contraction coupling. In the third part of my dissertation, I studied four cysteines in the RyR1 carboxy-terminal domain that are conserved among all isoforms of ryanodine receptors and inositol 1,4,5-triphosphate receptors, a second family of Ca^{2+} release channels. When I tested mutation to serine of these four cysteines (C4876S, C4882S, C4958S, C4961S) in RyR1, I found that Ca^{2+} release function was eliminated. However, DHPR Ca^{2+} current enhancement was partially maintained suggesting that tetramerization of RyR1 was unaffected since the receptor could functionally interact with the DHPR.

Jennifer J. O'Brien

Department of Anatomy and Neurobiology

Colorado State University

Fort Collins, CO 80523

Spring 2002

ACKNOWLEDGMENTS

First and foremost, I would especially like to thank Kurt Beam. Through his advice and teaching, he has shown me how to better analyze and criticize my own and other people's data, how to better think through a problem, and ultimately how to become a better scientist.

Thanks to the rest of my committee, Sue Kinnamon, Kathy Partin, and Mike Tamkun, for their guidance, feedback, and willingness to help along the way, especially in my job search.

Kathy Parsons, Lindsay Grimes, and Michael van Oosten provided indispensable technical assistance, primary cell culturing, and maxi-prep production. I am grateful for all their help.

The rest of the members of the lab taught me experimental procedures and gave me advice along the way, and I thank them.

Special thanks to Theodore Roth for all his computer-related technical assistance. He not only wrote software for me (Leak subtraction program, Ca^{2+} calibration program, and many little time and energy saving scripts), he taught me how to use Linux which helped me maintain sanity while writing my dissertation.

And finally, thanks to my parents, my family and friends who supported me while I was out here in Colorado.

DEDICATION

To all those who promote education, creativity, and open mindedness

Contents

Signature Page ii

Abstract iii

Acknowledgments v

Dedication vi

Introduction 1

0.1 Importance of studying ryanodine receptors 1

0.2 Basic muscle physiology 2

0.3 Introduction to excitation-contraction (EC) coupling 2

0.4 Ryanodine receptors 4

0.5 Dihydropyridine receptors 10

0.6 Underlying mechanisms of EC coupling 11

0.7 Cardiac- versus skeletal-type EC coupling 14

0.8 A region in α_{1S} integral for skeletal-type EC coupling 15

0.9 Regions of RyR1 involved in skeletal-type EC coupling 16

0.10 Retrograde signaling 18

0.11 Hypotheses 19

1 Ca^{2+} Activation of RyR1 Is Not Necessary For The Initiation Of Skeletal-Type EC Coupling 21

1.1 Introduction 22

1.2 Experimental procedures 24
1.3 Results 30
1.4 Discussion 40

2 A Region In RyR1 That Interacts With the α_{1S} II-III Loop In Yeast Two-Hybrid Plays a Functional Role In Skeletal-type EC Coupling 46
2.1 Introduction 47
2.2 Experimental procedures 49
2.3 Results 51
2.4 Discussion 58

3 The Mutation C4958S In RyR1 Disables Ca^{2+} Release But Not Enhancement of α_{1S} Ca^{2+} Currents 64
3.1 Introduction 65
3.2 Experimental procedures 70
3.3 Results 73
3.4 Discussion 79

Appendices 83

A The Central Core Disease Mutation I4897T: Construction and Preliminary Experiments 84

B Testing of Chimeras With RyR3 Versus RyR2 Background Sequence 88

List of Abbreviations 90

Bibliography 92

List of Figures

1 Diagram of the triad junction 3

2 Location of transmembrane domains in α_{1S} 11

3 Diagram of RyR1 17

1.1 Bilayer studies of E4032A-RyR1 33

1.2 Ca^{2+} transients seen in E4032A-RyR1 expressing myotubes 34

1.3 Estimation of the SR Ca^{2+} load 36

1.4 Evidence of skeletal-type EC coupling with E4032A-RyR1 37

1.5 Enhancement of the DHPR Ca^{2+} currents by E4032A-RyR1 38

1.6 Effects of caffeine on E4032A-RyR1 Ca^{2+} release 39

1.7 Possible mechanisms of DHPR and Ca^{2+} activation of RyR1 42

2.1 Percent contractions with R16-Chimera 53

2.2 R16-Chimera mediated Ca^{2+} currents and Ca^{2+} transients 55

2.3 Analysis of R16-RevChimera 57

2.4 Analysis of Mac-Chimera 59

3.1 Alignment of IP_3R and RyR isoforms 69

3.2 Ca^{2+} currents seen with each cysteine mutant 75

3.3 Ca^{2+} transients in C4958S-RyR1 expressing cells 76

3.4 Slow SR Ca^{2+} leak with C4958S-RyR1 in CPA 78

3.5 Inactivation of α_{1S} Ca^{2+} currents in the presence of C4958S-RyR1 . . 79

A.1 Preliminary analysis of I4897T-RyR1 87

Introduction

0.1 Importance of studying ryanodine receptors

One of three isoforms of the ryanodine receptor calcium (Ca^{2+}) release channel is located in the sarcoplasmic reticular membrane of skeletal muscle. Mutations in this receptor directly cause the diseases malignant hyperthermia (MH) and central core disease (CCD). People with MH are susceptible to muscle rigidity, fever, and hypermetabolism when exposed to anesthetics and muscle relaxants (MacLennan and Phillips, 1992). If these symptoms are not immediately treated, the person could die from ventricular fibrillation, pulmonary edema, or neurological damage (MacLennan and Phillips, 1992). CCD is a more severe disease which begins in infancy. The patients suffer from hypotonia and muscle weakness and are prone to MH (Loke and MacLennan, 1998). The symptoms of both diseases are thought to derive from the excessive release of Ca^{2+} from the sarcoplasmic reticulum (SR) due to point mutations in the skeletal isoform of the ryanodine receptor. Studying the role of the ryanodine receptor in muscle contraction and understanding the structure-function relationships of the ryanodine receptor will allow for more accurate targeting for treatments of both diseases.

0.2 Basic muscle physiology

The skeletal isoform of the ryanodine receptor (RyR1) is a critical element in the contraction of striated muscle. It lies within the membrane of the SR which acts as a Ca^{2+} store for the cell. Within a muscle fiber, there is a bundle of fibrils enveloped by the SR and plasma membrane (left panel of Fig. 1). Each myofibril consists of the contractile apparatus which primarily contains actin and myosin strands (Rayment et al., 1993; Cooke, 1986). Invaginations of the plasma membrane called transverse tubules, or t-tubules, extend the contact of the extracellular membrane to each fibril in the bundle allowing a connection or junction to be formed between the SR and plasma membrane. This creates a functional bridge from extracellular signals to the contractile elements in the fibrils. Muscle contraction is driven by the movement of actin filaments by myosin. In brief summary, the troponin complex blocks the interaction between actin and myosin. Binding of Ca^{2+} to this complex triggers a release of this inhibition, thereby allowing the myosin head to bind the actin filament and complete the power stroke (Phillips Jr et al., 1986). Thus, Ca^{2+} plays a crucial role in the contraction of each muscle fiber.

0.3 Introduction to excitation-contraction (EC) coupling

The increase in the concentration of cytoplasmic Ca^{2+} necessary for the initiation of muscle contraction is triggered by depolarization of the muscle fiber. Acetylcholine receptors are concentrated in the plasma membrane of the muscle fiber at the synaptic junction with a motor neuron. Release of acetylcholine from the neuron

activates the acetylcholine receptors on the muscle fiber which then allows an influx of cations to depolarize the muscle plasma membrane. The depolarization propagates along the plasma membrane into the t-tubules via voltage-gated sodium channels. In the triad junction, where the t-tubule closely associates with the SR membrane (see Fig. 1), the signal from the nerve is converted into the mechanical muscle contraction. This conversion is known as excitation-contraction (EC) coupling (García and Beam, 1994b).

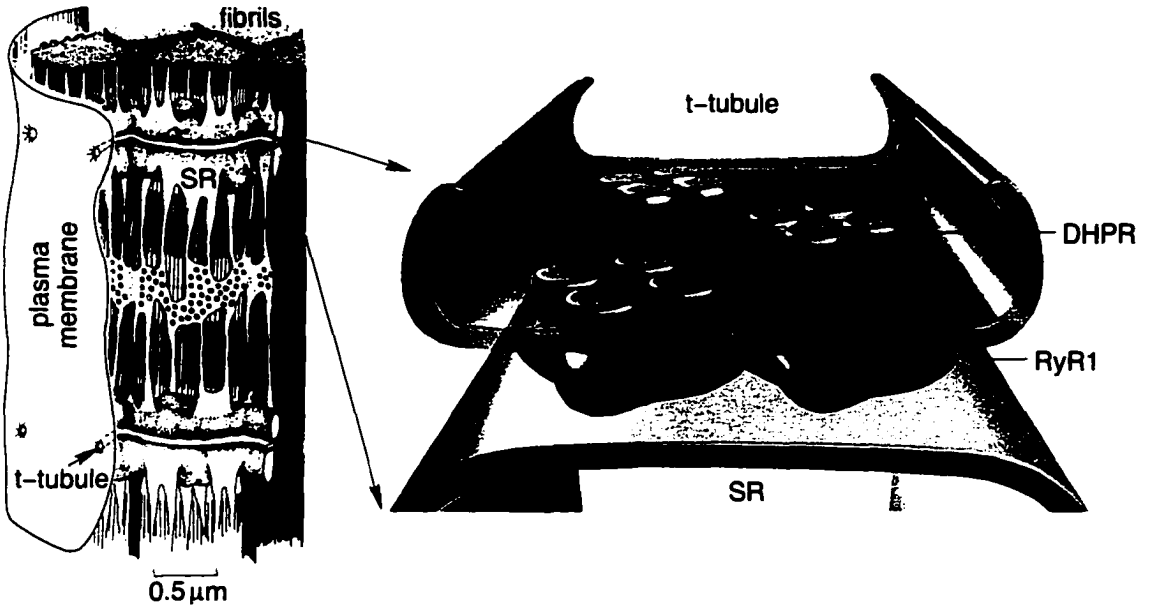

Figure 1: The diagram illustrates the location of the DHPRs and RyR1s in the triad junction of the muscle fiber. On the left is a depiction of a muscle fiber the length of one sarcomere (from Hille, 2001). On the right is a simplified model of the skeletal muscle triad junction, where the membranes of the t-tubule and SR are in close association. Each gray cylinder represents a single skeletal DHPR and each black square pillow represents a single RyR1 homotetramer.

The two main proteins involved in EC coupling in striated muscle are the skeletal isoform of the L-type voltage-gated Ca^{2+} channel or dihydropyridine receptor (α_{1S} or DHPR) and RyR1 (arrangement shown in Fig. 1). Activation of the DHPR

in the plasma membrane triggers the opening of RyR1 which in turn releases Ca^{2+} into the cytoplasm. It is this increase in cytoplasmic Ca^{2+} that relieves the inhibition between the actin and myosin filaments thus initiating muscle contraction. In order to better convey how these two proteins communicate between the plasma and SR membranes, I will begin by describing each receptor, then explain what is known about how these two receptors communicate, and finally summarize the studies I have carried out to better understand the functioning of the ryanodine receptor and its role in EC coupling.

0.4 Ryanodine receptors

0.4.1 Identification

Ryanodine receptors were first identified in electron microscopy images of muscle fibers. They appeared as large dense masses that bridged the gap between the t-tubule and the SR (Franzini-Armstrong, 1970). Clara Franzini-Armstrong called these large masses "feet" (Franzini-Armstrong, 1970) and proposed that they served as the EC coupling signal across the triad junction (Franzini-Armstrong and Nunzi, 1983). Later, the ryanodine receptor was purified from both cardiac and skeletal muscle and demonstrated to be the protein comprising the foot structures (Inui et al., 1987a,b). Yet the function of the ryanodine receptors was not resolved.

Although it was known that Ca^{2+} was released from the SR presumably via channel proteins and that ryanodine receptors were the "feet" of the triad junction, it was not initially clear that the channel proteins in the SR and the ryanodine receptors were one and the same. Direct recordings of the SR membrane in lipid

bilayers identified a Ca^{2+} release channel sensitive to ATP (Smith et al., 1985). This Ca^{2+} release channel protein was purified (Lai et al., 1988) and confirmed to be the ryanodine receptor by comparative ryanodine binding and expression and single channel measurements in lipid membranes (Imagawa et al., 1987; Smith et al., 1988). Subsequently, the sequence and primary structure were determined and functional expression of the cDNA demonstrated that the expression of this sequence was sufficient to create the full channel (Takeshima et al., 1989; Zorzato et al., 1990; Penner et al., 1989). For RyR1, the 5037 amino acid sequence encodes about a 560 kDa polypeptide that makes up only one of the four subunits required to form a complete receptor. Comparison of the electron microscopy images and ryanodine binding of the purified receptor to that of the "feet" structures confirmed that the purified receptor was indeed the "foot" protein (Inui et al., 1987a,b).

Since the first characterization of the ryanodine receptor in skeletal muscle, three isoforms have been discovered. RyR1 is the predominant form found in mammalian skeletal muscle and it has also been shown to be expressed in Purkinje cells in the brain (Sharp et al., 1993; Kuwajima et al., 1992). RyR2, the cardiac isoform, is expressed in the muscle of the heart (Inui et al., 1987a; Anderson et al., 1989; Nakai et al., 1990) and in parts of the brain (Kuwajima et al., 1992). Most recently, RyR3, the ubiquitously expressed isoform has been identified. It was originally cloned from brain (Hakamata et al., 1992) but found to be localized to many other tissues (Giannini et al., 1992, 1995) including mammalian skeletal muscle (Flucher et al., 1999). The relevant differences of the isoforms will be discussed when cardiac and skeletal-type EC coupling are compared.

0.4.2 Correlation of structural and functional properties

All three isoforms of the ryanodine receptor are thought to share similar structural features, although many of the most basic tertiary structural properties of the protein have not yet been fully elucidated. There are no known interactions between the subunits of different isoforms; ryanodine receptors exist in the membrane as homotetramers. Information from hydrophobicity plots suggests that the number of transmembrane domains could range somewhere between four (Takeshima et al., 1989) and twelve (Zorzato et al., 1990). Tryptic digestion of the exposed regions of the receptor has been shown to leave the regions of the protein roughly corresponding to the hypothesized four transmembrane domains intact (Chen et al., 1993). More recently, the comparison of RyR2 and RyR1 hydrophobic domains and conserved sequences suggested that many of the putative transmembrane domains in the Zorzato model are not present in RyR2. This observation led to an intermediary hypothesis stating that there are 6 domains (Tunwell et al., 1996). Regardless of the theory being considered, all potential transmembrane domains are located in 20% of the protein from the carboxy (C-) terminus. The remaining amino (N-) terminal portion creates the large cytoplasmic foot region (Takeshima et al., 1989; Zorzato et al., 1990) and the region including the C-terminal tail following the transmembrane domains is also cytoplasmic (Grunwald and Meissner, 1995). The C-terminal domain alone, after the N-terminal domain had been removed, was able to function as a channel suggesting that the transmembrane domains are sufficient to control channel function (Bhat et al., 1997). Furthermore, primary subunit-subunit interactions are localized

to the C-terminal region supporting the idea (see also the cryo-electron microscopy work described below) that all four subunits are needed for channel function and potentially forming a single opening (Wu et al., 1997).

Recently, structure-function analysis of the ryanodine receptor has provided information leading to the theory that the pore is formed by the cytoplasmic loop between the third and fourth transmembrane domains (in the Takeshima model) or by the second to last transmembrane domain of the Zorzato model (Balshaw et al., 1999; Zhao et al., 1999; Gao et al., 2000). Specifically, it has been proposed that the selectivity filter is composed of the conserved amino acids GGIG, 4895–4898 in RyR1, due to their similarity to the selectively filter of the KcsA channel and their impairment of Ca^{2+} release when mutated (Lynch et al., 1999; Balshaw et al., 1999; Zhao et al., 1999; Gao et al., 2000). Mutation and deletion experiments continue to reveal structural properties of the ryanodine receptor, but due to its large size and inaccessible location within the cell, it has been challenging to fully and confidently map the sequence to the structure. Other parallels between the amino acid sequence and the functional properties of the receptor will be further discussed below in terms of EC coupling and my own studies.

Cryo-electron microscopy of RyR1, RyR2, and RyR3 has provided three dimensional models of each isoform of the complete receptor (Radermacher et al., 1994; Sharma et al., 1998, 2000). Addition of proteins and antibodies to RyR1 during imaging has helped to map on the three dimensional model where binding sites and important regions may be located. For example, calmodulin was found to bind on the side of the "foot" region (Wagenknecht et al., 1994) and the C-terminal tail was

confirmed to be located in the cytoplasm near the transmembrane domains (Benacquista et al., 2000). Imaging of RyR1 in its active state, in the presence of Ca^{2+} and AMP-PCP a nonhydrolyzable analog of ATP, revealed a single pore in the transmembrane domain of the channel and openings at the four corners of the "foot" region, referred to as the clamps (Serysheva et al., 1999). A combination of the modeling studies and the sequence analysis has begun to provide a picture of RyR1 along with information about how the structure of the Ca^{2+} release channel relates to its function.

As stated above, all isoforms of the ryanodine receptor act as Ca^{2+} activated Ca^{2+} release channels. Functional characterization of the channels in lipid bilayers and HEK293 cells has shown that they have poor cation selectivity and no anion permeability (Smith et al., 1988; Meissner, 1994; Chen et al., 1997). Their cation permeability is greater for the divalent ions, specifically $Ba^{2+} > Sr^{2+} > Ca^{2+} > Mg^{2+}$ (Yoshida and Imai, 1997), and their conductance for these ions is very high (Smith et al., 1988). Ryanodine receptors are activated by moderate increases in the cytoplasmic Ca^{2+} concentration and inactivated by high concentrations (hence biphasic/bell-shaped dependence), suggesting the presence of both high and low affinity binding sites for Ca^{2+}, respectively (Ashley and Williams, 1990; Bull and Marengo, 1993; Györke and Fill, 1993). Interestingly, RyR1 has about a 10-fold higher affinity for Ca^{2+} at its inactivation site than RyR2. Exploiting the differences in Ca^{2+} affinity between the two isoforms, two labs constructed chimeric receptors, in which an amino acid region of one isoform was substituted into the corresponding region of the other isoform, and found from these chimeras that the inactivation site was localized to the

C-terminal region (Du and MacLennan, 1999; Nakai et al., 1999). Detailed information on the kinetics of ryanodine receptors is difficult to acquire because, at present, the only way to measure single channel currents through the receptor is by using lipid bilayers (extracts of SR membrane formed across a hole into a planar bilayer in which ryanodine receptors were reconstituted). Results from these experiments cannot predict how the channel behaves in physiological conditions.

0.4.3 Regulation by endogenous and exogenous factors

Behavior of the ryanodine receptor is regulated by many agents. I will focus on a few important to my work. RyR2 can be fully activated by Ca^{2+} alone, but RyR1 can only be partially activated unless adenine nucleotides such as ATP or potentiators such as caffeine are present (Smith et al., 1986). Since the myoplasmic levels of ATP (3–9 mM) (Godt and Maughan, 1988), are similar to those able to affect the ryanodine receptor in experimental conditions (Meissner, 1994), it could potentially act as a potentiator of RyR1 activation *in vivo*. Caffeine is thought to activate RyR1 while in the presence of Ca^{2+} by decreasing the threshold for activation by Ca^{2+} as demonstrated by its ability to shift the Ca^{2+} activation curve for RyR1 (Meissner et al., 1997). Mg^{2+}, an inhibitor of the ryanodine receptor, may play a role in regulation of the receptor. Acting as a competitive antagonist to the high affinity Ca^{2+} binding site (Meissner et al., 1997; Laver et al., 1997) Mg^{2+} is able to decrease Ca^{2+} induced Ca^{2+} release via RyR1 (Meissner et al., 1986; Smith et al., 1986) at concentrations close to the estimated resting myoplasmic concentration of 1 mM (Westerblad and Allen, 1992; Konishi et al., 1993). The plant alkaloid ryanodine, for which the

receptor was named, binds to the receptor with high affinity and specificity. At high concentrations it acts to inhibit the receptor. Yet at low concentrations, it specifically binds to the open state of the ryanodine receptor; therefore, many use it as a tool for studying activation (Buck et al., 1992). It remains unclear how exactly these endogenous and exogenous molecules act on ryanodine receptor function particularly during EC coupling.

0.5 Dihydropyridine receptors

The dihydropyridine receptor (DHPR) is the channel that communicates with the ryanodine receptor during EC coupling. Although its role is equally important to that of the ryanodine receptor, only its role in EC coupling, specifically, its ability to trigger the ryanodine receptor will be discussed (detailed below). The DHPR is an L-type voltage-gated Ca^{2+} channel found in the t-tubule membrane within the triad junction (Fosset et al., 1983). Originally it was identified by its high affinity for dihydropyridines including the antagonist nifedipine and the agonist Bay K 8644. In the cell, the DHPR exists as a complex in which the α_1 subunit forms the channel, the α_2 and γ subunits adjacent to the channel within the membrane, the β subunit is attached to the cytoplasmic side of α_1 and the δ subunit is covalently bonded to the extracellular portion of α_2 (Takahashi et al., 1987). The channel forming subunit, α_1, has four sections, I–IV, that each have six transmembrane domains, S1–S6, as defined by its amino acid sequence (Fig. 2; Tanabe et al., 1987). Two isoforms of α_1 important for EC coupling are from skeletal muscle (α_{1S}) and cardiac muscle (α_{1C}). A major difference between the two channels, aside from tissue specific localization, is that α_{1C}

activates faster than α_{1S}. Thus, in response to an action potential in physiological conditions, the Ca^{2+} influx via the DHPR is much greater in the presence of α_{1C} than α_{1S} (Tanabe et al., 1991; Dirksen and Beam, 1996). This observation plays a key role in the differences between EC coupling in cardiac versus skeletal muscle.

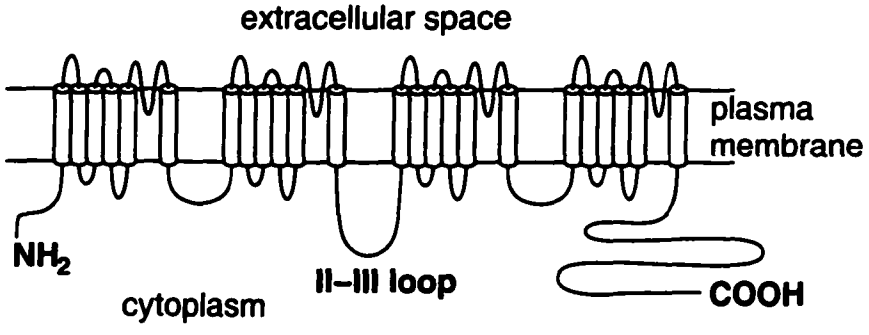

Figure 2: This diagram of α_{1S} shows the relative location of the transmembrane domains. Each group of six transmembrane domains is numbered I–IV from left to right. The center, cytoplasmic loop is known as the II-III loop.

0.6 Underlying mechanisms of EC coupling

The preceding detail concerning the properties of the receptors that together are the core of EC coupling provided the background for the following explanation of how these two receptors act to transmit the signal linking the depolarization of the muscle plasma membrane to the contraction of the muscle fiber. The DHPR was the first receptor/channel to be characterized as having a key role in EC coupling. When all the currents on a skeletal muscle fiber were blocked, a measurable charge movement still remained. This charge movement was hypothesized to be a moving protein linking the t-tubule membrane to the "feet" (Schneider and Chandler, 1973). Identification of the protein that acted as the voltage sensor resulted from studies

of both dihydropyridine binding (Rios and Brum, 1987) and mice with muscular dysgenesis (mdg; Beam et al., 1986). Dihydropyridines blocked the voltage sensor and Ca^{2+} release suggesting that the DHPR is involved (Rios and Brum, 1987). These stillborn mdg mice had no slow Ca^{2+} currents in their muscle cells (Beam et al., 1986). EC coupling was restored after microinjection of DHPR cDNA into cultured muscle cells from mdg mice (dysgenic cells) demonstrating that the DHPR was responsible for the slow Ca^{2+} current (Tanabe et al., 1988). Specifically, it was shown that dysgenic cells lack the α_{1S} subunit of the DHPR (Knudson et al., 1989). Thus, expression of α_{1S} in dysgenic myotubes also restored the charge movement of the t-tubule membrane (Adams et al., 1990). Together, the results led to the conclusion that the α_{1S} subunit of the DHPR acts as both a voltage-gated Ca^{2+} channel and the voltage sensor in skeletal-type EC coupling.

The ryanodine receptor, as explained above, is the Ca^{2+} release channel that helps to regulate the initiation of muscle contraction. In addition, it is thought to provide the bridge across the triad junction that transfers a signal from the voltage sensor, the DHPR, to trigger Ca^{2+} release. Do the DHPR and ryanodine receptor mechanically interact or does the influx of Ca^{2+} via the DHPR activate the ryanodine receptor? In the absence of extracellular Ca^{2+}, hence no Ca^{2+} influx, skeletal muscle was able to contract but cardiac muscle was not (Armstrong et al., 1972). Furthermore, skeletal-type EC coupling was not affected by a mutation in the pore region of the DHPR α_{1S} subunit that eliminated Ca^{2+} influx through the channel (Dirksen and Beam, 1999) reinforcing the findings of previous studies that had used channel blockers or Ca^{2+}-free solutions which may have had confounding effects on the cells.

Thus, it appears that a mechanical interaction between the DHPR and ryanodine receptor is present in skeletal muscle, but cardiac muscle depends on Ca^{2+} to transfer the EC coupling signal. This interaction is isoform specific; skeletal-type EC coupling is dependent upon the presence of α_{1S} (Knudson et al., 1989) and RyR1 (Takeshima et al., 1994), but cardiac cells predominantly express α_{1C} and RyR2.

Physical evidence of an interaction between the skeletal DHPR and RyR1 was originally shown with freeze fracture techniques. The "feet" in the SR membrane align in an alternate pattern with tetrads which are particles found in groups of four in the facing t-tubule membrane as shown the right panel of Fig. 1 (Block et al., 1988). Tetrads are absent in dysgenic muscle cells (Franzini-Armstrong et al., 1991) but can be restored by expressing α_{1S} demonstrating that the α_{1S} and the rest of the DHPR complex are the proteins that constitute each particle in the tetrad (Takekura et al., 1994). In dyspedic muscle cells which lack functional endogenous RyR1s neither "feet" nor tetrads were present (rather there was a random arrangement of particles in the plasma membrane in place of the tetrads), but the junctional membranes remained closely associated (Takekura et al., 1995). Injection of RyR1 into the dyspedic cells restored the unordered array of particles into tetrads (Protasi et al., 1998). Accordingly, the DHPRs require the presence of the RyR1s to form tetrads suggesting that there is a physical link between the two proteins but each protein is not required for the proper membrane association of the other. In cardiac muscle, tetrads are seen highlighting the skeletal specific nature of the interaction (Sun et al., 1995). Cosedimentation and cross-linking experiments have further given support to the idea that the DHPR and RyR1 are physically associated (Marty et al.,

1994; Murray and Ohlendieck, 1997) although whether or not the interactions occur under physiological conditions has not been determined.

0.7 Cardiac- versus skeletal-type EC coupling

Underlying the physiological differences between skeletal- and cardiac-type EC coupling are the differences in the properties of the α_1 and ryanodine receptor isoforms found in their respective tissues. EC coupling in cardiac muscle is believed to occur through Ca^{2+} induced Ca^{2+} release (CICR); it is the influx of Ca^{2+} through α_{1C} that activates RyR2 (Fabiato, 1983). Activation of RyR2 is much lower when the cell is held at voltages near the reversal potential for the α_{1C} Ca^{2+} currents than at voltages able to trigger the peak Ca^{2+} current amplitudes. This results in a bell-shaped voltage dependence of Ca^{2+} release via RyR2. When RyR2 was expressed in dyspedic myotubes (in the presence of endogenous skeletal DHPR complexes), no contractions were observed in the absence of extracellular Ca^{2+} unlike when RyR1 is expressed in these cells (Nakai et al., 1997). Likewise, in the converse situation, α_{1C} does not trigger the activation of RyR1 when expressed in dysgenic myotubes (Tanabe et al., 1990b; García et al., 1994). Specifically, myotubes expressing α_{1C} release SR Ca^{2+} and contracted under electrical stimulation, but this Ca^{2+} release was abolished in the presence of Ca^{2+} channel blockers (Tanabe et al., 1990b). Depolarization evoked Ca^{2+} release, measured while in whole-cell patch clamp mode, showed a bell-shaped voltage dependence which reflects the U-shaped dependence of the Ca^{2+} entry via α_{1C} supporting the idea that the activation of RyR1 is triggered by CICR (García et al., 1994). Normal myotubes, in contrast, showed a sigmoidal-shaped voltage

dependence independent of Ca^{2+} influx which instead parallels that of the degree of intramembrane charge movement associated with α_{1S} (García and Beam, 1994a). In normal conditions during an action potential (versus an unnatural 200 ms pulse), it is likely that RyR2 is exposed to a greater concentration of Ca^{2+} influx via α_{1C} than is RyR1 upon activation of α_{1S}. This is due to the fact that the α_{1C} Ca^{2+} currents are faster and activate at more negative potentials than α_{1S} causing a greater influx of Ca^{2+} through α_{1C} (Tanabe et al., 1990b). In addition, RyR2 is more sensitive to activation by Ca^{2+} than RyR1 (Zimanyi and Pessah, 1991) further promoting the efficiency of CICR in cardiac cells versus a direct interaction like that in skeletal cells.

0.8 A region in α_{1S} integral for skeletal-type EC coupling

The creation of chimeric channels, proteins in which corresponding amino acid regions of two isoforms are exchanged, takes advantage of the unique properties of each receptor isoform to determine what structural regions are important for the functioning of the receptors, in this case, in EC coupling. A series of chimeras with background sequence of α_{1C} and different cytoplasmic regions replaced by α_{1S} revealed that the loop between repeats II and III of α_{1S} is sufficient to transfer skeletal-type EC coupling function onto an otherwise cardiac channel (Tanabe et al., 1990a). Additional chimera studies between α_{1S} and α_{1C} narrowed down the important region within the II-III loop to amino acids 725–742 of α_{1S} (Nakai et al., 1998b). Other labs formulated a different hypothesis concerning which amino acids within the II-III loop were important for EC coupling by testing the ability of different peptides of

the loop to activate RyR1 in lipid bilayers (El Hayek et al., 1995). Both types of experiments had flaws preventing a single hypothesis from being accepted, specifically, the sequence between the II-III loop of both α_{1S} and α_{1C} is highly conserved so different regions of each isoform could have overlapping or unpredictable effects and the peptides of the loop could access regions of RyR1 that the loop, when attached to the rest of α_{1S}, might not otherwise have access to. Two experiments provided convincing evidence that amino acids 725–742 are important. A chimera made with house fly (*Musca domestica*) DHPR, which has very few conserved amino acids in the II-III loop compared to α_{1S}, as background and the region 720–764 of α_{1S} exchanged into the loop was able to support skeletal-type EC coupling when expressed in dysgenic myotubes (Wilkens et al., 2001). In addition, scrambling the loop sequence, which was shown to activate RyR1 in peptide experiments (681–690), had no effect on function of the whole α_{1S} protein during skeletal-type EC coupling (Proenza et al., 2000). Thus, the amino acids 725–742 are likely to either directly or indirectly (via a possible intermediary protein) interact with RyR1.

0.9 Regions of RyR1 involved in skeletal-type EC coupling

Similar chimeric studies were performed on the ryanodine receptor to determine the region with which the II-III loop interacted. As with α_{1S} and α_{1C}, chimeras were made between RyR1 and RyR2 to exploit the differences in function between the two isoforms. Three regions of highly divergent sequence between RyR1 and RyR2 are named as follows: D1, 4254–4631 of RyR1 and 4210–4562 of RyR2; D2,

1342–1403 of RyR1 and 1353–1397 of RyR2; D3, 1872–1923 of RyR1 and 1852–1890 of RyR2 (see Fig. 3; Sorrentino and Volpe, 1993). Deletion of the D2 region in RyR1

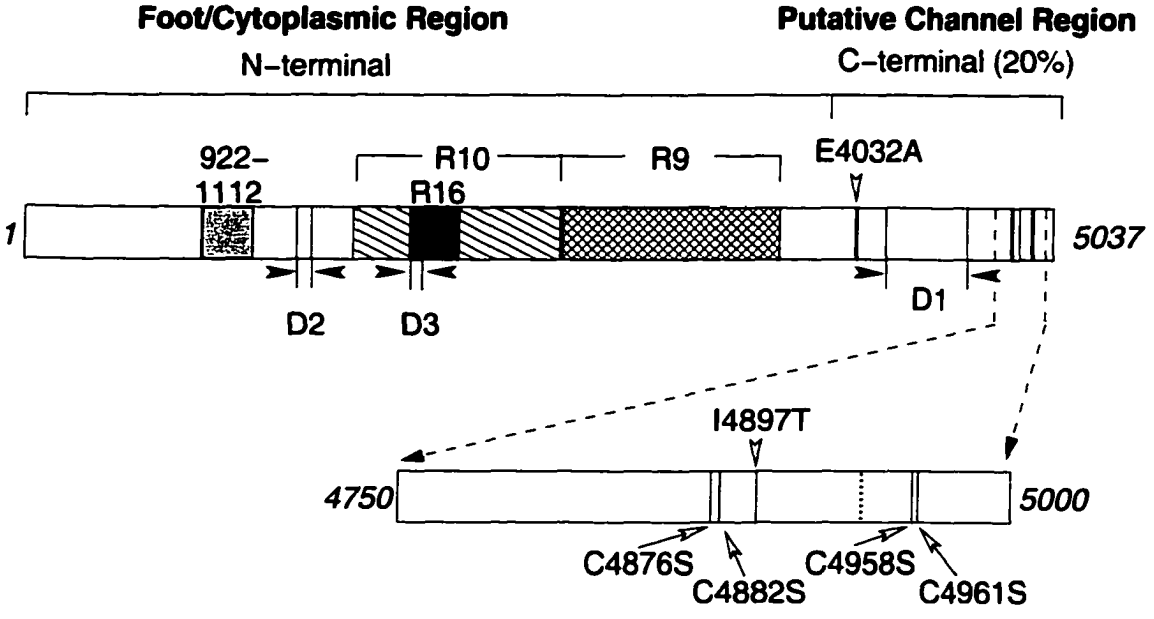

Figure 3: This diagram shows the important regions of RyR1 that will be discussed. The top bar represents the amino acid sequence encoding the full RyR1 protein and the bottom bar represents an enlarged portion of the C-terminal domain. The dashed line on the bottom bar denotes the end of the last putative transmembrane domain. Both bars are drawn to scale.

eliminated skeletal-type EC coupling, but replacement of the deleted region with the corresponding RyR2 region recovered RyR1's function (Yamazawa et al., 1997). These results could be interpreted to mean that the deletion caused enough structural change to damage the function of RyR1 or that D2 works in concert with another region to transfer the signal. Reverse chimera studies, with RyR2 background sequence, have confirmed that D2 is unlikely to be solely important in communication with the DHPR. Of possibly greater importance is the D3 region since the chimera R10 (1635–2636 of RyR1) containing D3 was sufficient to restore skeletal-type EC coupling (Nakai et al., 1998a). Interestingly, both this region and R9 (2659–3720) of

RyR1 were able to support retrograde signaling, or signaling back to the DHPR (discussed below), in the presence of an RyR2 background (Fig. 3; Nakai et al., 1998a). As one might have expected, it appears that the potential regions of interaction with the DHPR on RyR1 are located in the cytoplasmic "foot" region.

0.10 Retrograde signaling

Not only does the DHPR signal to RyR1, but RyR1 also feeds back onto the DHPR. When RyR1 is absent, as in the case of dyspedic myotubes, the DHPR Ca^{2+} currents are small. Expression of RyR1 restores or enhances the amplitude of the Ca^{2+} currents but expression of RyR2 does not (Nakai et al., 1996, 1997). Activation, conductance, and expression of the DHPR are all influenced by the presence of RyR1 (Avila and Dirksen, 2000). The chimeras R9 and R10, previously mentioned, were capable of enhancing Ca^{2+} currents suggesting that multiple or overlapping sites within these areas are important for interaction with the DHPR (Nakai et al., 1998a). As in skeletal-type EC coupling, the amino acids, 720–764 of the II-III loop of the DHPR are essential for retrograde signaling (Grabner et al., 1999). Ca^{2+} may play a role in regulating the expression of the DHPR. Prolonged decrease in Ca^{2+} release, due to a mutation in RyR1, prevented increased DHPR expression seen with wild type RyR1 (Avila et al., 2001). Thus, the functional and physical presence of RyR1 is required for full DHPR activity.

0.11 Hypotheses

0.11.1 Ca^{2+} activation of RyR1 is not necessary for the initiation of skeletal-type excitation-contraction coupling

During skeletal-type EC coupling, RyR1 can be activated in the absence of Ca^{2+} entry through an interaction with the α_{1S} II-III loop of the DHPR. Resting concentrations of myoplasmic Ca^{2+} may be sufficiently high to contribute to the activation of RyR1 during this process. The DHPR may allosterically cause a decrease in the Ca^{2+} sensitivity of RyR1 thus allowing activation of RyR1 by resting Ca^{2+} concentrations. A point mutation of a highly conserved glutamate in RyR3 (E3885A) caused a 10,000 fold increase in the threshold for activation by Ca^{2+} (Chen et al., 1998). The corresponding mutation in RyR1 (E4032A) was studied to determine the effect of the decreased Ca^{2+} sensitivity of RyR1 on skeletal-type EC coupling.

0.11.2 A region in RyR1 that interacts with the α_{1S} II-III loop in yeast two-hybrid plays a functional role in skeletal-type EC coupling

The specific region on RyR1 that interacts with the α_{1S} II-III loop has not been elucidated. Previous work with chimeras between RyR1 and RyR2 showed that the skeletal region R9 (2659–3720) was able to support retrograde signaling and the region R10 (1635–2636) was able to support both retrograde and orthograde signaling with the DHPR (Nakai et al., 1998a). Interaction with yeast two-hybrid was shown between amino acids 720–765 of the α_{1S} II-III loop and amino acids 1837–2168 (sR16, within R10) of RyR1 (Proenza, 1999). Using a biochemical approach (specifically use of affinity columns) to determine what regions of RyR1 bound to the α_{1S} II-III loop,

the MacLennan lab identified amino acids 922–1112 as a potential interactor, while the corresponding region of RyR2 (933–1126) was unable to interact (Leong and MacLennan, 1998). To determine the importance of each region in retrograde and orthograde signaling, I tested two chimeras when expressed in dyspedic myotubes, one with the sR16 region exchanged into RyR2 and one with 933–1126 of RyR2 exchanged into RyR1.

0.11.3 The mutation C4958S in RyR1 disables Ca^{2+} release but not enhancement of α_{1S} Ca^{2+} currents

Due to their ability to form covalent bonds with one another, cysteines usually play an important role in maintaining the structural integrity, or subunit-subunit interactions, of a protein. In the C-terminal domain of all isoforms of the ryanodine receptor and inositol triphosphate receptors (IP_3Rs), another family of Ca^{2+} release channels, two pairs of conserved cysteines have been identified. Because IP_3Rs share common properties with ryanodine receptors including homotetramerization and relative cation permeability, it is probable that either pair of cysteines is involved in subunit interactions or channel formation and function. To test this hypothesis, I expressed four RyR1 constructs, each containing a mutation of one of the four cysteines mentioned above, in dyspedic myotubes to show what effects the mutation has on RyR1 function. Detailed analysis was continued on the mutation C4958S in RyR1.

My contributions to collaborative projects are included in the appendix.

Chapter 1

Ca^{2+} Activation of RyR1 Is Not Necessary For The Initiation Of Skeletal-Type EC Coupling

The chapter will be published in the *Biophysical Journal* with the following list of authors: Jennifer J. O'Brien[†], Wei Feng[‡], Paul D. Allen[§], S. R. Wayne Chen[¶], Isaac N. Pessah[‡], and Kurt G. Beam[†]. Wei Feng in Isaac N. Pessah's lab contributed the methods, data, and figure (Fig. 1.1) for the single channel recordings. Paul D. Allen originally supplied us with the dyspedic myotubes and S. R. Wayne Chen constructed the mutant, E4032A-RyR1. I performed the rest of the experiments.

[†]Dept. of Anatomy and Neurobiology, Colorado State University, Fort Collins, CO 80523
[‡]Dept. of Molecular Biosciences, Univ. of California Davis, Davis, CA 95616
[§]Dept. of Anesthesia, Brigham & Women's Hospital, Boston, MA 02115
[¶]Dept. of Physiology and Biophysics, University of Calgary, Calgary, Alberta T2N 4N1, Canada

1.1 Introduction

Ryanodine receptors are intracellular Ca^{2+} release channels, currently known to be encoded in mammals by three distinct genes. RyR1 and RyR2 are the predominant forms in skeletal muscle and cardiac muscle, respectively (Takeshima et al., 1989; Zorzato et al., 1990; Nakai et al., 1990), and RyR3 is ubiquitously expressed (Hakamata et al., 1992; Giannini et al., 1992). All three isoforms can be activated by an elevation in cytoplasmic Ca^{2+}. In cardiac muscle, activation of RyR2 by cytoplasmic Ca^{2+} plays a major role in excitation-contraction (EC) coupling. Specifically, depolarization of cardiac muscle cells activates a voltage-gated L-type Ca^{2+} channel, which contains α_{1C} as its principle subunit; the resulting influx of Ca^{2+} provides an increase in cytoplasmic Ca^{2+} sufficient for activating RyR2 to release Ca^{2+} from the sarcoplasmic reticulum (Fabiato, 1985; Nabauer et al., 1989). An elevation of intracellular Ca^{2+} can also serve to activate RyR1, but the role of this pathway is uncertain. Thus, even though skeletal muscle expresses large numbers of L-type Ca^{2+} channels (containing α_{1S} as the principle subunit), EC coupling in skeletal muscle persists after Ca^{2+} influx through α_{1S} is blocked by removal of extracellular Ca^{2+} (Armstrong et al., 1972) or by channel blockers (Gonzalez-Serratos et al., 1982). Therefore, a mechanical interaction with α_{1S} may be responsible for activating RyR1 during "skeletal-type" EC coupling (Rios and Brum, 1987; Tanabe et al., 1990a) and the role of Ca^{2+}-activation during this initial triggering of RyR1 remains unclear (e.g. Lamb et al., 2001).

Recently, it has been reported that a glutamate conserved in all three RyR isoforms has an important role in Ca^{2+} activation. Specifically, mutation of this glutamate to alanine in RyR2 (E3987A) and in RyR3 (E3885A) caused a 1,000–10,000-fold increase in the EC50 for activation by Ca^{2+}, as measured by recordings of channels reconstituted into bilayers (Chen et al., 1998; Li and Chen, 2001). The corresponding mutation (E4032A) in RyR1 also inhibits activation by Ca^{2+} (Fessenden et al., 2001). Here, we have used expression in dyspedic mouse myotubes, which lack endogenous RyR1 (Takeshima et al., 1994; Buck et al., 1997), to compare the effects of the E4032A mutation on the activation by Ca^{2+} of single ryanodine receptor channels reconstituted into planar lipid bilayers and the activation of intracellular Ca^{2+} release by depolarization of myotubes via the whole-cell technique. We found that the E4032A mutation causes >100-fold suppression in RyR1 activity in bilayers in response to Ca^{2+}, but only a ~5-fold reduction in depolarization induced Ca^{2+} release in myotubes. This residual Ca^{2+} release occurred via skeletal-type coupling because it showed a sigmoidal dependence on test potential and persisted after the block of Ca^{2+} influx via L-type Ca^{2+} current. Thus, Ca^{2+} activation of RyR1 does not appear to be essential for the initiation of skeletal-type EC coupling although it might be important for the overall functioning of EC coupling. In agreement with Avila et al. (2001), retrograde signaling, whereby RyR1 increases the L-type Ca^{2+} current carried by α_{1S} (Nakai et al., 1996) was little affected by the E4032A mutation. Therefore, Ca^{2+} release from RyR1 does not appear to play a major role in the retrograde signal from RyR1 to α_{1S}.

1.2 Experimental procedures

1.2.1 Mutagenesis

The mammalian expression plasmid (E4032A-RyR1-pCDNA3), in which the point mutation E4032A was introduced into RyR1, was constructed by the overlap extension method (Ho et al., 1989) using polymerase chain reaction (PCR). The "outer" two oligonucleotides used are: forward, 5′ GTGTTCAACAGCCTCACCGA 3′ and reverse, 5′ GAACTGCTTCTGGCTGTCCA 3′. The oligonucleotides for the E4032A mutation are: forward, 5′ GTCCCTACTGGCAGGGAACGTGGT 3′ and reverse, 5′ CCACGTTCCCTGCCAGTAGGGACA 3′. The sequence of the PCR product was confirmed by DNA sequencing. The *Xho*I (12018)–*Stu*I (12224) fragment was removed from the PCR product and was used to replace the corresponding wild-type region in the *Xho*I (12018)–*Xba*I (3′ end) fragment of the RyR1 cDNA in pBluescript. The *Xho*I (12018)–*Xba*I (3′ end) fragment containing the E4032A mutation was subcloned into the RyR1 cDNA in pHSVprPUC vector lacking the *Xho*I (6466)–*Xho*I (12018) fragment, which was added back subsequently to form the full length E4032A-RyR1 cDNA. The full length E4032A-RyR1 cDNA (*Hind*III–*Xba*I) was transferred from pHSVprPUC to pCDNA3 to form the expression plasmid E4032A-RyR1-pCDNA3.

1.2.2 Single channel analysis

For the measurements of single ryanodine receptor channels, ryanodine receptor cDNAs were expressed in 1B5 myotubes. The 1B5 cells were cultured in DMEM (Dulbecco's Modified Eagle Medium, GIBCO/BRL, Germantown, MD) containing

20% fetal bovine serum in collagen-coated 100 mm polystyrene plates (Protasi et al., 1998; Moore et al., 1998). When the cells attained 30–50% confluence, they were differentiated within a 20% CO_2 incubator at 37°C for 5 days in 5% heat-inactivated horse serum in DMEM before infection with RyR-cDNA containing viruses (Wang et al., 2000). Briefly, cDNA encoding either wild-type RyR1 or E4032A-RyR1 was added to differentiated 1B5 myotubes at a concentration of 3–5 $\times$ 10^5 infectious units (IU)/ml. Cells were harvested and sarcoplasmic reticulum (SR) prepared 48 hrs after infection.

Crude membrane homogenates from 1B5 myotubes expressing E4032A-RyR1 were prepared as described previously (Moore et al., 1998) and subsequently loaded onto a sucrose gradient consisting of layers of 10%, 27% and 45% w/w sucrose, 10 mM HEPES pH 7.4. After sedimentation of the crude membranes on this gradient at 40,000 $\times$ g for 1 hr at 4°C, the 27–45% interface containing heavy SR membranes was isolated and diluted in 10 mM HEPES, pH 7.4 and subsequently pelleted at 110,000 $\times$ g for 1 hr. The pellet was resuspended in 10% sucrose, 10 mM HEPES, pH 7.4, divided into small aliquots and either used immediately or stored at −80°C for no more than two weeks.

Heavy SR membrane vesicles were fused with an artificial bilayer lipid membrane (BLM) composed of a 5:2 mixture of natural phosphatidylethanolamine and phosphatidylcholine (PE:PC 5:2 mixture) at 50 mg/ml in decane. The BLM was formed across a 200 to 250 μm hole in a polystyrene cup separating two chambers (cis and trans) each 0.7 ml. Vesicles (0.1–5 μg protein) were added to the cis chamber in the presence of 200 μM Ca^{2+}. The cis and trans chambers contained 500 mM CsCl,

20 mM HEPES (pH 7.4), and 100 mM CsCl, 20 mM HEPES (pH 7.4), respectively. After fusion, 300 μM EGTA was added to the cis chamber to prevent additional fusion events. The cis chamber was then perfused with a solution composed of 500 mM CsCl, 20 mM HEPES, pH 7.4 (asymmetrical CsCl 5:1 cis:trans). A patch-clamp amplifier (Dagan, model 3900) was used to measure currents through a single channel. The data were filtered at 1 kHz (low-pass, 8-pole Bessel filter, Warner Instrument Corp, CT) before acquisition at 10 kHz by a DigiData 1200A (Axon Instruments, Foster City, CA). Experimental reagents were added to the cis chamber and stirred for 30 sec. Subsequent channel gating behavior was recorded for 1–20 min using Axoscope 8.0 (Axon Instruments). Single-channel data from BLM experiments were analyzed using pCLAMP6 (Axon Instruments), and Fig. 1.1 was prepared using Origin 4.0 (Microcal, Northampton, MA).

1.2.3 Expression of cDNA in primary myotubes

Primary cultures of dyspedic mouse myotubes were obtained as previously described (Nakai et al., 1996; Rando and Blau, 1994). At 6–7 days after initial plating, a single nucleus of each cell was microinjected with 0.3 μg/μl of either E4032A-RyR1-pCDNA3 or RyR1-pCIneo (Nakai et al., 1998a) and 0.2 μg/μl of an expression plasmid (Jurman et al., 1994) for the surface antigen CD8. All constructs were derived from the rabbit cDNA for that protein. Approximately 48 hours later, the medium was removed from injected myotubes and replaced with external recording solution (see below) containing beads coated with CD8 antibody (Dynabeads M-450, Dynal AS, Oslo, Norway), which allowed identification of cells that were expressing CD8 and

thus also candidates to be expressing the ryanodine receptor construct of interest. Alternatively, the ryanodine receptor cDNA was injected together with 0.04 μg/μl cDNA for green fluorescent protein (Grabner et al., 1998). After 48 hours, the GFP-positive myotubes, while bathed in DMEM (Dulbecco's Modified Eagle Medium, GIBCO/BRL, Germantown, MD), were tested for the ability to contract in response to stimulation (100 V, 10 ms) via an extracellular pipette which was filled 150 mM NaCl and positioned with its tip near ($\sim$30 μm) the cell.

1.2.4 Measurement of Ca^{2+} currents and Ca^{2+} transients

Ca^{2+} currents and Ca^{2+} transients were recorded simultaneously (García et al., 1994) using a combination of the whole-cell patch technique and fluorometric monitoring of myoplasmic Ca^{2+} by means of Fluo-3 which was included in the "internal solution" (composition given below). Patch pipettes were pulled from borosilicate glass and had resistances of 1.6 to 2.0 MΩ when filled with internal solution. After a seal was obtained between the patch pipette and a myotube, the cell was washed to remove any Fluo-3 that might have leaked into the bath from the pipette. A period of >5 min was allowed after breaking into whole-cell mode in order that Fluo-3 could diffuse throughout the myotube. Cells were held at -80 mV and control currents were measured by steps to -110 mV. Cell capacitance was determined by integration of the control current and used to normalize Ca^{2+} currents (pA/pF). Additionally, the average of ten control currents was digitally scaled and subtracted from test currents to correct for linear components of leakage and capacitative current. The voltage

protocol for test currents consisted of a 1 sec prepulse to −30 or −20 mV to inactivate T-type current, followed by a 50 ms repolarization to −50 mV, followed by a 200 ms step to the test potential, a 125 ms step to −50 mV and finally a return to the holding potential.

For the measurement of fluorescence, a rectangular slit and iris diaphragm were adjusted so that the illumination from a 75W xenon bulb and was restricted to a segment of the myotube that avoided both surrounding cells and the patch pipette. To prevent prolonged exposure of cells to this illumination, a digitally controlled shutter was opened 1 sec prior to the test step and closed immediately after the return to the holding potential. Fluorescence emission was recorded with standard filters for fluoroscein (excitation centered at 470 nm with half-height width of 20 nm, dichroic 510 nm long pass, emission 520 nm long pass) and a photometer system (Biomedical Instrumentation Group, U. of Pennsylvania). Data were acquired and analyzed with a PDP-11/73 computer system (INDEC, Sunnyvale, CA).

For the measurement of changes of myoplasmic calcium in response to application of caffeine or cyclopiazonic acid (CPA), intact myotubes were rinsed with serum-free DMEM and then incubated for 1 hr at 37°C in serum-free DMEM containing 5.5 μM Fluo-3AM (Molecular Probes, Eugene, OR). After loading, the cells were returned to normal culture medium (DMEM with serum) and placed in the incubator for a minimum of 30 minutes prior to experimentation. Fluorescence responses were recorded with pClamp 8.0 (Axon Instruments). To normalize for differences in loading with Fluo-3AM, changes in fluorescence (ΔF) in response to CPA were normalized by the baseline fluorescence, which was determined as the resting fluorescence

of the loaded myotube after subtraction of the signal from a corresponding area of the culture dish that lacked myotubes.

1.2.5 Solutions

The internal solution contained (in mM): 145 Cs-glutamate, 8 MgATP (1 mM free Mg^{2+}), 2 CsCl, 10 HEPES, 10 EGTA, and 0.5 K_5 Fluo-3 (Molecular Probes, Eugene, OR). The external solution used for measuring Ca^{2+} currents and Ca^{2+} transients contained (in mM): 145 TEACl, 10 HEPES, 10 $CaCl_2$, and 0.003 TTX. To test the effects of Cd^{2+} plus La^{3+} (0.5 and 0.1 mM, respectively) or of caffeine (1 or 10 mM), individual, patch-clamped myotubes were analyzed before and after the external solution was replaced with external solution containing the indicated substances. The effect of CPA (30 μM) was studied on individual, intact cells bathed in Rodent Ringers solution which contained (in mM) 145 NaCl, 10 HEPES, 5 KCl, 2 $CaCl_2$, 1 $MgCl_2$. In myotubes expressing RyR1, TTX (3 μM) was added to block Ca^{2+} release triggered by spontaneous action potential activity. The effects of caffeine and CPA were tested on only a single myotube per culture dish because the actions of these agents were not found to be easily reversible.

1.2.6 Analysis

Because intracellular Ca^{2+} release was reduced several-fold for E4032A-RyR1, I characterized release in terms of ΔF, the change in fluorescence from baseline (F), rather than as $\Delta F/F$, because ΔF was quite stable during the course of an experiment, whereas the baseline fluorescence gradually increased, apparently due to incomplete

removal of myoplasmic Ca^{2+}. Additionally, ΔF was measured 40 ms after the onset of depolarization to help reduce the contribution of the entry of extracellular Ca^{2+} due to Ca^{2+} current. Values of ΔF were plotted versus test potential (V) and fitted according to the equation:

$$\Delta F = \Delta F_{max} / \left(1 + \exp - \frac{(V - V_{\frac{1}{2}})}{k_F}\right) \tag{1.1}$$

where ΔF_{max} is the maximum fluorescence change, $V_{\frac{1}{2}}$ is the potential eliciting a half-maximal ΔF, and k_F is a parameter related to the steepness of voltage dependence. In addition to measuring amplitude, we visually fitted a straight line to the onset of the transient to determine the initial slope (in ΔF/ms).

Data are reported as mean $\pm$ s.e.m. and exclude cells which had peak Ca^{2+} currents less than 1 pA/pF and transients indistinguishable from baseline noise, on the assumption that these cells were likely expressing CD8 but not the ryanodine receptor construct. Statistical comparisons were made with the Student's t-test.

1.3 Results

To analyze the effects of the E4032A mutation at the single channel level, wild-type and mutant RyR1 were produced by transduction of myotubes obtained by differentiation of 1B5 cells, an immortal myogenic cell line lacking a functional copy of the native RyR1 gene. As observed after reconstitution of native RyR1 from rabbit skeletal muscle junctional SR, wild-type RyR1 channels isolated from transduced 1B5 myotubes have been shown to exhibit large conductance events (>400 pS for

100 mM Cs^+) with rapid, full conductance gating transitions that are sensitive to modulation by Ca^{2+}, Mg^{2+}, caffeine, adenine nucleotides, ryanodine and ruthenium red (Moore et al., 1998; Wang et al., 2000). Consistent with this previous work, we found that reconstituted wild-type RyR1 was strongly activated by exposure on the cis side to 100 μM Ca^{2+} (P_o ranging from 0.64 to 0.95, averaging 0.88 ± 0.08, $n = 9$), whereas the reconstituted E4032A-RyR1 was not (P_o too low to be measured, data not shown). In fact, several attempts to activate E4032A-RyR1 by cis exposure to a combination of activators (100 μM free Ca^{2+}, 2 mM ATP and 2 mM caffeine) yielded very negligible gating activity (Fig. 1.1, top panel, $P_o < 0.0001$). Thus, the E4032A mutation severely impairs activation by Ca^{2+} compared to wild-type RyR1 isolated from 1B5 myotubes and measured under similar conditions (Wang et al., 2000). We also examined the behavior of E4032A-RyR1 in the presence of mM Ca^{2+} in the cis solution since mM Ca^{2+} was found to cause measurable activation (P_o of 0.016) of RyR3 bearing the mutation (E3885A) homologous to that of E4032A-RyR1 (Chen et al., 1998). When Ca^{2+} was raised to 1–5 mM, channel activity of E4032A-RyR1 exhibited only a modest enhancement (not shown), but reached a discernible level when a combination of strong activators was included in the cis chamber (Fig. 1.1, middle and bottom panels). However, unlike wild-type RyR1 and E3885A-RyR3, the gating activity of E4032A-RyR1 remained extremely low (typically $P_o < 0.005$) under all the conditions tested. The inability to cause an appreciable P_o for E4032A-RyR1 makes it difficult to quantify the effects of the mutation on Ca^{2+} activation. However, comparison of P_o for wild-type RyR1 in 100 μM Ca^{2+} (0.88) with the maximal P_o that we observed for E4032A-RyR1 under any condition (< 0.005 in 2 mM Ca^{2+}, 2 mM

ATP and 2 mM caffeine) suggests a >100-fold decrement in the maximal ability of Ca^{2+} to cause activation, alone or together with other strongly activating ligands.

To determine if the E4032A mutation affects the ability of RyR1 to mediate EC coupling, the mutant protein was expressed in dyspedic myotubes which lack endogenous RyR1 (Takeshima et al., 1994), but do express other key proteins of the triad junction, including α_{1S} (Buck et al., 1997). When cells expressing E4032A-RyR1 were focally stimulated (100 V, 10 ms), no evoked contractions were observed in the 28 cells tested, whereas all 13 cells expressing wild-type RyR1 contracted when stimulated. Thus, the E4032A mutation impairs the ability of RyR1 to mediate EC coupling. To obtain a more quantitative estimate of this impairment, I used the whole-cell variant of the patch clamp technique together with Fluo-3 to measure Ca^{2+} transients (transient increases in cytoplasmic Ca^{2+} as indicated by changes in dye fluorescence). As shown in Figure 1.2a, depolarization caused Ca^{2+} release via E4032A-RyR1, but this was about 5-fold smaller than for RyR1. Specifically, at +40 mV, ΔF for E4032A-RyR1 expressing cells was 35.31 ± 4.47 ($n = 28$) compared to 181.67 ± 20.36 ($n = 27$) for RyR1 (significantly different, $p \ll 0.001$). The rate of fluorescence increase ($\Delta F/ms$) at +40 mV showed a similar reduction from 7.84 ± 1.18 ($n = 27$) for RyR1 to 1.54 ± 0.20 for E4032A-RyR1 ($n = 28$). No transients were observed in dyspedic myotubes ($n = 10$). The amplitude of Ca^{2+} transients for E4032A-RyR1 showed a sigmoidal dependence on voltage similar to that of RyR1 (Fig. 1.2b).

In principle, the reduced Ca^{2+} transients for E4032A-RyR1 could have resulted from the mutant channel having caused an increased leak of Ca^{2+} from the SR and

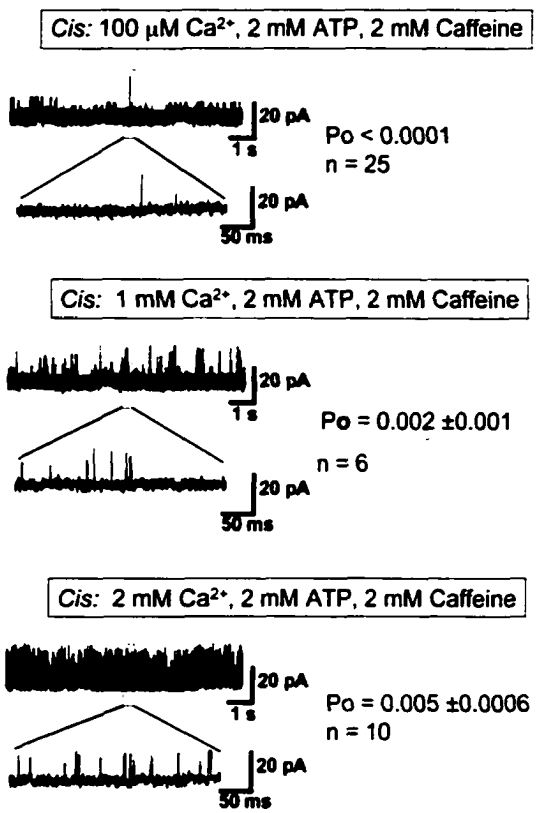

Figure 1.1: E4032A-RyR1 reconstituted into bilayer lipid membranes after expression in 1B5 myotubes is negligibly activated by physiological and pharmacological agonists of RyR1. Top panel: Of approximately 100 fusion events for E4032A-RyR1, 25 contained rare and very brief transitions to the open state that prevented calculation of P_o in the presence of cis 100 μM Ca^{2+}, 2 mM ATP, and 2 mM caffeine ($P_o < 0.0001$, $n = 25$). Middle panel: Increasing cis Ca^{2+} to 1 mM resulted in a measurable elevation in P_o ($P_o = 0.002 \pm 0.001$, $n = 6$). Bottom panel: In the presence of 2 mM Ca^{2+}, the average P_o determined for E4032A-RyR1 was 0.005 ± 0.0006 ($n = 10$).

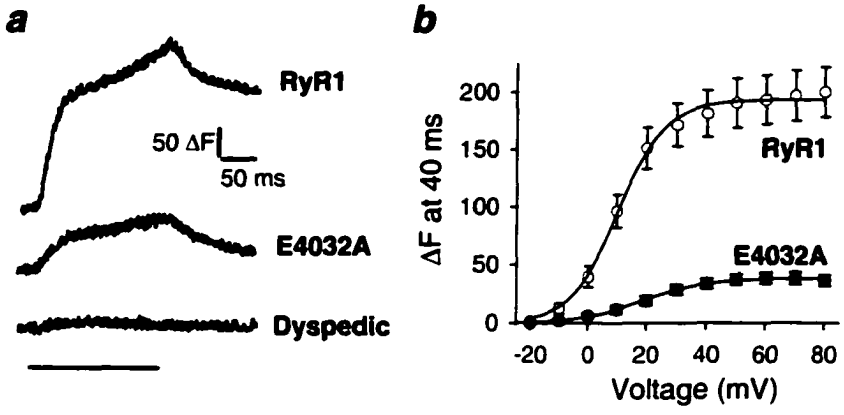

Figure 1.2: The mutation E4032A in RyR1 reduces depolarization induced Ca^{2+} release. (a) Representative Ca^{2+} transients (ΔF) from control dyspedic myotubes and dyspedic myotubes expressing E4032A-RyR1 or RyR1. The transients were elicited by a 200 ms depolarization to +40 mV (black bar). (b) Voltage dependence of the Ca^{2+} induced increase of fluorescence measured 40 ms after the onset of depolarization for E4032A-RyR1 (n = 28) and RyR1 (n = 27). Ca^{2+} transients were absent in dyspedic myotubes (n = 10; not shown). The smooth curves represent best-fits of the Boltzmann expression (Eq. 1.1) with values of k_F = 10.66 and 8.13 mV, and $V_{\frac{1}{2}}$ = 18.34 and 10.36 mV, for E4032A-RyR1 and wild-type RyR1, respectively.

thus a decreased quantity of Ca^{2+} available to be released. Thus, I assessed the SR Ca^{2+} content by means of the increase in myoplasmic Ca^{2+} that occurred after the addition of cyclopiazonic acid (CPA) to block the SR Ca^{2+} pump. These experiments were carried out on intact, Fluo-3AM loaded myotubes in order to maintain the cells in a state close to physiological. Fig. 1.3a illustrates a myotube expressing wild-type RyR1 which responded to the addition of CPA to the bath by a slow increase of myoplasmic Ca^{2+} that was associated with three rapid spikes of Ca^{2+} release. These spikes likely represent Ca^{2+} induced Ca^{2+} release and were typically observed in myotubes expressing wild-type RyR1 (5 of 6 cells examined). Since the spikes were larger than the peak of the slow Ca^{2+} increase, it is apparent that not all the Ca^{2+}

in the SR store is being released through leak in the presence of CPA. Such spikes were not observed when myotubes expressing E4032A-RyR1 were exposed to CPA, although these cells did display a slow increase of myoplasmic Ca^{2+} (Fig. 1.3a, lower trace). The data should be interpreted under the assumption that the initial decrease in fluorescence seen in the presence of CPA is probably due to photobleaching, since the cells were washed in Rodent Ringers prior to the wash-in of CPA and were exposed to fluorescent illumination for an extended period of time. The average amplitude of the slow Ca^{2+} leak in cells expressing wild-type RyR1 was similar ($p > 0.1$) to that of cells expressing E4032A-RyR1 (Fig. 1.3b), averaging 0.59 $\pm$ 0.11 $\Delta F/F$ ($n = 8$) and 0.78 $\pm$ 0.16 $\Delta F/F$ ($n = 6$), respectively. Therefore, it appears that the Ca^{2+} content of the SR in cells expressing E4032A-RyR1 does not differ from that of cells expressing wild-type RyR1.

The results above show that although E4032A-RyR1 does not release enough Ca^{2+} to mediate electrically evoked contractions, it does support depolarization evoked Ca^{2+} transients of small amplitude. To determine whether Ca^{2+} release via E4032A-RyR1 reflects skeletal-type EC coupling, Ca^{2+} transients were measured in individual cells for a test pulse to +40 mV immediately before and after addition of 0.5 mM Cd^{2+} and 0.1 mM La^{3+} (nonspecific Ca^{2+} channel blockers) to the bathing medium. This addition effectively blocked Ca^{2+} current (Fig. 1.4a, lower sets of traces), without altering the amplitude of the Ca^{2+} transients for either RyR1 or E4032A-RyR1 (Fig. 1.4a, upper set of traces; Fig. 1.4b). These results, together with the sigmoidal voltage dependence of the transients (Fig. 1.2b) imply that E4032A-RyR1 is able to mediate skeletal-type EC coupling.

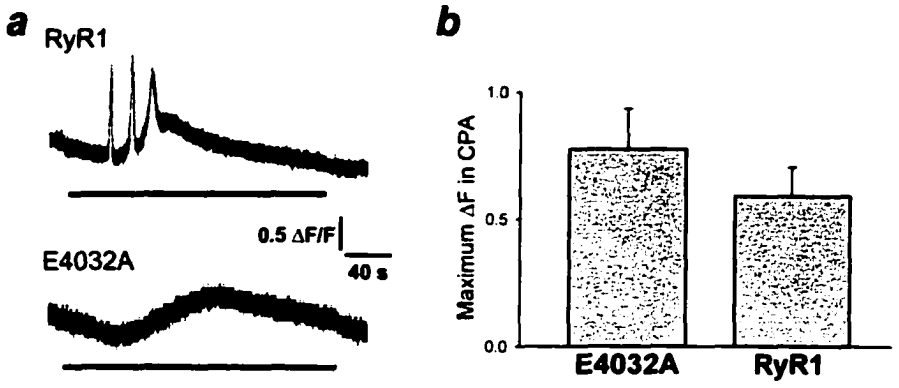

Figure 1.3: The SR Ca^{2+} content is similar in myotubes expressing E4032A-RyR1 or wild-type RyR1. (a) Response of Fluo-3AM loaded myotubes expressing either RyR1 (upper trace) or E4032A-RyR1 (lower trace) to block of the SR Ca^{2+} pump by cyclopiazonic acid (CPA). For both cells, there was a slow increase of myoplasmic Ca^{2+} in response to CPA. Three transient Ca^{2+} spikes occurred during the rising phase of this slow increase in the cell expressing wild-type RyR1. The horizontal bar beneath each trace indicates the period of exposure to CPA. (b) The average amplitude of the slow increase of myoplasmic Ca^{2+} for E4032A-RyR1 ($n = 8$) was not significantly different ($p > 0.1$) from that of RyR1 ($n = 6$). The amplitude for RyR1 expressing myotubes was estimated as the maximum deviation from baseline after the cessation of any Ca^{2+} spikes.

In addition to receiving the EC coupling signal from α_{1S}, RyR1 transmits a retrograde signal which acts to increase the magnitude of the L-type Ca^{2+} current produced by α_{1S} (Nakai et al., 1996). Figure 1.5 illustrates representative L-type Ca^{2+} currents (a) and average peak current versus voltage relationships (b) for dyspedic myotubes and myotubes expressing RyR1 or E4032A-RyR1. Although having similar voltage dependence, the peak currents differed considerably in magnitude for the three groups. At +30 mV, peak current density for E4032A-RyR1 (-6.53 ± 0.54 pA/pF, $n = 28$) was much larger ($p \ll 0.001$) than for dyspedic myotubes (-1.35 ± 0.30 pA/pF, $n = 10$), but not quite as large ($p < 0.005$) as for wild-type RyR1 (-10.11 ± 0.79 pA/pF, $n = 35$).

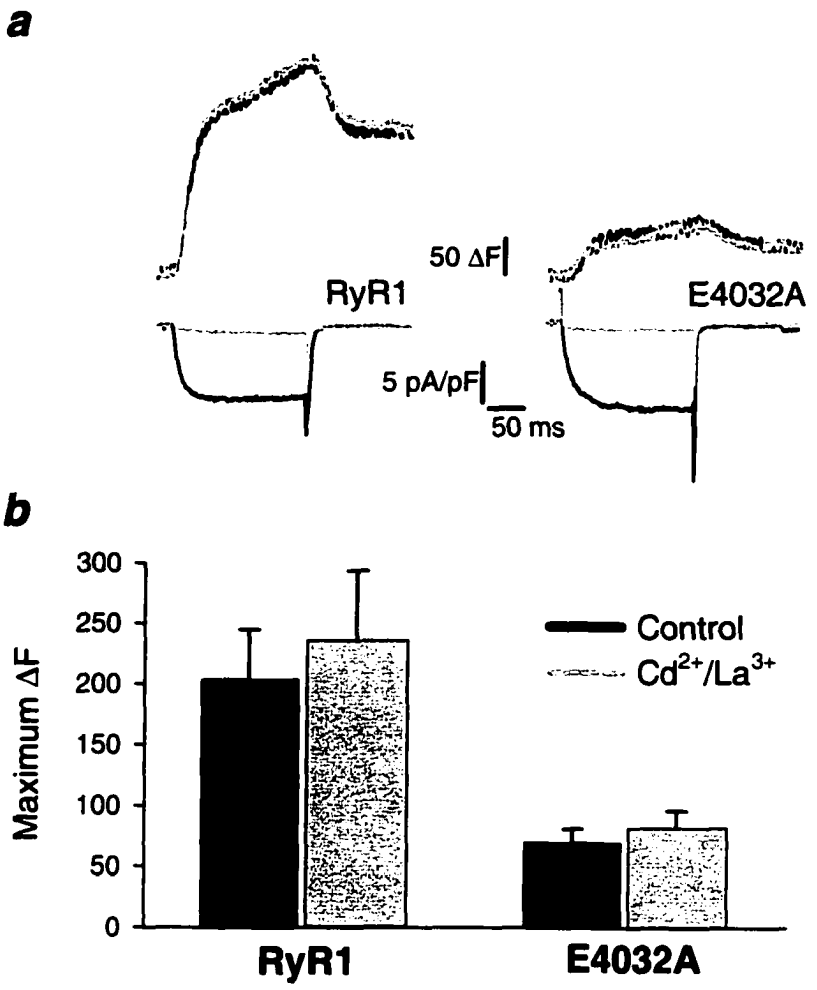

Figure 1.4: E4032A-RyR1 supports skeletal-type EC coupling. (a) Representative Ca^{2+} transients and Ca^{2+} currents recorded at +40 mV before (black) and after (gray) application of Cd^{2+} and La^{3+} to block Ca^{2+} entry. The transients before and after the block of Ca^{2+} current almost completely overlapped, indicating that, like RyR1, E4032A-RyR1 supports skeletal-type EC coupling. (b) Average Ca^{2+} transient amplitude at +40 mV was not significantly different before (black) and after (gray) application of Cd^{2+} and La^{3+} for either RyR1 ($n = 7$, $p > 0.5$) or E4032A-RyR1 ($n = 7$, $p > 0.5$).

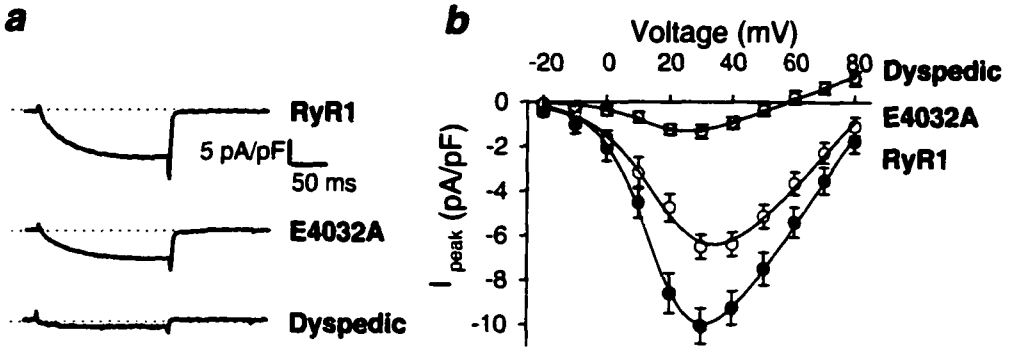

Figure 1.5: The E4032A mutation of RyR1 slightly impairs retrograde signaling. (a) Representative peak Ca^{2+} currents (at +20 mV) from control, E4032A-RyR1-expressing and RyR1-expressing dyspedic myotubes. (b) Average peak current versus voltage relationships for dyspedic myotubes (n = 10) and dyspedic myotubes expressing E4032A-RyR1 (n = 28) or RyR1 (n = 35).

Because caffeine is a potentiator of Ca^{2+} induced Ca^{2+} release (Meissner et al., 1997), it was of interest to determine whether caffeine affected depolarization evoked Ca^{2+} release via E4032A-RyR1. The application of 10 mM caffeine to myotubes at the holding potential caused a large release of Ca^{2+} in RyR1 expressing myotubes (113.36 $\pm$ 28.76 ΔF, n = 4) but caused no release in E4032A-RyR1 expressing myotubes (n = 7; Fig. 1.6a). This difference provides additional support for the idea that the E4032A mutation impairs Ca^{2+} activation. Despite having little effect on E4032A-RyR1 at the holding potential, 10 mM caffeine did cause a large increase in the amplitude of the depolarization induced Ca^{2+} transient (Fig. 1.6b), which on average was about 4-fold (ΔF increased from 20.6 $\pm$ 3.0 to 78.2 $\pm$ 12.4, n = 10, $p < 0.001$). In the presence of 10 mM caffeine, the ΔF versus voltage relationship for E4032A-RyR1 remained sigmoidal, although steeper and somewhat left shifted compared to control (Fig. 1.6c). Additionally, caffeine increased the initial rate of

rise of the Ca^{2+} transient in E4032A-RyR1 expressing cells from 0.81 ± 0.13 to 3.25 ± 0.58 ΔF/ms ($n = 10$, $p \ll 0.001$).

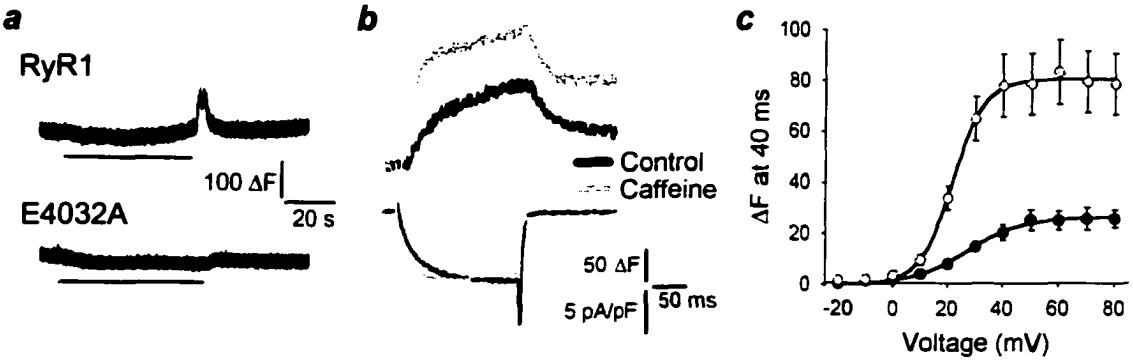

Figure 1.6: Caffeine enhances depolarization induced Ca^{2+} release for E4032A-RyR1. (a) Caffeine (10 mM) causes Ca^{2+} release from RyR1 expressing myotubes at the holding potential (−80 mV), but not from myotubes expressing E4032A-RyR1. Similar responses were obtained from a total of 8 cells expressing E4032A-RyR1 ($\Delta F = 0$) and 4 cells expressing RyR1 ($\Delta F = 113.36 \pm 28.76$). Bath perfusion (horizontal bar) was used to introduce 10 mM caffeine which then remained for the duration of the experiment. (b) Representative Ca^{2+} transients (top) and Ca^{2+} currents (bottom) at +40 mV before (black) and after (gray) the application of 10 mM caffeine. (c) Voltage dependence of the Ca^{2+} transients measured in E4032A-RyR1 expressing myotubes before and after application of 10 mM caffeine ($n = 10$). The data has been fitted with Eq. 1.1 as shown by the smooth curve. The values for k_F are 9.87 and 5.89 mV and for $V_{\frac{1}{2}}$ are 27.13 and 21.69 mV before and after caffeine was applied.

In addition to increasing the amplitude of the Ca^{2+} transient in myotubes expressing E4032A-RyR1, the application of 10 mM caffeine also caused the half-rise time for activation of Ca^{2+} current to decrease from 23.4 ± 2.2 ms to 11.6 ± 0.6 ms ($n = 10$, $p < 0.001$). The effect of caffeine on the rate of activation of Ca^{2+} current appeared to be unrelated to its effect on Ca^{2+} release. First, the half-rise time for activation of Ca^{2+} current in the absence of caffeine was similar ($p > 0.15$) in cells expressing wild-type RyR1 (18.1 ± 1.3 ms, $n = 35$) to that in cells expressing E4032A-RyR1 (21.2 ± 1.7 ms, $n = 28$), despite the fact that Ca^{2+} release flux was several-fold

lower for E4032A-RyR1 (see above). Second, 10 mM caffeine caused half-rise times for Ca^{2+} current in four cells expressing wild-type RyR1 to decrease from 18.0 ± 2.0 ms to 10.3 ± 0.3 ms, despite causing a reduction in the amount of calcium released (maximum ΔF fell from 355.3 ± 60.5 to 139.3 ± 52.9, presumably because the caffeine caused a loss of Ca^{2+} from the SR).

1.4 Discussion

In this paper, we have characterized the consequences of the mutation E4032A on the function of RyR1. Expression in 1B5 dyspedic myotubes followed by reconstitution into planar lipid bilayers demonstrated that E4032A-RyR1 is not appreciably activated by Ca^{2+}, even when the additional strong activators caffeine and ATP are also present. Expression in primary dyspedic myotubes followed by whole-cell measurements showed that the E4032A mutation reduced depolarization induced Ca^{2+} release about 5-fold, as compared to wild-type RyR1, and as a result impaired the ability of RyR1 to mediate EC coupling. This reduction did not appear to be secondary to a reduction in the SR Ca^{2+} content which appeared to be similar for cells expressing E4032A- and wild-type RyR1 based on the increase in myoplasmic Ca^{2+} that occurred after the addition of CPA. The Ca^{2+} release that did occur for E4032A-RyR1 appeared to reflect skeletal-type EC coupling both because its amplitude showed a sigmoidal voltage dependence and because it persisted after the addition of extracellular Cd^{2+} and La^{3+} to block Ca^{2+} influx. In addition to being

able to mediate EC coupling (at a reduced level), E4032A-RyR1 was also able to cause retrograde enhancement of L-type Ca^{2+} current via α_{1S}. Compared to control dyspedic cells, the L-current density was ~5-fold larger for E4032A-RyR1 expressing myotubes, a retrograde enhancement somewhat smaller than that found for wild-type RyR1 (7.5-fold).

The results reported here raise the question of whether there is a direct relationship between activation of RyR1 by α_{1S} (in response to depolarization) and the activation of RyR1 by Ca^{2+}. Figure 1.7 illustrates two extreme possibilities for the relationship between the two modes of activation. In scheme (1), the two modes of activation are completely independent, whereas in scheme (2) the only function of the α_{1S} is to lower the threshold for activation by Ca^{2+} such that resting Ca^{2+} is sufficient to cause activation. Scheme (2) can be viewed as the converse of the proposal that α_{1S} functions to raise the threshold for the inhibition of RyR1 by Mg^{2+} (Lamb and Stephenson, 1991, 1994). If scheme (1) were correct, it might be possible to abolish activation by Ca^{2+} without any effect on depolarization induced Ca^{2+} release. If scheme (2) were correct, then eliminating activation by Ca^{2+} would also abolish activation by α_{1S}. An argument against scheme (2) is that the E4032A mutation does not abolish depolarization induced Ca^{2+} release, although one could argue that E4032A-RyR1 has sufficient residual Ca^{2+} sensitivity to support a reduced level of depolarization induced release. However, the effect of the mutation on depolarization induced release is trivial compared to its effect on Ca^{2+} activation. Specifically, the bilayer experiments indicate that the E4032A mutation depressed activation by Ca^{2+} by more than 100-fold, whereas the reduction in depolarization induced release was

only 5-fold. Thus, it seems unlikely that Ca^{2+} activation plays an obligatory role in depolarization induced release.

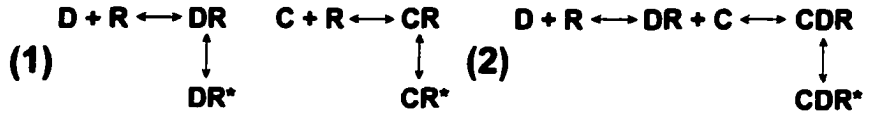

Figure 1.7: Two schemes indicating pathways for activation of RyR1 (R), with horizontal arrows indicating reversible binding steps, and vertical arrows indicating conformation changes that convert RyR1 to the active state, indicated by the asterisk (*). According to scheme (1), depolarization causes a domain of the α_{1S} (D, possibly the II-III loop) to bind to and activate RyR1 independently of the activation occurring in response to Ca^{2+} (C). In scheme (2), the binding of D cannot by itself induce activation, which requires Ca^{2+}. Specifically, the binding of D increases the affinity of RyR1 for Ca^{2+} so that the threshold for activation is below that of the resting myoplasmic concentration.

Because the E4032A mutation affects activation of RyR1 both by depolarization (as shown in myotubes) and by Ca^{2+} (as shown in bilayers), it is possible that the two activation pathways interact with one another in intact cells. Such an interaction could take place either in the same ryanodine receptor molecule or between different ryanodine receptor molecules. In the latter case, for example, the Ca^{2+} initially released from some ryanodine receptors in response to depolarization could induce release from adjacent ryanodine receptors via Ca^{2+} activation (Rios and Pizarro, 1991; Schneider, 1994). Put another way, ΣCa^{2+} = VGCR + CICR, where ΣCa^{2+} is the total amount of Ca^{2+} released by depolarization, part of which is from ryanodine receptors activated directly by DHPRs (VGCR) and part from ryanodine receptors secondarily activated by Ca^{2+} (Rios and Pizarro, 1991; Schneider, 1994). Accordingly, the interpretation of the 5-fold reduction in depolarization induced Ca^{2+} release in myotubes expressing E4032A-RyR1 depends on knowing whether the mutation affects

only CICR. If this were the case, one would conclude that CICR is responsible for the bulk of total Ca^{2+} release and that VGCR contributes only a relatively small fraction (~20%). Alternatively, it is common that synergistic interactions occur between ligands that activate an allosteric protein; that is, activation of a single ryanodine receptor by depolarization would be potentiated by Ca^{2+}, and activation of an ryanodine receptor by Ca^{2+} would be potentiated by depolarization. Thus, a mutation which depressed CICR might well be expected to depress VGCR as well. However, even if the two activation pathways were completely independent, there is no reason why the E4032A mutation could not affect both.

Caffeine is widely thought to act on ryanodine receptors by reducing the threshold for activation by Ca^{2+} (e.g. Meissner et al., 1997). Thus, it is of interest that the application of 10 mM caffeine caused a ~4-fold augmentation in the depolarization evoked release of Ca^{2+} by E4032A-RyR1 without having any discernible effect at the holding potential. This augmentation seems difficult to explain if the only effect of caffeine is on the Ca^{2+}-activation threshold. In bilayers, Ca^{2+} caused minimal activation of E4032A-RyR1, even when 2 mM caffeine was present (Fig. 1.1). Thus, rather than simply shifting the apparent Ca^{2+}-activation threshold by enhancing the binding affinity of the activator site for Ca^{2+}, caffeine may have the more general effect on ryanodine receptors of reducing the energy of channel activation and shifting the equilibrium toward the open state.

A limitation in our comparison of the properties of wild-type RyR1 and E4032A-RyR1 is that we have no independent measure of the expression level or junctional targeting of the mutant protein. However, it seems unlikely that expression or targeting

is significantly altered since E4032A-RyR1 caused a substantial increase in the amplitude of L-type Ca^{2+} current compared to that in uninjected dyspedic cells. This result suggests that E4032A-RyR1 is expressed at a level similar to that of RyR1 and is like RyR1 in being able to increase the magnitude of current normalized by the number of α_{1S} subunits in the plasma membrane (Nakai et al., 1996; Avila et al., 2001). Avila et al. (2001) also found that retrograde signaling by E4032A-RyR1 was similar to that of RyR1, although E4032A-RyR1 lacked the ability to cause an up-regulation of the number of α_{1S} subunits in the plasma membrane that occurs on the time scale of several days. Because E4032A-RyR1 was able to mediate retrograde enhancement of Ca^{2+} current despite a greatly reduced orthograde signaling (EC coupling), it suggests that the two processes are not tightly linked. Further support for this idea is that caffeine caused a large increase in depolarization induced Ca^{2+} release by E4032A-RyR1 without much effect on the amplitude of L-type current (Fig. 1.6). Thus, it does not seem likely that Ca^{2+} release is the signal for retrograde enhancement of L-type current.

The depression of Ca^{2+} activation by the E4032A mutation could mean that the mutation directly affects the Ca^{2+} binding site for activation (Chen et al., 1998; Li and Chen, 2001). An alternative possibility is that the E4032A mutation induces a folding error which impairs channel opening conformation changes (Fessenden et al., 2001). According to this latter interpretation, calcium would be less effective at overcoming the impairment of channel opening than would orthograde activation via the DHPR and this orthograde activation would be directly potentiated by caffeine. However, no matter which interpretation is correct, the essential conclusion from our

work is that Ca^{2+} activation of RyR1 is not essential for the initiation of skeletal-type EC coupling.

Chapter 2

A Region In RyR1 That Interacts With the α_{1S} II-III Loop In Yeast Two-Hybrid Plays a Functional Role In Skeletal-type EC Coupling

This work has been published (*Journal of Biological Chemistry* 2002. 277:6530–5) with the following authors: Catherine Proenza[‡], Jennifer J. O'Brien[†], Junichi Nakai[‡], Santwana Mukherjee[§], Paul D. Allen[§], and Kurt G. Beam[†]. I have rewritten the paper to focus only on the experiments I have performed and to include the preliminary data from studies with the Mac-Chimera. When discussing the yeast two-hybrid experiments that were included in the original paper, I referenced Catherine Proenza's dissertation. Junichi Nakai from Kurt G. Beam's lab made R16-Chimera, Santwana Mukherjee from Paul D. Allen's lab made R16-RevChimera, and David H. MacLennan's[¶] lab made Mac-Chimera.

[‡]Dept. of Physiology, Colorado State University, Fort Collins, CO 80523
[†]Dept. of Anatomy and Neurobiology Colorado State University, Fort Collins, CO 80523
[§]Department of Anesthesia, Brigham & Women's Hospital, Boston, MA 02115
[¶]Banting and Best Dept. of Medical Research, University of Toronto, Toronto, Ontario M5G 1L6, Canada

2.1 Introduction

Excitation-contraction coupling in muscle cells is the conversion of the depolarization of the plasma membrane to contraction of the muscle fiber. This conversion is mediated by the communication between the DHPR, an L-type voltage-gated Ca^{2+} channel in the t-tubule membrane, and the ryanodine receptor, a Ca^{2+} activated Ca^{2+} release channel in the SR membrane. EC coupling in cardiac muscle cells involves activation of the cardiac isoform of the ryanodine receptor, RyR2, by Ca^{2+} entry through the α_{1C} subunit of the DHPR. Alternatively, EC coupling in skeletal muscle cells is not dependent on the influx of Ca^{2+} via the α_{1S} subunit of the DHPR to activate the skeletal isoform of the ryanodine receptor, RyR1. In this case, DHPRs align with the RyR1s in the opposing membrane and communicate via protein-protein interaction either directly with RyR1 or via an intermediary protein. In addition, the presence of RyR1 serves to enhance the size of the α_{1S} Ca^{2+} currents thus implicating a bi-directional signal between the receptors.

Potential regions of interaction between these two receptors have been elucidated. Expression of chimeras, made with regions of α_{1S} replacing the corresponding region of α_{1C}, in dysgenic myotubes that lack endogenous α_{1S}, has shown that the cytoplasmic loop between repeats II and III of α_{1S}, specifically amino acids 720–765, is essential for the occurrence of skeletal-type EC coupling (Nakai et al., 1998b; Grabner et al., 1999; Tanabe et al., 1990a). Similarly, the complementary, putative region of functional interaction on RyR1 was determined using chimeras between RyR1 and RyR2. The region R10, skeletal sequence 1635–2636, was able to confer skeletal-type

function onto RyR2 whereas the region R9, skeletal sequence 2659–3720, was only able to restore retrograde signaling (Nakai et al., 1998a). Though functionally important, if these regions of α_{1S} and RyR1 interact directly to mediate bi-directional communication has not been confirmed.

Use of peptide binding and biochemical assays has led to varying results in the identification of the putative regions of interaction between α_{1S} and RyR1. In contrast to the chimera work, the peptide of amino acids 671–690 in the α_{1S} II-III loop (peptide A) has been shown to activate RyR1 (El Hayek et al., 1995; Dulhunty et al., 1999). In RyR1, the sequence 922–1112 was found to bind to the α_{1S} II-III loop in an affinity column whereas the corresponding region 933–1126 of RyR2 was not (Leong and MacLennan, 1998). An interaction between the α_{1S} II-III loop segment 719–767 and the RyR1 segment sR16, 1837–2168, was detected in yeast two-hybrid experiments (Proenza, 1999). Interestingly, much less reaction took place between α_{1S} 719–767 and cR16, the corresponding cardiac region to sR16, and no interaction was detected between the segment encompassing the peptide A region and sR16 or other segments of R9 and R10 (Proenza, 1999). Of note, one of three highly divergent regions between RyR1 and RyR2 sequence (D3) lies within sR16 (Sorrentino and Volpe, 1993). The relative positions of the potentially important regions in RyR1 described above are mapped to the RyR1 amino acid sequence in Figure 3 on page 17. These results from the different binding assays suggest that either pair of strong interactors described above may play key roles in mediating skeletal-type EC coupling.

Since few tests have been done in actual muscle fibers to confirm the physiological importance of the varied putative regions of interaction, it has not been

determined which regions are necessary for skeletal-type EC coupling or other functional interactions between α_{1S} and RyR1. In this study, I have expressed chimeras of RyR1 and RyR2 in dyspedic myotubes to determine whether or not the biochemically active regions sR16 and 922–1112 are necessary and sufficient to support skeletal-type EC coupling. Analysis of electrically evoked contractions and whole cell patch clamping paired with simultaneous cytoplasmic Ca^{2+} measurements suggests that sR16 plays a role in skeletal-type EC coupling while the region 922–1112 does not. From these data it remains unclear if there are other roles for these regions or if multiple regions act in concert to fully control skeletal-type coupling.

2.2 Experimental procedures

2.2.1 Preparation of chimeras

R16-Chimera, with the amino acid sequence 1–1817 of RyR2, 1837–2154 of RyR1, 2118–4968 of RyR2, was constructed in the pCDNA3 vector by Junichi Nakai. Hence, the region 1837–2154 of RyR1 (sR16) replaced the corresponding region in RyR2, 1817–2154 (roughly cR16 which was 1816–2142) within a background sequence of RyR2. The inversion of this chimera, R16-RevChimera which contained amino acids 1–1645 of RyR1, 1636–2121 of RyR2, and 2158–5037 of RyR1, was created in Paul Allen's lab by Santwana Mukherjee. Members of the MacLennan lab constructed the chimera, Mac-Chimera, which is made up of amino acids 1–922 of RyR1, 933–1126 of RyR2, 1112–5037 of RyR1. The control receptor sequences, RyR2 and RyR1, were incorporated into the pCIneo vector (Nakai et al., 1997, 1998a).

2.2.2 Primary culture and microinjection of cDNA

The dyspedic myotube cultures were prepared as described in Section 1.2.3 on page 26. Seven to eight days following plating of the myotubes, 0.3 $\mu g/\mu L$ of the cDNA construct of interest was coinjected with either 0.04 $\mu g/\mu L$ GFP (for contraction data) or 0.2 $\mu g/\mu L$ CD8 antigen cDNA (for physiology experiments) into a single nuclei of each dyspedic myotube. As before, the cells incubated 48 hr to allow for expression of the injected proteins before performing experiments.

2.2.3 Electrically evoked contractions, whole cell patch clamp and Ca^{2+} measurements

Contractions were measured as described in Section 1.2.3 on page 26, except the bath solutions used were Ca^{2+}-free Rodent Ringers (in mM: 145 NaCl, 10 HEPES, 5 KCl, 3 $MgCl_2$, pH 7.4) and Cd^{2+} plus La^{3+} Rodent Ringers (145 NaCl, 10 HEPES, 5 KCl, 2 $CaCl_2$, 1 $MgCl_2$, 0.5 $CdCl_2$, 0.1 $LaCl_3$). The latter solution was only used with cells expressing R16-RevChimera.

Simultaneous measurement of the whole cell Ca^{2+} currents and intracellular Ca^{2+} levels were performed as described in Section 1.2.4 on page 27. Due to the contamination of Ca^{2+} currents from T-type channels, despite the use of the 1 sec prepulse, the maximum amplitude of each Ca^{2+} current trace was measured after 150 ms into the 200 ms test pulse. This did not affect the RyR1 data since the maximum amplitudes of each current trace occurred near the end of the test pulse. In addition, the maximum amplitude of each Ca^{2+} transient was measured at its true maximum for the entire 200 ms test pulse, not at time 40 ms into the pulse as

was described in Section 1.2.4. Cells with measured capacitance above 800 pF were eliminated from analysis because they were too large to maintain a reliable voltage clamp. All measurements not mentioned, solutions, and analyses were not changed from those described previously.

2.2.4 Analysis of Mac-Chimera

All data collected after the acquisition of the data from RyR1, RyR2, R16-Chimera and R16-RevChimera expressing myotubes (Mac-Chimera) and comparisons to that data (RyR1) were measured as $\Delta F/F$ where the baseline was recorded from that preceding the first voltage step and used for all the voltage steps within a run (-20 to $+80$ mV). This method compensates for the increases in the baseline fluorescence described in Section 1.2.6 on page 29.

2.3 Results

2.3.1 R16-Chimera

The region sR16 of RyR1 has been shown to interact with a region of the α_{1S} II-III loop, but neither the complete protein in its natural tertiary structural form nor physiological conditions in which these regions would normally associate were used in these experiments (Proenza, 1999). For the following experiments, a chimeric receptor was used in which the region 1837–2154 was inserted into RyR2 and the corresponding region of RyR2, 1817–2118, was removed. Due to cloning limitations, the swapped regions do not exactly correspond to sR16, 1837–2168, nor cR16, 1819–2142, yet high sequence conservation in that region leaves only a difference of three

amino acids (RyR1 to RyR2: E2157A, C2158S, and I2167S). The chimeric receptor R16-Chimera was expressed in dyspedic myotubes which are null for RyR1. To test if myotubes expressing R16-Chimera could support skeletal-type EC coupling, the myotubes were electrically stimulated in the absence of extracellular Ca^{2+} (Ca^{2+}-free Rodent Ringers). R16-Chimera expressing cells exhibited frequent spontaneous contractions as previously described for RyR2 (Nakai et al., 1997) and other chimeras with RyR2 background sequence (Nakai et al., 1998a) making it difficult to determine whether or not electrical stimulation was eliciting observable contractions. Three out of a total of 30 R16-Chimera expressing myotubes tested contracted with stimulation whereas none of the wild-type RyR2 expressing cells (out of 33) contracted (Fig. 2.1). Almost all wild-type RyR1 expressing myotubes (10 out of 13) were able to contract with stimulation, suggesting that the R16-Chimera is only able to mediate weak skeletal-type EC coupling.

Since only a few cells were able to support observable skeletal-type EC coupling, it is possible that the level of Ca^{2+} being released in response to depolarization is larger than that of RyR2 but lower than the threshold required to trigger a full contraction. Indeed, depolarization evoked Ca^{2+} transients displayed an intermediary response between that of wild-type RyR1 and wild-type RyR2. Amplitudes of the Ca^{2+} transients measured from myotubes expressing R16-Chimera before and after the addition of Cd^{2+} and La^{3+} to the bath solution were not equal as seen with wild-type RyR1, rather, the responses varied enough to justify classifying them into two categories (Fig. 2.2a). The skeletal-like category encompasses the 80% ($n = 10$) of the R16-Chimera expressing myotubes that had measurable Ca^{2+} transients in

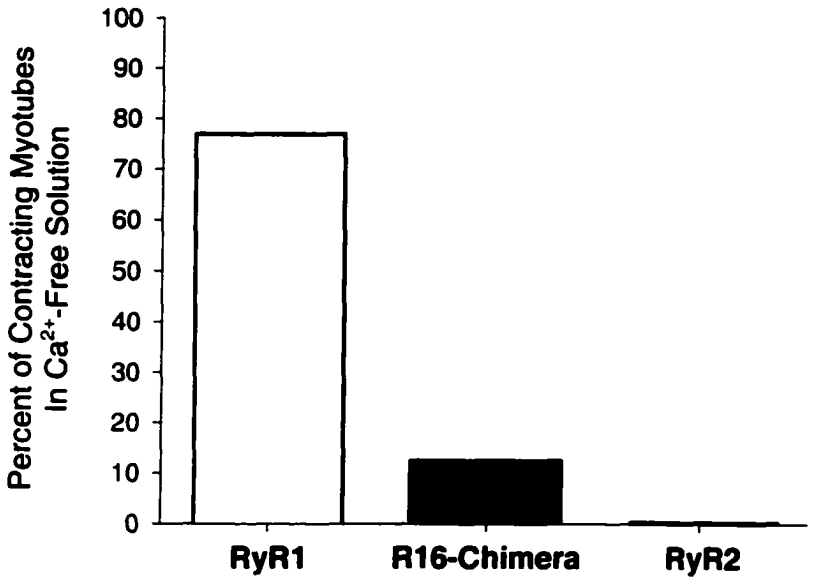

Figure 2.1: R16-Chimera supports weak skeletal-type excitation-contraction coupling. Wild-type RyR1 (n = 33), R16-Chimera (n = 30), and wild-type RyR2 (n = 13) expressing dyspedic myotubes were bathed in Ca^{2+} free Rodent Ringers and tested for their ability to support electrically evoked contractions. The number of myotubes that contracted in these conditions were recorded as a percentage of the total number of expressing cells tested.

the presence of Cd^{2+} and La^{3+}, three of which had equal Ca^{2+} transient amplitudes relative to that of their control conditions. The other 20% were grouped into the cardiac-like category in which the Ca^{2+} transients were eliminated by the block of Ca^{2+} influx via α_{1S}. Overall, the amplitudes of the R16-Chimera Ca^{2+} transients in the presence of Cd^{2+} and La^{3+} were 67.2 $\pm$ 8.0% of Ca^{2+} transients of the same cell in control conditions. Further evidence that R16-Chimera is able to support a weak level of skeletal-type EC coupling was found in the sigmoidal voltage dependence of the Ca^{2+} transient amplitudes like that of wild-type RyR1 (Fig. 2.2b). Despite the similarity in voltage dependence, the Ca^{2+} transients measured at +30 mV with the

R16-Chimera (45.0 ± 10.4 ΔF, $n = 22$) were significantly smaller ($p < 10^{-8}$) than those with wild-type RyR1 (312.0 ± 31.7 ΔF, $n = 29$), but they were significantly larger ($p < 0.05$) than those with wild-type RyR2 (6.6 ± 6.6 ΔF, $n = 10$). Thus, R16-Chimera is able to support a greater degree of skeletal-type EC coupling function than wild-type RyR2.

Both the orthograde EC coupling signal and the retrograde Ca^{2+} current enhancement signal have been shown to be mediated by the same amino acid domain in α_{1S} (Nakai et al., 1998b; Grabner et al., 1999). To determine if this is also true with RyR1, I analyzed the Ca^{2+} currents in myotubes expressing R16-Chimera. On average, the maximal Ca^{2+} current density measured at the peak voltage was -4.04 ± 0.44 pA/pF ($n = 33$) for cells expressing R16-Chimera (Fig. 2.2c). This result was significantly smaller ($p < 10^{-10}$) than that of wild-type RyR1 expressing cells (-10.02 ± 0.79 pA/pF, $n = 35$) but was similar to that of wild-type RyR2 (-3.11 ± 0.56 pA/pF, $n = 10$, $p > 0.1$). From these data, it appears that R16-Chimera is unable to support retrograde signaling to α_{1S}.

2.3.2 R16-RevChimera

If the sR16 region of RyR1 is necessary and not only sufficient (as shown) for maintaining skeletal-type EC coupling, then removal of this region should eliminate all skeletal-type function from RyR1. Amino acids 1645–2154 were removed from RyR1 by substituting them with the corresponding region of RyR2 (1637–2118). The resulting chimera (R16-RevChimera) was not the exact reverse of R16-Chimera; 179 adjacent residues, 1637–1816, in addition to cR16 were replaced into the larger and

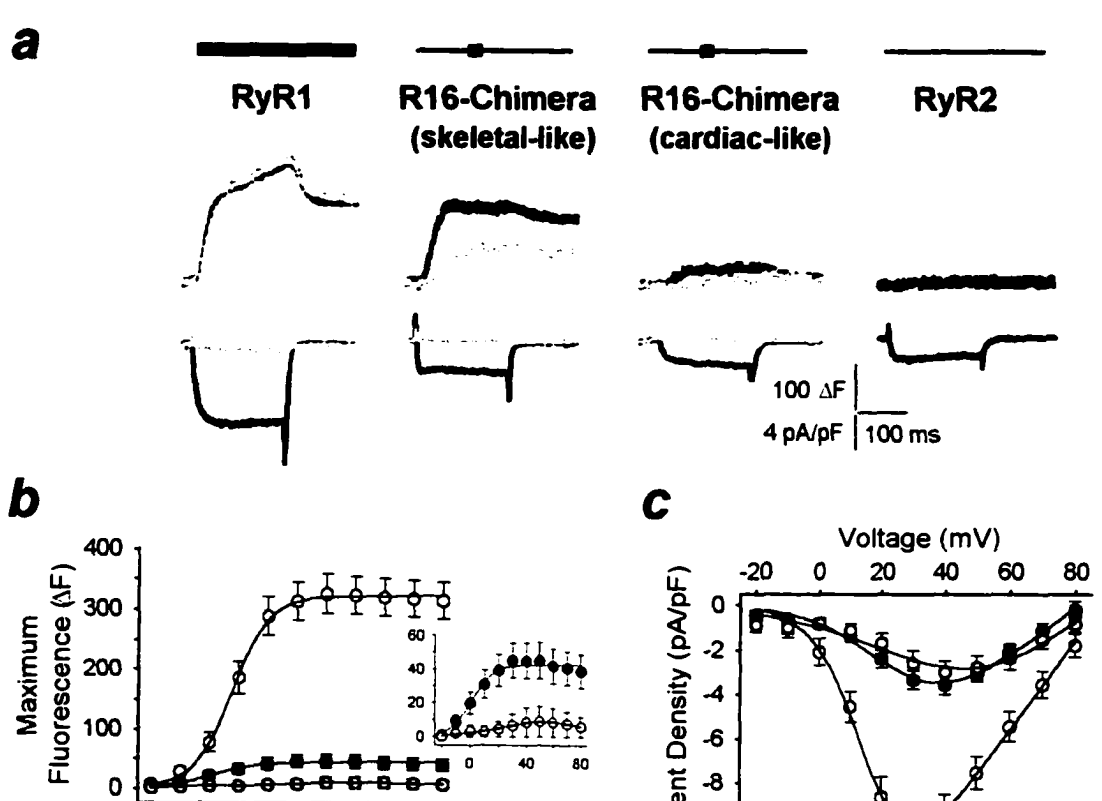

Figure 2.2: There is a gain of function with R16-Chimera over that of wild-type RyR2 but not to the level of wild-type RyR1. (a) The lines above the traces represent the RyR1 portion (thick lines) and the RyR2 portion (thin lines) of the amino acid sequence of each construct. Representative Ca^{2+} currents taken at +40 mV (bottom traces, black) were blocked by bath application of 0.5 mM Cd^{2+} and 0.1 mM La^{3+} (bottom traces, gray) in wild-type RyR1, R16-Chimera and wild-type RyR2 expressing myotubes (left to right). The corresponding Ca^{2+} transients elicited during the test pulse are shown in the top traces (control is black, in Cd^{2+} and La^{3+} is gray). Due to the range of responses seen with R16-Chimera, the traces were grouped into skeletal-like and cardiac-like as described in Section 2.3.1. (b) Average depolarization induced Ca^{2+} transient amplitudes for wild-type RyR1 (white circles, $n = 29$), R16-Chimera (black circles, $n = 22$), and wild-type RyR2 (gray circles, $n = 10$) expressing myotubes in the control external solution are shown in the graph. The inset shows an enlargement of the R16-Chimera and RyR2 data to emphasize the sigmoidal shape of the voltage dependence of R16-Chimera in comparison to the bell-shaped dependence of RyR2. (c) The average Ca^{2+} current density-voltage relationships are shown for wild-type RyR1 (white circles, $n = 35$), R16-Chimera (black circles, $n = 33$), and wild-type RyR2 (gray circles, $n = 10$).

still corresponding region of RyR1. Expression of R16-RevChimera fully restored skeletal-type EC coupling in dyspedic myotubes. Depolarization induced Ca^{2+} transients seen with R16-RevChimera were not affected by the block of Ca^{2+} currents via α_{1S} by Cd^{2+} and La^{3+} (Fig. 2.3a). In addition, both the amplitudes of the Ca^{2+} transients seen with R16-RevChimera (336.7 ± 63.8 ΔF, $n = 6$) and the voltage dependence of these transients (sigmoidal) were equivalent to that of wild-type RyR1 (see above and Fig. 2.3b top graph). Similarly, R16-RevChimera enhanced the Ca^{2+} currents (-11.24 ± 2.47 pA/pF, $n = 6$) to the level of wild-type RyR1 (Fig. 2.3b bottom graph). These data support the idea that sR16 is not necessary for skeletal-type function.

2.3.3 Mac-Chimera

To test the functional significance of the biochemically interactive region 922–1112 of RyR1, I used a chimera in which the corresponding region 933–1126 of RyR2 replaced 922–1112 in RyR1 (Mac-Chimera). Of the myotubes expressing Mac-Chimera ($n = 26$), 69.2% contracted with electrical stimulation while in media (~2 mM Ca^{2+}) compared to 100% of myotubes expressing RyR1 ($n = 13$). Skeletal-type EC coupling was not eliminated in Mac-Chimera as demonstrated by the 47.1% of the Mac-Chimera expressing cells ($n = 17$) that supported electrically evoked contractions while bathed in Cd^{2+} and La^{3+} containing Rodent Ringers solution. The percentage is smaller than that seen with RyR1 in Ca^{2+}-free solution (76.9%, see above). Interpretations should be made under consideration that the data for the chimera in Cd^{2+} and La^{3+} was collected from a single culture that may have had cells

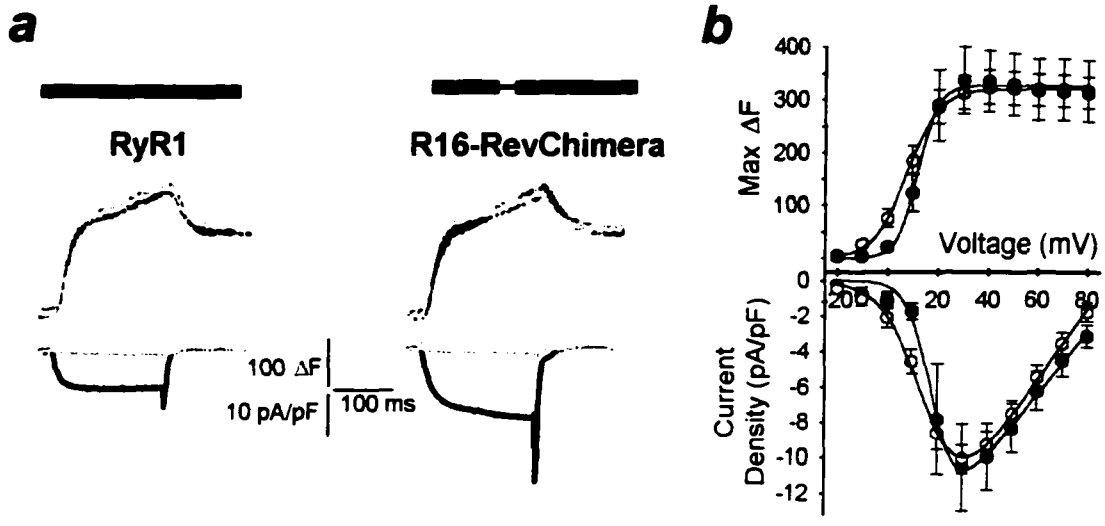

Figure 2.3: R16-RevChimera has no effect on skeletal-type EC coupling in myotubes. (a) The lines above the traces show the RyR1 (thick lines) and RyR2 (thin lines) amino acid sequences used to create the constructs. Representative Ca^{2+} currents (bottom traces) and Ca^{2+} transients (top traces) at +50 mV are shown from wild-type RyR1 and R16-RevChimera expressing myotubes. The black traces are data recorded from the cell in control conditions and the gray traces are data recorded in the presence of 0.5 mM Cd^{2+} and 0.1 mM La^{3+}. (b) The average depolarization induced Ca^{2+} transient amplitudes for both wild-type RyR1 (white circles, $n = 29$) and R16-RevChimera (black circles, $n = 6$) are similar at all voltage potentials. (c) Likewise, the Ca^{2+} current densities, displayed by the current-voltage relationships, for wild-type RyR1 (white circles, $n = 35$) and R16-RevChimera (black circles, $n = 6$) were equivalent on average.

that were less robust, more covered in fibroblasts, or more tightly bound to the dish than the previous cultures used. Due to this fact, it is likely that this limited sample may not have been truly representative.

Results from the electrophysiological experiments support the data from the contraction experiments. In myotubes expressing Mac-Chimera, the Ca^{2+} transients recorded at +40 mV were smaller (0.81 $\pm$ 0.26 $\Delta F/F$, $n = 3$) than those of wild-type RyR1 (4.35 $\pm$ 0.79 $\Delta F/F$, $n = 24$), but they maintained a sigmoidal voltage

dependence characteristic of RyR1 and were significantly larger than those of wild-type RyR2 (0.06 ± 0.06 $\Delta F/F$, $n = 10$; Fig. 2.4a). No statistics were performed due to the extremely small sample size of the Mac-Chimera data (error bars were included for illustrative purposes). To demonstrate that there is no contribution of Ca^{2+} influx via α_{1S} or CICR to the amplitude of the Ca^{2+} transients, the Ca^{2+} transients in the presence of Cd^{2+} and La^{3+} were measured. Blocking Ca^{2+} influx did not affect the amplitude of the Ca^{2+} transients (Fig. 2.4b), further supporting the ideas that (despite the small amplitude of the Ca^{2+} transients) the Ca^{2+} transients are caused by Ca^{2+} efflux and skeletal-type EC coupling is not eliminated by the chimera. The retrograde signal is not being transmitted via the 922–1112 region as shown by the similarity ($p > 0.5$) of the voltage dependence and the average amplitude at +30 mV of the Ca^{2+} currents in both Mac-Chimera (−14.56 ± 3.20 pA/pF, $n = 10$) and wild-type RyR1 (−14.12 ± 1.51 pA/pF, $n = 41$) expressing cells and the difference ($p \ll 0.001$) from wild-type RyR2 (−2.60 ± 0.59 pA/pF, $n = 10$; Fig. 2.4c).

2.4 Discussion

In this study, I described the role in skeletal-type EC coupling of regions of RyR1 that were thought to be important in the potential interaction between the DHPR α_{1S} subunit II-III loop and RyR1. It is apparent from the data that the two regions studied, sR16 and 922–1112, are not the amino acid sequences unique to RyR1 necessary for mediating skeletal-type EC coupling. Yet, these two regions appear to play a role in the function of RyR1; that is, sR16 is able to transfer weak skeletal-type

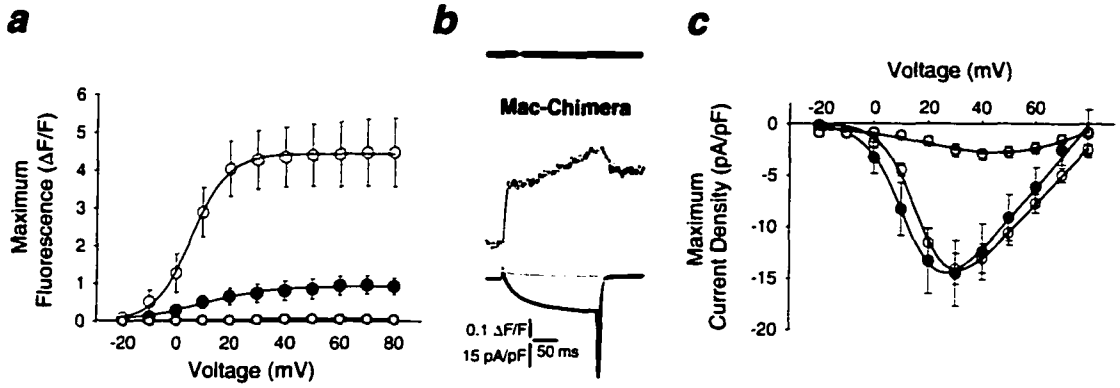

Figure 2.4: The chimera, Mac-Chimera, supports skeletal-type excitation contraction coupling despite a potential impairment of its Ca^{2+} release function. (a) Average maximal amplitudes of the depolarization induced Ca^{2+} transients are shown for Mac-Chimera expressing myotubes (black circles, $n = 3$), wild-type RyR1 expressing cells (white circles, $n = 24$), and wild-type RyR2 expressing cells (gray circles, $n = 10$). *Note*: The fluorescence data were measured in $\Delta F/F$ units versus ΔF units as in the previous figures. (b) Representative Ca^{2+} transients (top traces) and Ca^{2+} currents (bottom traces) from a Mac-Chimera expressing cell recorded at +40 mV before (black lines) and after exposure to Cd^{2+} and La^{3+} (gray lines). The line diagram represents the RyR1 (thick lines) and RyR2 (thin lines) sequences in the chimeric construct. (c) The average amplitudes of the Ca^{2+} current densities for Mac-Chimera (black circles, $n = 10$), wild-type RyR1 (white circles, $n = 41$), and wild-type RyR2 expressing cells are shown (gray circles, $n = 10$).

function onto an otherwise cardiac receptor and removal of 922–1112 from RyR1 by replacement with the corresponding cardiac region may affect the activation of RyR1 during EC coupling (although the data is preliminary).

2.4.1 R16-Chimera and R16-RevChimera

A functional interaction was seen between R16-Chimera, but not wild-type RyR2, and the skeletal DHPR. Although the Ca^{2+} transients measured in the presence of R16-Chimera were small, they were larger than those seen with RyR2 and had a more sigmoidal shape to their voltage dependence. Blocking of Ca^{2+} influx via α_{1S}

by Cd^{2+} and La^{3+} only partially inhibited the Ca^{2+} transients in most of the R16-Chimera expressing cells. The ability of R16-Chimera expressing cells to mediate spontaneous contractions suggests that the expression level of the chimera and the SR Ca^{2+} load are sufficient to release enough Ca^{2+} to reach the threshold necessary to mediate a contraction, but it does not eliminate the possibility that these mechanisms may be impaired. Focusing on the R16-Chimera studies alone, it appears that the sR16 region is sufficient to support a weak level of skeletal-type EC coupling.

In contrast to the above data supporting the role of sR16 in skeletal-type EC coupling, R16-RevChimera, which is roughly the inverse of R16-Chimera, had no effect on the Ca^{2+} transients. Thus, the sR16 region plays a role in skeletal-type EC coupling as shown by R16-Chimera, but it is not necessary as shown by the lack of an effect upon "removal" of sR16. The sR16 region cannot be dismissed, because it is able to transfer a small degree of skeletal-type EC coupling to RyR2. Yet it is unlikely to be the sole region of interaction between the DHPR and RyR1. Since the larger section surrounding sR16, R10, can mediate skeletal-type coupling (Nakai et al., 1998a), the amino acid sequence of sR16 may be smaller than that necessary for a full functional interaction. Alternatively, sR16 could work in concert with other non-adjacent regions of RyR1 to communicate with the DHPR.

Considering that the cR16 region did interact with the Sk53 region of the α_{1S} II-III loop, although to a lesser extent than sR16 (Proenza, 1999), this region of RyR2 may carry functional importance. Instead, the structures of the RyR1 and RyR2 segments used in yeast two-hybrid experiments may differ from those found in the intact protein (see Proenza (1999) for a discussion of yeast two-hybrid techniques).

Despite the fact that the sequence homology between sR16 and cR16 is about 75% and that these regions encompass one of the highest stretches of divergence (D3, Sorrentino and Volpe, 1993), the three dimensional configuration may be similar enough to bind weakly to Sk53 in yeast two-hybrid studies and maintain the structure and function of the rest of the protein when in the presence of RyR1 as in R16-RevChimera. Another possibility is that the presence of the sR16 region in an otherwise cardiac receptor may be sufficient to allow the skeletal DHPR and R16-Chimera to align atop one another as would wild-type RyR1 but not RyR2. Thus, other portions of RyR2 which would not normally be exposed to the DHPR could then support a weak functional interaction. Similarly, the sR16 region may be exposed to the DHPR when in RyR1, but not as conveniently as when substituted into RyR2 consequently preventing it from interacting efficiently with the DHPR.

Retrograde signaling does not appear to be controlled by communication from the sR16 region of RyR1 to the skeletal DHPR. On average, the α_{1S} Ca^{2+} current amplitude seen in R16-Chimera expressing myotubes was equivalent to that of wild-type RyR2 expressing myotubes. Likewise, the presence of the R16-RevChimera did not affect enhancement of the Ca^{2+} currents. These combined results are surprising considering a single region of α_{1S} is thought to mediate bi-directional signaling (Grabner et al., 1999). Complicated results were found with R9 and R10 in which both regions of RyR1 were able to transfer retrograde function onto RyR2 but only R10 supported skeletal-type EC coupling (Nakai et al., 1998a). It is possible that the region required for retrograde signaling overlaps R9 and R10 excluding sR16 or that the sR16 segment is too small to maintain retrograde signaling on its own. In either

circumstance, sR16 is insufficient and unnecessary for full enhancement of the Ca^{2+} currents via α_{1S}.

2.4.2 Mac-Chimera

Because the data concerning Mac-Chimera is preliminary, I hesitate to state my conclusions as final. The region 922–1112 of RyR1 may not be necessary for skeletal-type EC coupling since the Ca^{2+} transients seen with Mac-Chimera have a sigmoidal shape to their voltage dependence and are sustained when the Ca^{2+} influx via α_{1S} is blocked. Additionally, retrograde signaling was fully intact in the presence of Mac-Chimera. In support of these conclusions, a chimera (R2) in which amino acids 1–1631 (encompassing 922–1112) of RyR1 were substituted into RyR2, did not express properties of bi-directional signaling (Nakai et al., 1998a). Taken together, the region 922–1112 has been found to be neither necessary nor sufficient to transfer skeletal-type function onto RyR2. It appears that Ca^{2+} release may be impaired as shown by the roughly 4-fold decrease in the amplitude of the Ca^{2+} currents in Mac-Chimera expressing cells. This degree of decrease is comparable to degree seen with E4032A-RyR1 (see Chapter 1). It is unlikely that these three data points with Mac-Chimera are representative given that the E4032A-RyR1 expressing myotubes were unable to contract with stimulation while the Mac-Chimera expressing myotubes were able to contract despite the similarity in the amount of Ca^{2+} release. Thus, the larger sample of contraction data collected from Mac-Chimera expressing cells is likely to be more representative than the small sample of Ca^{2+} transient data.

2.4.3 Summary

The biochemical and yeast two-hybrid interaction studies provided a useful basis for studying potential functional regions of interaction between RyR1 and the skeletal DHPR, but functional significance cannot be presupposed from the results. In the case of the ryanodine receptor this statement is especially true since very little is known about its three dimensional structure and thus whether or not the sequences in question, sR16 and 922–1112, are fully exposed to the α_{1S} II-III loop in physiological conditions. It can be concluded, though, sR16 is likely to play some role in skeletal-type EC coupling and that 922–1112 is not likely to play a strong role.

Chapter 3

The Mutation C4958S In RyR1 Disables Ca^{2+} Release But Not Enhancement of α_{1S} Ca^{2+} Currents

This work will be published as a collaboration with the following order of authors: Jennifer J. O'Brien[†], Doug Wingrove[§], Paul D. Allen[§], and Kurt G. Beam[†]. Doug Wingrove was a member of the Allen lab when he made all four of the individual cysteine mutant constructs (C4876S, C4882S, C4958S, C4961S) in RyR1. I performed all of the other experiments. Some of the data are still in preliminary form.

[†]Dept. of Anatomy and Neurobiology, Colorado State University, Fort Collins, CO 80523
[§]Dept. of Anesthesia, Brigham and Women's Hospital, Boston, MA 02115

3.1 Introduction

Ryanodine receptors serve to release Ca^{2+} from the endo/sarcoplasmic reticulum Ca^{2+} store. The three isoforms, RyR1 and RyR2, which are important for the mediation of EC coupling in skeletal and cardiac muscle respectively, and the ubiquitously expressed isoform RyR3, share about 65–70% homology in amino acid sequence. Inositol 1,4,5-triphosphate receptors (IP_3Rs) comprise a second family of Ca^{2+} release channels expressed in the endoplasmic reticulum in a myriad of cell types. These two families of Ca^{2+} release channels have both high conserved sequence conservation in their C-terminal portions and common channel function.

In both the ryanodine and IP_3 receptor families, the channel forming region of the protein is located in the C-terminal portion of the sequence while the other roughly 80% of the protein is cytoplasmic. It has been estimated that the ryanodine receptor contains anywhere from four to twelve transmembrane domains (Takeshima et al., 1989; Zorzato et al., 1990; Tunwell et al., 1996) and IP_3Rs contain six transmembrane domains (Furuichi et al., 1989; Mignery et al., 1989; Michikawa et al., 1994). As would be predicted, these C-terminal membrane spanning regions constitute the channel portion of each receptor (Bhat et al., 1997; Mignery et al., 1989). In addition, the cytoplasmic C-terminal tail region following the putative transmembrane domains plays an important, yet unidentified, role in channel function in each of the receptors (Gao et al., 1997; Miyazaki et al., 1992).

Ryanodine receptors are only expressed as homotetramers (Lai et al., 1988; Takeshima et al., 1989) whereas IP_3Rs are capable of forming both homotetramers

(Furuichi et al., 1989; Mignery et al., 1989; Maeda et al., 1991) and heterotetramers (Monkawa et al., 1995). The important domain in the maintenance of the subunit-subunit interactions for each receptor family is the C-terminal domain (Meissner et al., 1989; Sayers et al., 1997; Miyawaki et al., 1991). Part of the cytoplasmic region in addition to the transmembrane domains of the ryanodine receptor may be involved in subunit interactions (Chen et al., 1993), yet the transmembrane domains alone are sufficient to form homotetramers of the IP_3Rs (Mignery and Sudhof, 1990). The apparent overlap between the regions implicated in subunit-subunit interactions of the ryanodine and IP_3 receptors suggests that the amino acids required for subunit binding may be conserved between the two Ca^{2+} release channel families.

Similarities in the structure of the Ca^{2+} release channel families are reflected in the similarities in their function. For example, while the ryanodine receptors are activated by increases in cytoplasmic Ca^{2+} or, as in skeletal muscle, by the direct interaction with the DHPR, the IP_3Rs are activated by IP_3 via G-protein coupled receptor activation. Interestingly, Ca^{2+} can also activate the IP_3R but as a coagonist in the presence of IP_3 (Finch et al., 1991). Activation of each receptor type shows a bell-shaped dependence on increasing Ca^{2+} concentrations (Ashley and Williams, 1990; Bull and Marengo, 1993; Györke and Fill, 1993; Iino, 1990). The importance of Ca^{2+} activation of both ryanodine and IP_3 receptors is paralleled by the recent data showing that the putative Ca^{2+} sensor has been identified at corresponding C-terminal glutamates, that is E4032 in RyR1, (Chen et al., 1998, and Chapter 1) and E2100 in IP_3R, (Miyakawa et al., 2001).

As the classification states, the Ca^{2+} release function is analogous between the ryanodine and IP_3 receptors. These Ca^{2+} release channel families display the same relative permeability to cations ($Ba^{2+} > Sr^{2+} > Ca^{2+} > Mg^{2+}$) and favor conduction of divalent cations over monovalent cations (Bezprozvanny and Ehrlich, 1994; Yoshida and Imai, 1997). Although the permeability is similar, the unitary conductance of these cations is smaller through the IP_3R channel than through the ryanodine receptor channel (Bezprozvanny and Ehrlich, 1994). Parallels between the overall structure and function of the C-terminal region, as suggested above by the conservation of the Ca^{2+} sensor, imply that the amino acids important for maintaining the structural and functional properties of the channel are likely to be conserved between the receptor families.

A potential amino acid that could play a role in the subunit-subunit interactions and channel functioning of ryanodine and IP_3 receptors is the cysteine residue. Cysteine pairs are able to form covalent, disulfide, bonds between their thiol side chains. This bonding can determine the three dimensional structure and rigidity of the protein as well as the redox sensitivity. Disulfide bonds can be easily broken with mild oxidizing reagents and thus reformed with reducing agents. Oxidizing reagents, acting through sulfides, have been shown to trigger Ca^{2+} release from the SR presumably via ryanodine receptors (Abramson and Salama, 1989). Experiments using physiological redox conditions on the cytoplasmic and lumenal sides of the ryanodine receptor have shown that redox activation may be important in normal cellular functioning and that the cysteines involved in this reaction may be located in the transmembrane domains (Feng et al., 2000). In addition, oxidation of IP_3Rs has been

shown to increase Ca^{2+} release, presumably by increasing the affinity of the receptor for IP_3 binding (Bootman et al., 1992; Hilly et al., 1993). One particular cysteine residue in RyR1, 3635, may be important for oxidation induced and calmodulin protected intersubunit interactions of the receptor (Porter et al., 1999), but the other cysteines involved in the normal subunit-subunit interactions and the activation of the channel have remained elusive.

There are two specific C-terminal cysteine pairs that are conserved among the ryanodine and IP_3 receptor families (Berridge, 1993). The first pair, in which only the cysteine residues themselves are conserved, is located at the cytoplasmic end of the fifth transmembrane domain of the IP_3Rs (Fig. 3.1). The relative structural location of the first pair in RyR1 is debatable due to the discrepancies in the different potential number of transmembrane domains. In addition, the entire motif TXCFICG containing the second pair of cysteines is conserved among the receptors in each group (Fig. 3.1). To determine if any of these four cysteines are important for either channel function or subunit-subunit interactions, I studied the effects on Ca^{2+} release and retrograde signaling of four RyR1 constructs each containing one of the cysteines mutated to a serine (C4876S-, C4882S-, C4958S-, and C4961S-RyR1) expressed in dyspedic myotubes. After obtaining preliminary results from all four mutants, I concentrated on evaluating the whole-cell Ca^{2+} currents and depolarization evoked Ca^{2+} transients in myotubes expressing C4958S-RyR1. This cysteine mutant appears to sustain a reduced level of retrograde signaling and to have drastically impaired Ca^{2+} release function.

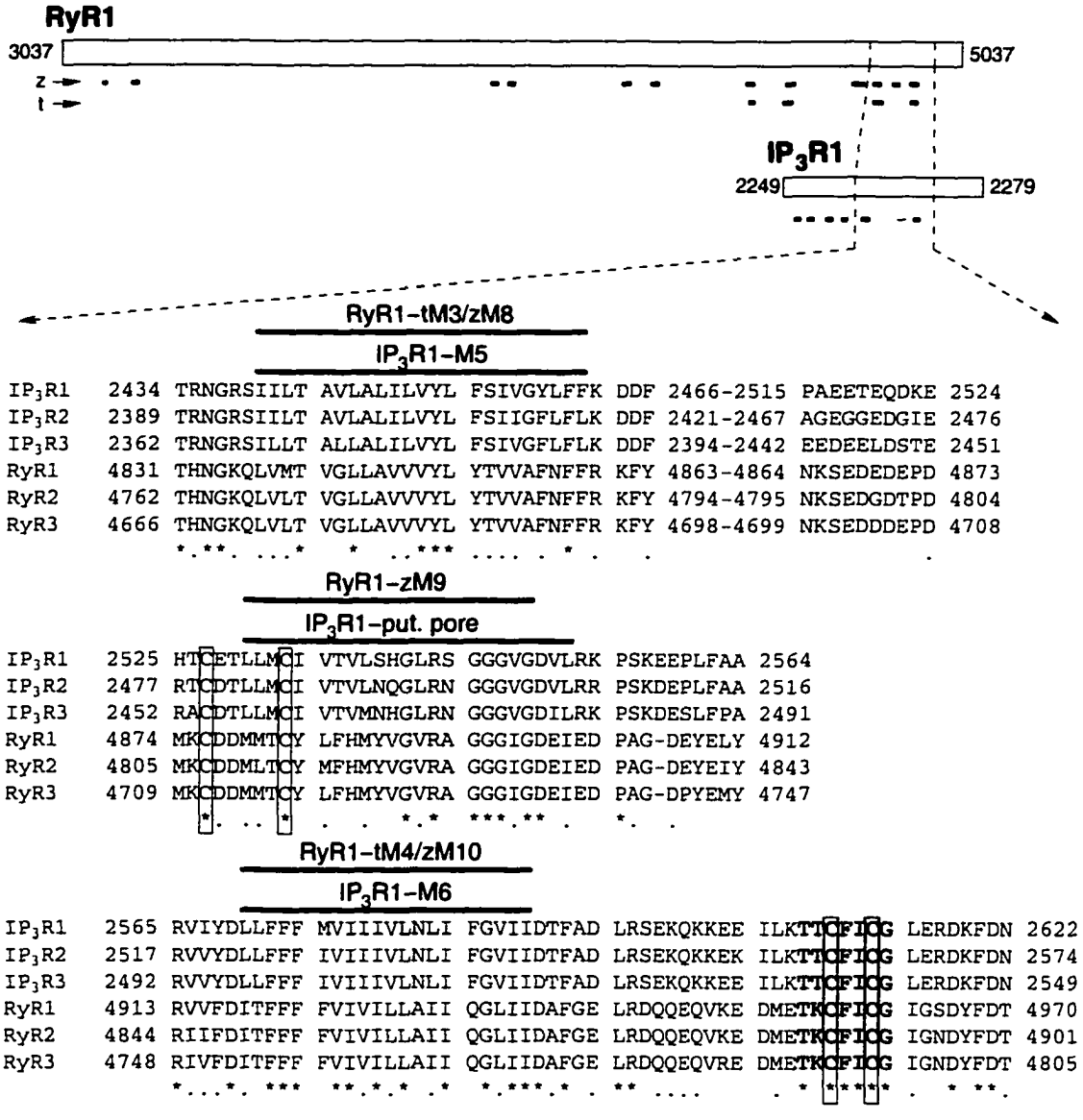

Figure 3.1: Alignment of C-terminal transmembrane domains (TMDs) of IP_3R and RyR isoforms. The C-terminal ends of IP_3R type 1 and RyR1 are represented by the white bars. Under RyR1, the top row of short lines (z) represents the location of the TMDs proposed by Zorzato et al. (1990) and the bottom row (t) represents the locations proposed by Takeshima et al. (1989). Under IP_3R1, the thick lines represent the TMDs as suggested by Furuichi et al. (1989) and the thin line shows the location of the putative pore region (Michikawa et al., 1994). The amino acid alignment of representative isoforms from each receptor family is based on that of Furuichi et al. (1989). Again, as indicated by the bars above the alignment, the TMDs are labeled z for the Zorzato model and t for the Takeshima model. Sequences: mouse IP_3R1, (Furuichi et al., 1989); mouse IP_3R2 and IP_3R3, (Ross et al., 1992); rabbit RyR1, (Takeshima et al., 1989); rabbit RyR2, (Nakai et al., 1990); rabbit RyR3, (Hakamata et al., 1992)

3.2 Experimental procedures

3.2.1 Preparation of myotubes

Myotube cultures were prepared as described in Section 1.2.3 on page 26. The control wild-type RyR1 was the same as used in the previous two Chapters. Doug Wingrove in the Allen lab created all four cysteine mutants (C4876S-, C4882S-, C4958S-, and C4951S-RyR1) in the pCIneo expression plasmid. Injection of these plasmid constructs into the nuclei of cultured dyspedic myotubes was performed as described in Section 1.2.3. CD8 was used as an indicator of expression for all of the studies using simultaneous recording of whole cell Ca^{2+} currents and Ca^{2+} transients, while GFP was coexpressed in cells ultimately used for contraction experiments and initial recordings of the Ca^{2+} currents alone.

3.2.2 Electrically evoked contractions

Electrically evoked contractions were triggered as described in Sections 1.2.3, 2.2.3. During the tests, the cells were bathed in either 2% media or Rodent Ringers (with Ca^{2+}) solutions. The 2% media included along with other compounds 25 mM HEPES in DMEM with glucose (Gibco/Invitrogen, Carlsbad, CA) which, among other compounds, has (in mM) 1.8 $CaCl_2$, 5.4 KCl, 0.8 $MgSO_4$, 154 Na^+ (total of NaCl, $NaHCO_3$, NaH_2PO_4). Since the ionic concentrations of 2% media and Rodent Ringers (2 mM Ca^{2+}) are quite similar, I pooled the data taken in the presence of each solution.

3.2.3 Measurement of Ca^{2+} currents and Ca^{2+} transients

The technique used to simultaneously record both the whole cell Ca^{2+} currents and increases in cytoplasmic Ca^{2+} concentrations (Ca^{2+} transients) was the same as described in Sections 1.2.4, 2.2.3 on pages 27, 50. Exceptions to the previous procedures are only applicable to those studies done with C4958S-RyR1.

The changes in methodology were brought about by the use of Clampex 8.0 and Clampfit 8.0 (Axon Instruments, Union City, CA) for data acquisition and analysis, respectively. An 8 ms pulse to the holding potential of -80 mV was added prior to the 50 ms prepulse to -50 mV and subsequent to the 1 sec conditioning pulse to -20 or -30 mV. The step to -50 mV for 125 ms following the test pulse was lengthened to 200 ms. Capacitance measurements were calculated from the integration of a series of depolarizing steps from the holding potential to -60 mV instead of hyperpolarizing steps to -110 mV. Leak current measurements were recorded and subtracted in an analogous manner to that described previously, but the subtraction was done offline using Leak Subtraction program (written by T. Roth). Even though a different program (Clampfit 8.0) was used, the analysis of the Ca^{2+} currents was similar to that of previous Chapters.

Recording of the Ca^{2+} transients was not changed with the move to new software. Removal of all ambient light and increases in the gain of the output signal during data acquisition may have altered the appearance of the raw data traces. To analyze the Ca^{2+} transients, the basal level of fluorescence from the first pulse recorded in that cell was used as the baseline for all following test pulses. The value

of the fluorescence during the test pulse was normalized dividing the change in the this fluorescence from the baseline by the baseline value ($\Delta F/F$) as done for Mac-Chimera (see Section 2.2.4). All other analysis was performed as described previously.

3.2.4 Recording and analysis of inactivation

Ca^{2+} current inactivation was measured using long depolarizing test pulses. All other conditions were the same as those used for the whole-cell patch clamp technique described above. Ca^{2+} transients were not measured in these experiments thus Fluo-3 was omitted from the internal, pipette solution. The conditioning pulse remained the same, but the subsequent steps were as follows: prepulse to -50 mV for 75 ms, test pulse between +20 to +40 mV for 2000 ms, postpulse to -50 mV for 75 ms. Because prolonged hyperpolarization can damage the cell, a 20 mV depolarizing step from the holding potential (using the same step function as for the test data) was used to measure the leak currents. Leak measurements were repeated 5 times and averaged before subtraction using the offline program, Leak Subtraction. Data acquisition was performed with Clampex 8.0.

The percent inactivation was calculated by subtracting the value of the current at time 1982 ms into the test pulse (a point chosen near the end) from the peak value of the current during the test pulse then dividing this difference by the peak current. Thus, when there is complete decay of the current, the inactivation is 100%. Time to peak was measured as the time beginning at the start of the test pulse until the current reached its peak value. These measurements were only performed on the long, 2 sec pulses. All data analysis of the long pulses was done with Clampfit 8.0.

3.2.5 Recording the effects of CPA

Cells were loaded with Fluo-3AM as explained in Section 1.2.4. To prevent photobleaching during prolonged exposure to the excitation wavelength (see decreasing baseline in Fig. 1.3), the shutter was only opened for 1 sec every 10 sec during the experiment. Fluorescence data was only recorded during these brief light exposures. Since the shutter requires settling time, the data before 200 ms into the light pulse was not used. Data points from 200 to 800 ms were averaged to account for the noise in the sample and plotted against the elapsed time at the start of the region being analyzed. Little to no changes in the amplitude of the fluorescence were seen during the 1 sec openings. The average of the data in the first few pulses before the application of CPA was used to determine the baseline level of fluorescence which was in turn used to calculate $\Delta F/F$. To measure the delay in the initial increase of fluorescence in the presence of Ca^{2+}, the time after the application of CPA at which the first steady increase of fluorescence occurred was recorded.

3.3 Results

To determine the significance of the cysteines C4876, C4882, C4958, and C4961 in RyR1 function, four RyR1 constructs were made each with a different, single cysteine mutation. Serine has a similarly charged side group (primary –OH) but is not as reactive in redox reactions as a cysteine residue. Furthermore, a double bond with oxygen (C=O) is formed upon oxidation instead a covalent bond with another serine or cysteine side chain. Thus, the cysteines in the four mutant RyR1s were

changed to serines to preserve the charge of the side group while removing reactivity (C4876S-RyR1, C4882S-RyR1, C4958S-RyR1, and C4961S-RyR1).

None of the four mutant RyR1s were able to mediate EC coupling. Each of the four cysteine mutants were expressed in dyspedic myotubes and tested for responsiveness to electrical stimulation. In the presence of extracellular Ca^{2+} ($\sim$2 mM), all 13 wild-type RyR1 expressing myotubes contracted yet none of the cysteine mutant expressing myotubes contracted (C4876S-RyR1 $n = 7$, C4882S-RyR1 $n = 2$, C4958S-RyR1 $n = 11$, and C4961S-RyR1 $n = 5$). Although some of the data are preliminary, it is apparent that removal of these C-terminal cysteines impairs function of RyR1.

It is possible that the expressing myotubes are unable to contract simply because expression, targeting, or tetramerization has been hindered by the presence of the mutation. Since enhancement of the DHPR α_{1S} Ca^{2+} currents is dependent on the association of RyR1 and the DHPR (Nakai et al., 1996), then the presence of the mutant RyR1s in the SR membrane can be indirectly measured by the occurrence of retrograde signaling. The average amplitudes of the peak Ca^{2+} current densities for C4876S-RyR1 (-12.09 ± 2.70 pA/pF, $n = 2$) C4882S-RyR1 (-12.20 ± 2.50 pA/pF, $n = 2$), and C4961S-RyR1 (-16.36 ± 4.18 pA/pF, $n = 3$) were similar to that of wild-type RyR1 (-15.51 ± 1.45 pA/pF, $n = 41$; Fig. 3.2a, no statistics were performed due to the small sample sizes of each group). Detailed analysis of C4958S-RyR1 expressing myotubes revealed that the Ca^{2+} currents measured at +30 mV were enhanced above the level seen in uninjected dyspedic myotubes (-5.54 ± 0.68 pA/pF, $n = 32$ versus -1.35 ± 0.30 pA/pF, $n = 10$, respectively, $p < 0.001$), but not to the level seen when wild-type RyR1 was expressed (-14.12 ± 1.51 pA/pF, $n = 41$, $p \ll 0.001$)

as shown in Fig. 3.2b,c. Despite the fact that retrograde signaling is impaired in cells expressing C4958S-RyR1, the currents were enhanced enough to suggest that the receptors are being expressed. This finding is supported by direct measurement of expression of C4958S-RyR1 in comparison to wild-type RyR1 when expressed in 1B5 cells, a myogenic cell line lacking endogenous RyR1 (Hurne et al., 2002).

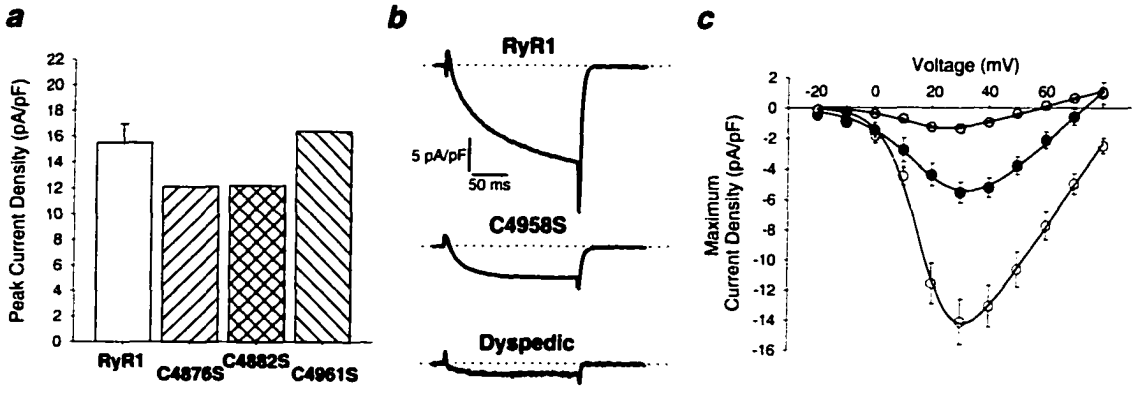

Figure 3.2: Ca^{2+} currents in C4958S-RyR1 expressing myotubes are smaller than those of wild-type RyR1 expressing myotubes but larger than those of uninjected dyspedic myotubes. (a) Preliminary data showing the average peak current densities for mutants C4876S- (n = 2), C4882S- (n = 2), and C4961S-RyR1 (n = 3) are similar to that of wild-type RyR1 (n = 41) when expressed in dyspedic myotubes. No error bars are shown since no statistics were performed. (b) Representative Ca^{2+} current traces at +30 mV from dyspedic myotubes expressing wild-type RyR1 (top) and C4958S-RyR1 (middle) and from uninjected dyspedic myotubes (bottom) are shown. (c) Ca^{2+} current-voltage relationships of dyspedic myotubes (gray circles; n = 10), C4958S-RyR1 expressing myotubes (black circles; n = 32), and wild-type RyR1 expressing myotubes (white circles; n = 41) are plotted.

Since it appears that C4958S-RyR1 is being expressed as a complete tetrameric protein in the SR membrane, the lack of electrically evoked contractions may be due to elimination of Ca^{2+} release or a reduction in the amount of Ca^{2+} release to that below the threshold required to elicit a visible contraction. In some of the cells expressing C4958S-RyR1, the Ca^{2+} transients were very small and in the rest of the cells they

were not even detectable (i.e. Fig. 3.3a). On average, the amplitude at +40 mV of the Ca^{2+} transients in C4958S-RyR1 expressing myotubes equaled 0.11 ± 0.05 ΔF/F (n = 8) which is significantly smaller ($p < 0.01$) than those seen with wild-type RyR1 (4.35 ± 0.79 ΔF/F, n = 24; Fig. 3.3b). Both the inset in Fig. 3.3b and the raw data traces in Fig. 3.3a show that the voltage dependence of the Ca^{2+} transients is bell-shaped reflecting the voltage dependence of the Ca^{2+} currents (see Fig. 3.2c). Considering the Ca^{2+} transients in wild-type RyR1 expressing cells display a sigmoidal voltage dependence, the Ca^{2+} transients are likely to be caused by Ca^{2+} influx via the DHPR α_{1S} subunit versus Ca^{2+} efflux through C4958S-RyR1.

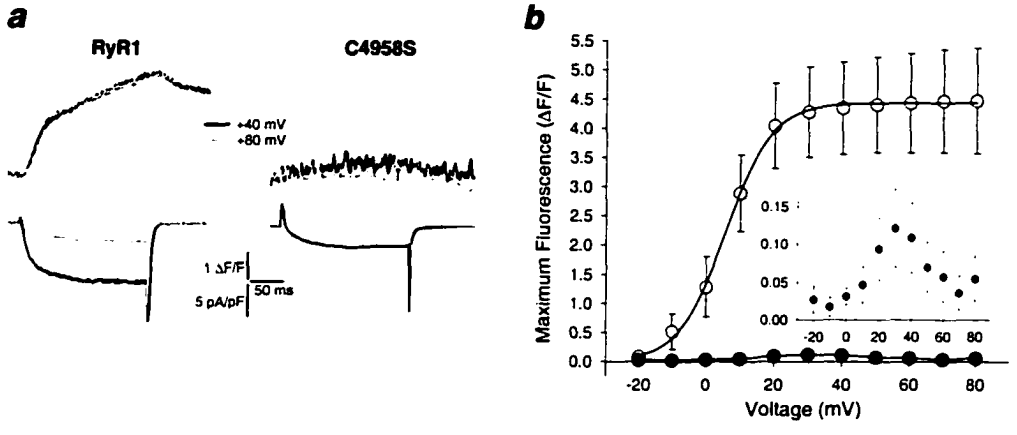

Figure 3.3: The Ca^{2+} transients with C4958S-RyR1 are very small and have a bell-shaped voltage dependence indicative of Ca^{2+} influx via α_{1S}. (a) Representative Ca^{2+} transients at +40 (black) and +80 mV (gray) for wild-type RyR1 and C4958S-RyR1 are shown. (b) Maximal Ca^{2+} induced fluorescence increase in wild-type RyR1 (white circles; n = 24) and C4958S-RyR1 (black circles; n = 8) expressing myotubes is plotted against the value of the test potential. The inset is an enlargement of the C4958S-RyR1 data to emphasize the bell-shape of the voltage dependence.

Lack of Ca^{2+} transients with C4958S-RyR1 could be explained either by an excess of Ca^{2+} leakage from the SR causing depletion of the Ca^{2+} load or by impairment

of the channel causing no Ca^{2+} to be released. To differentiate between these two possibilities, the Ca^{2+} content of the SR was indirectly measured by blocking the Ca^{2+} pumps with CPA and recording the slow increase in myoplasmic Ca^{2+} presumably due to leak. As illustrated in Fig. 3.4, the maximal increase in fluorescence following application of CPA to C4958S-RyR1 (0.97 ± 0.30 $\Delta F/F$, $n = 6$) was comparable to that of wild-type RyR1 expressing cells (1.44 ± 0.08 $\Delta F/F$, $n = 3$, $p > 0.1$). It is unknown what channels the Ca^{2+} from the SR escapes through; therefore, CPA was applied to uninjected dyspedic myotubes to resolve whether or not ryanodine receptors act as the gate for the Ca^{2+} leak. The increase in myoplasmic Ca^{2+} was, though variable, similar to that of C4958S-RyR1 ($p > 0.5$) and wild-type RyR1 ($p > 0.5$) expressing myotubes (1.45 ± 0.93 $\Delta F/F$, $n = 4$). Interestingly, the increase in Ca^{2+} in the presence of CPA was delayed relative to that of wild-type RyR1 expressing cells (19.9 ± 5.8 sec, $n = 3$) in both dyspedic (117.2 ± 30.2 sec, $n = 4$, $p < 0.05$) and C4958S-RyR1 expressing cells (106.4 ± 27.6 sec, $n = 6$, $p > 0.05$) which were not significantly different from one another ($p > 0.5$). Conceivably, the initial increase seen with wild-type RyR1 could be due to leak through RyR1 and CICR. The above data support the idea that the cysteine mutation impairs the channel in such a way to prevent Ca^{2+} efflux into the cytoplasm.

Calmodulin mediates the Ca^{2+} dependent inactivation of the cardiac DHPR channel, α_{1C} (Zühlke et al., 1999; Peterson et al., 1999; Qin et al., 1999). Recent data suggest that α_{1S} inactivation may also be regulated by Ca^{2+}-calmodulin (Stroffekova et al., 2001; Stroffekova and Beam, 2002). Thus, changes in the cytoplasmic concentrations of Ca^{2+} may alter the inactivation of the DHPR α_{1S} Ca^{2+} currents. Since

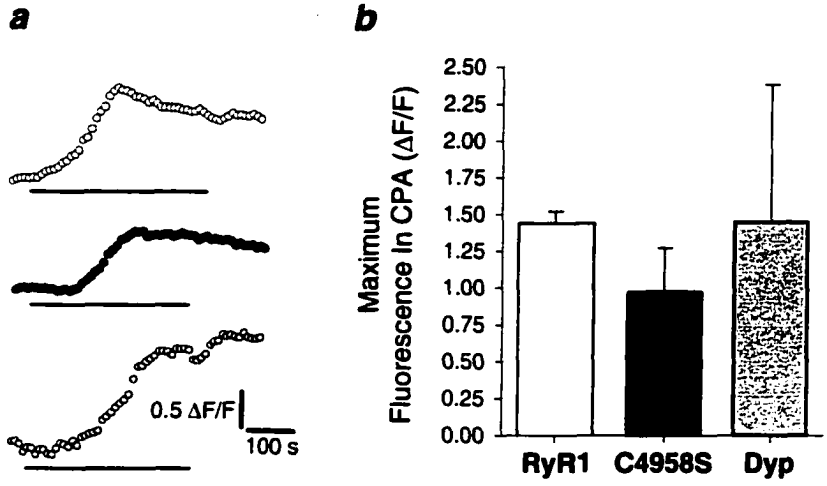

Figure 3.4: SR Ca^{2+} load does not appear to be affected by C4958S-RyR1. (a) Traces from wild-type RyR1 expressing (white circles), C4958S-RyR1 expressing (black circles), and uninjected dyspedic (gray circles) myotubes represent responses to bath application of 30 μM CPA. The data were recorded during 1 sec acquisitions every 10 sec. (b) Average maximal fluorescence increases during exposure to 30 μM CPA are plotted in the bar graph for C4958S-RyR1 (black circles; $n = 6$), wild-type RyR1 (white circles; $n = 3$), and dyspedic myotubes (gray circles, $n = 4$).

C4958S-RyR1 appears to prevent depolarization induced Ca^{2+} release from the SR, this lack of a local increase in myoplasmic Ca^{2+} near α_{1S} during activation of both receptors may affect inactivation of α_{1S}. The percent inactivation of C4958S-RyR1 during a 2 sec test pulse to peak current voltage (+20 to +40 mV) was not significantly different ($p > 0.05$) from that of wild-type RyR1 as illustrated in the representative traces in Fig. 3.5 (C4958S-RyR1: 66 $\pm$ 8%, $n = 16$; RyR1: 59 $\pm$ 6%, $n = 12$). Interestingly, the activation rate of the Ca^{2+} currents in C4958S-RyR1 expressing cells as measured by the time to peak during the 2 sec test pulses was 179 $\pm$ 35 ms ($n = 16$) which was significantly faster ($p > 0.05$) than those of wild-type RyR1 (330 $\pm$ 67 ms, $n = 12$). Perhaps this is due to a larger contribution of dyspedic Ca^{2+} current, which

has previously been shown to activate faster than RyR1 expressing and normal myotubes (Nakai et al., 1996), in C4958S-RyR1 expressing cells compared to that of wild-type RyR1 expressing cells.

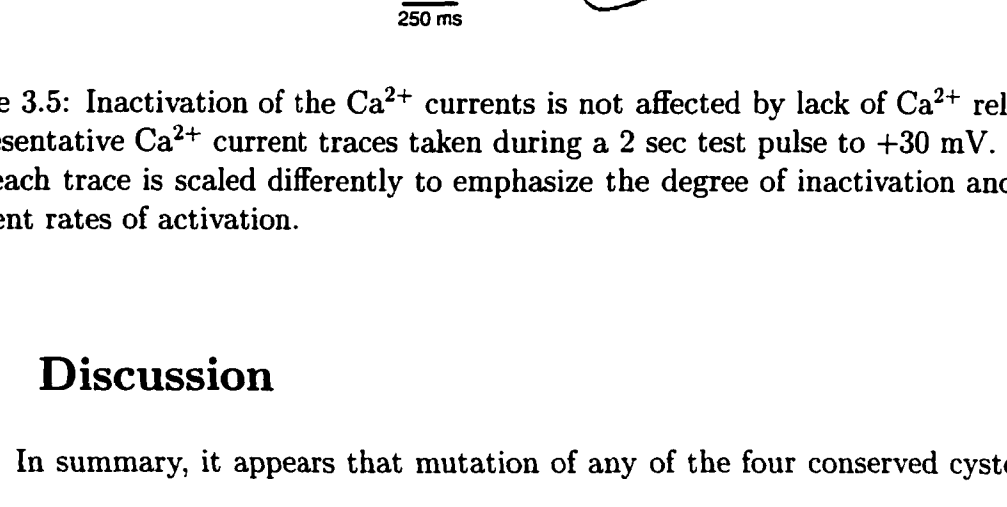

Figure 3.5: Inactivation of the Ca^{2+} currents is not affected by lack of Ca^{2+} release. Representative Ca^{2+} current traces taken during a 2 sec test pulse to +30 mV. Note that each trace is scaled differently to emphasize the degree of inactivation and the different rates of activation.

3.4 Discussion

In summary, it appears that mutation of any of the four conserved cysteines may not prevent homotetramerization of the ryanodine receptor subunits but does inhibit Ca^{2+} release. Thorough analysis of the C4958S mutant RyR1 revealed that the Ca^{2+} transients are indeed completely eliminated with this mutation and that the Ca^{2+} currents are partially, but not completely, enhanced. In addition, the rate of activation of the Ca^{2+} currents in the presence of C4958S-RyR1 was faster than that with wild-type RyR1 which suggests that a greater number of DHPRs are uncoupled from C4958S-RyR1s than with wild-type RyR1 leading to a greater contribution of the fast dyspedic Ca^{2+} currents. The lack of Ca^{2+} release from the SR had little effect on the putative calmodulin mediated inactivation of the Ca^{2+} currents. Even though

the function these cysteines have in the ryanodine receptor is not known, it is clear that their role is important for proper channel function.

The cysteine residue 4958 in RyR1 does not alone mediate the subunit-subunit interactions required for homotetramerization of the ryanodine receptor protein complex. Although the Ca^{2+} currents measured in C4958S-RyR1 expressing cells are smaller than those in wild-type RyR1 expressing cells, they are significantly larger than currents in uninjected dyspedic myotubes. Thus, the mutant channel is able to support a somewhat weakened level of retrograde signaling. The amount of protein expressed in C4958S-RyR1 and wild-type RyR1 virally-infected 1B5 cells is similar (Hurne et al., 2002) indicating that the decrease in Ca^{2+} current enhancement is unlikely to be simply due to decreased expression of the mutant channel. Instead, the difference may be due to a slight inhibition of the coupling between the DHPR and C4958S-RyR1. Reasons for this are unclear. One possibility is that the subunits are weakly associated, but not completely dissociated, because C4958 may be one of a set of cysteines necessary to maintain the tetrameric complex. Alternatively, mutation of the cysteine may cause enough overall structural modifications in the protein to decrease the likelihood of another region of RyR1 to communicate with the DHPR. Finally, the individual subunits may be able to successfully target to the junction without being formed into a complete protein, but this is only possible if the proteins are formed into tetramers after being inserted into the membrane.

The conclusion that the mutation of cysteine 4958 does not affect homotetramerization is based solely on its functional effects and not on direct physical evidence. Thus, it is possible that the mutation alters the ability of RyR1 to be

properly targeted to the junction. In addition, impairment of RyR1 by the mutation may affect the targeting of other proteins to the junction which could ultimately change the DHPR Ca^{2+} currents or the functioning of RyR1. My experiments were unable to address the likelihood of these other potential conclusions.

Elimination of the Ca^{2+} transients by the mutation C4958S in RyR1 suggests that the cysteine residue C4958 in some way plays an important role in the functioning of the ryanodine receptor channel. Extremely small Ca^{2+} transients, relative to the size of those seen with wild-type RyR1, were seen in some of the cells expressing C4958S-RyR1. The bell-shaped voltage dependence of the transients is characteristic of Ca^{2+} influx via the DHPR α_{1S} subunit and not of wild-type RyR1 Ca^{2+} release. Thus these small Ca^{2+} transients are probably due to increases in Ca^{2+} entering the myoplasm from the extracellular space and not the SR. Given that CPA caused an equal increase in myoplasmic Ca^{2+}, I can only conclude that the mutant receptor is not damaged enough to cause the entire store of Ca^{2+} to leak out of the SR because the release during block of the Ca^{2+} pumps does not cause complete depletion of the Ca^{2+} store (see fast Ca^{2+} spikes in Chapter 1, Fig. 1.3). Further evidence that the mutant receptor is unable to release Ca^{2+} is provided by the delay in Ca^{2+} leak of both dyspedic and C4958S-RyR1 in comparison to wild-type RyR1 expressing myotubes. The fast initial increase in Ca^{2+} seen with wild-type RyR1 could be due to leak through the receptors and the activation of the receptors by the increase in myoplasmic Ca^{2+}, or the coupled DHPRs may create a larger influx of Ca^{2+} via leak than uncoupled channels. This implies that C4958S-RyR1 cannot leak Ca^{2+} nor sustain CICR.

Since C4958 is located in the cytoplasmic portion of the C-terminus (see Fig. 3.1), it is unlikely that the cysteine is involved in the structure-function of the pore itself. C4876 and C4882 are adjacent to the putative pore region in both IP_3Rs and ryanodine receptors (Ramos-Franco et al., 1999; Balshaw et al., 1999; Zhao et al., 1999), but more analysis on the effects of the mutants on ryanodine receptor function are necessary before attempting to draw any parallels. The cysteines in the C-terminal tail of RyR1 may cause any number of alterations to the channel and its function including conformation changes and inhibition of activation, but my studies are not sufficient to derive a single conclusion. Another option is that poor subunit-subunit interactions may affect the assembly of the channel itself considering cryo-electron microscopy images (Radermacher et al., 1994; Serysheva et al., 1999) and analysis of the conductance states in the presence of variable size cations (Anyatonwu et al., 2002) have shown that a single channel opening appears to be formed by all four subunits. Finally, activation of RyR1 by changes in the redox potential could have been impaired by the removal of the cysteine residue, but further analysis on the single channel level would be necessary to support this idea.

Because I found little difference between the inactivation of DHPR Ca^{2+} currents in C4958S-RyR1 and wild-type RyR1 expressing myotubes, little can be concluded concerning the role of calmodulin in the inactivation of α_{1S}. Ca^{2+} release may not be affecting the actions of calmodulin, rather the local increase in concentration caused by Ca^{2+} influx via α_{1S} or resting concentrations of Ca^{2+} may be sufficient to trigger calmodulin mediated inactivation as seen with α_{1C} (Neely et al., 1994). Since Ca^{2+} currents are enhanced in the presence of C4958S-RyR1, although not as

strongly as with wild-type RyR1, Ca^{2+} influx or resting myoplasmic Ca^{2+} alone may also be sufficient to trigger calmodulin mediated modifications.

Overall, the C-terminal cysteines C4876, C4882, C4958, and C4961 are important structural features in the functioning of RyR1. Specifically, C4958 is integral to allow RyR1 to release Ca^{2+}. Considering that this cysteine and the other cysteine residues are located near the putative pore regions of both IP_3 and ryanodine receptors (Ramos-Franco et al., 1999; Balshaw et al., 1999; Zhao et al., 1999), cysteine reactivity may contribute to the structure-function relationships of the channel of each receptor family.

Appendix A

The Central Core Disease Mutation I4897T: Construction and Preliminary Experiments

The complete studies regarding I4897T-RyR1 were completed by Guillermo Avila in Robert Dirksen's lab and published (Guillermo Avila[§], Jennifer J. O'Brien[†], and Robert T. Dirksen[§]. 2001. *Proc. Natl. Acad. Sci.* 98:4215–20). I contributed to the preliminary work as detailed below.

Typically, mutations in RyR1 associated with malignant hyperthermia MH and CCD are clustered in two N-terminal domains of the receptor, amino acids 35–614 and 2162–2458 (Loke and MacLennan, 1998). The first mutation localized outside these domains, specifically in the C-terminal region of RyR1, was discovered in an afflicted family in Mexico (Lynch et al., 1999). Studies of the equivalent mutation made in rabbit RyR1 cDNA (I4897T) revealed that the mutation caused the receptor to leak Ca^{2+} from the SR into the cytoplasm (Lynch et al., 1999). This result corresponds to previous research suggesting that MH and CCD are triggered by excess

[§]Dept. of Pharmacology and Physiology, University of Rochester, Rochester, NY 14642
[†]Dept. of Anatomy and Neurobiology, Colorado State University. Fort Collins, CO 80523

release of Ca^{2+} from the SR (Loke and MacLennan, 1998). Since the function of I4897T-RyR1 was studied in HEK293 cells, both the Dirsken lab and I decided to determine what effect the mutation had on EC coupling in muscle cells. I will not discuss the findings of the Dirksen lab, rather I will simply explain the work that I had done.

Using the overlapping extension method of site directed mutagenesis (Ho et al., 1989), the I4897T mutation was incorporated into RyR1-pCIneo (Nakai et al., 1998a). First, two overlapping segments of RyR1-pCIneo were replicated using PCR. The primers that covered the overlapping region contained the basepair change (ATC to ACC) necessary to make the appropriate amino acid change (I to T). Upper segment primers were 5′ ACCTGGCGGGTGCAGGG 3′ forward and 5′ ATCTCGTCCCCGGTGCCTC 3′ reverse and lower segment primers were 5′ AGGCACCGGGGACGAGAT 3′ forward and 5′ ATCTCCCCCTGAACCTGAAAC 3′ reverse. A standard PCR protocol was used with an annealing temperature of 60°C. The resulting DNA from the PCR was isolated from a 1% agarose gel using the Promega DNA Wizard Clean Up kit (Promega Corp., Madison, WI). These two PCR fragments were annealed together using PCR in a second step in which the overlapping fragment ends acted as primers coupled with the upper segment forward primer and the lower segment reverse primer. The final, complete segment was sequenced (by Macromolecular Resources, Fort Collins, CO) to confirm that the mutation was properly incorporated. Both the mutation bearing final segment and the template RyR1-pCIneo were cut with restriction enzymes *Xba*I and *Bst*Z17I (New England BioLabs, Inc., Beverly, MA). The cut final segment and RyR1-pCIneo, with base pairs 13880–15111 removed,

were ligated together with high concentration T4 DNA polymerase. The region in which the mutation was incorporated was shown to be correct by sequencing, but the rest of the I4897T-RyR1 plasmid was not. All experiments done with I4897T-RyR1 expressed in dyspedic myotubes were performed as described in Chapter 1.

Mutation I4897T in rabbit RyR1 appears to eliminate EC coupling. When expressed in dyspedic myotubes, only 4 out of 18 cells supported electrically evoked contractions in media (~2 mM Ca^{2+}). Since fully enhanced Ca^{2+} currents were seen with I4897T-RyR1 (at +30 mV: -10.90 ± 2.19 pA/pF, $n = 10$) like that of wild-type RyR1 (-10.11 ± 0.79 pA/pF, $n = 35$) and unlike that of uninjected dyspedic myotubes (-1.35 ± 0.30 pA/pF, $n = 10$), the mutant receptor is being expressed and properly targeted to the triad junctions where it can communicate with the DHPRs (Fig. A.1b). Interestingly, the Ca^{2+} transients recorded from I4897T-RyR1 expressing myotubes were smaller (0.88 ± 0.32 $\Delta F/F$, $n = 10$) than those with wild-type RyR1 (4.35 ± 0.79 $\Delta F/F$, $n = 24$) and had a bell-shaped voltage dependence indicative of Ca^{2+} influx (Fig. A.1a,c). From this preliminary data, it appears that the receptor is impaired in such a way as to eliminate Ca^{2+} release instead of causing excessive leak of Ca^{2+} through the channel as seen in earlier studies (Lynch et al., 1999).

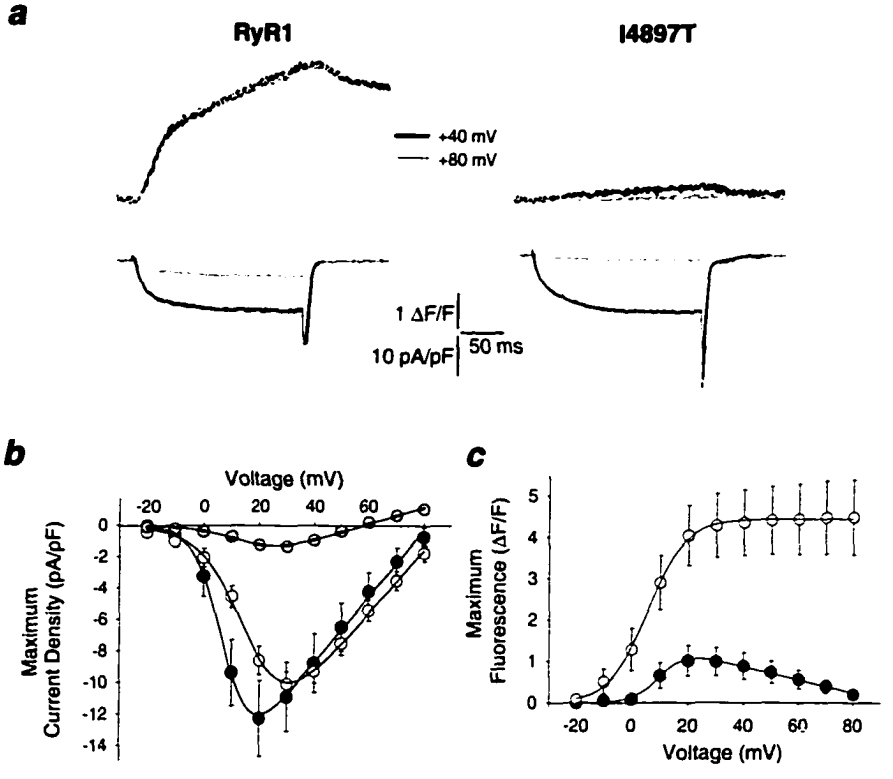

Figure A.1: The mutation I4897T in RyR1 does not affect retrograde signaling to the DHPR but does seem to eliminate Ca^{2+} release from the SR. (a) Ca^{2+} currents (lower sets of traces) and Ca^{2+} transients (upper sets of traces) from wild-type RyR1 and I4897T-RyR1 expressing myotubes are represented. The black traces were recorded at +40 mV and the gray traces were recorded at +80 mV. (b) Average Ca^{2+} current amplitudes in dyspedic myotubes (gray circles, $n = 10$) and myotubes expressing wild-type RyR1 (white circles, $n = 35$) and I4897T-RyR1 (black circles, $n = 10$) are plotted against the test potential. (c) At each test potential, the average maximal increase in fluorescence is shown for wild-type RyR1 (white circles, $n = 24$) and I4987T-RyR1 (black circles, $n = 10$) expressing cells. Since the data were treated as preliminary, no statistics were performed. Error bars were included for illustrative purposes.

Appendix B

Testing of Chimeras With RyR3 Versus RyR2 Background Sequence

Chimeras made with RyR2 and RyR1 sequence can be difficult to interpret because both receptors share involvement in EC coupling even though the means of transferring the EC coupling signal differ. The sequence homology of RyR3 to that of the other ryanodine receptors is slightly less than that between RyR1 and RyR2. Furthermore, RyR3 is not known to be involved in mammalian EC coupling. Thus, chimeras made with sequence from RyR1 and RyR3 may provide cleaner results. Thus, Claudio Perez in Paul D. Allen's lab constructed a set of chimeras in which regions of RyR1 were substituted into RyR3 to determine what regions of RyR1 are sufficient to transfer skeletal-type function onto RyR3, much like Junichi Nakai had done with RyR1/RyR2 chimeras (Nakai et al., 1998a). These constructs were expressed in 1B5 cells, a myogenic dyspedic cell line lacking endogenous RyR1. To confirm the results found with the 1B5 cells, I tested two of the chimeras by expressing them into primary cultures of dyspedic myotubes. Electrically evoked contractions were elicited as described in previous Chapters. I found that both in media and

in Cd^{2+} and La^{3+} Rodent Ringers solutions, the constructs Ch-17 (1–1577:RyR3, 1681–2217:RyR1, 2083–4873:RyR3) and Ch-9 (1–2507:RyR3, 2642–3770:RyR1, 3620–4873:RyR3) showed frequent spontaneous contractions. Specifically, in Cd^{2+} and La^{3+}, 2 out of 35 Ch-17 expressing cells contracted with stimulation and 15 out of 35 cells contracted spontaneously. This result corresponds to that seen with R16-Chimera which is roughly the equivalent RyR2 chimera (Fig. 2.1). With Ch-9, 10 out of 24 cells contracted with stimulation and 7 out of 24 contracted spontaneously. Surprisingly, the Ch-9 chimera corresponds to the R9 chimera made with RyR2, yet Junichi Nakai found that skeletal-type EC coupling was not supported by his chimera. This discrepancy further brings to focus the complicated nature of the means of communication between the DHPR and RyR1 during skeletal-type EC coupling and the importance of subtle differences in tertiary structure of a protein on its function.

List of Abbreviations

α_1 channel forming subunit of L-type voltage gated Ca^{2+} channels

α_{1C} cardiac isoform channel forming subunit of the dihydropyridine receptor

α_{1S} skeletal isoform channel forming subunit of the dihydropyridine receptor

BLM bilayer lipid membrane

C-terminal carboxy-terminal

Ca^{2+} ionic calcium

CCD central core disease

CICR Ca^{2+} induced Ca^{2+} release

CPA cyclopiazonic acid

DHPR dihydropyridine receptor

DMEM Dulbecco's Modified Eagle Medium

EC coupling excitation-contraction coupling

EGTA ethylene glycol-bis(aminoethylether) N,N,N′,N′-tetraacetic acid

GFP green fluorescent protein

HEK293 cells human embryonic kidney cell line

IP_3 inositol 1,4,5-triphosphate

IP_3R inositol 1,4,5-triphosphate receptor

MH malignant hyperthermia

mdg muscular dysgenesis

N-terminal amino-terminal

PCR polymerase chain reaction

RyR1 skeletal isoform of the ryanodine receptor

RyR2 cardiac isoform of the ryanodine receptor

RyR3 ubiquitously expressed isoform of the ryanodine receptor

s.e.m. standard error of the mean

SR sarcoplasmic reticulum

TMDs transmembrane domains

t-tubules transverse tubules

Bibliography

Abramson J and Salama G (1989), Critical sulfhydryls regulate calcium release from sarcoplasmic reticulum. *Journal of Bioenergetics and Biomembranes* 21:283–94.

Adams B, Tanabe T, Mikami A, Numa S, and Beam K (1990), Intramembrane charge movement restored in dysgenic skeletal muscle by injection of dihydropyridine receptor cDNAs. *Nature* 346:569–72.

Anderson K, Lai F, Liu Q, Rousseau E, Erickson H, and Meissner G (1989), Structural and functional characterization of the purified cardiac ryanodine receptor-Ca^{2+} release channel complex. *Journal of Biological Chemistry* 264:1329–35.

Anyatonwu G, Buck E, and Ehrlich B (2002), Analyzing the pore of the ryanodine receptor. *Biophysical Journal* 82:113a, abstract.

Armstrong C, Bezanilla F, and Horowicz P (1972), Twitches in the presence of ethylene glycol bis(-aminoethyl ether)-N,N'-tetracetic acid. *Biochimica et Biophysica Acta* 267:605–8.

Ashley R and Williams A (1990), Divalent cation activation and inhibition of single calcium release channels from sheep cardiac sarcoplasmic reticulum. *Journal of General Physiology* 95:981–1005.

Avila G and Dirksen R (2000), Functional impact of the ryanodine receptor on the skeletal muscle L-type Ca(2+) channel. *Journal of General Physiology* 115:467–80.

Avila G, O'Connell K, Groom L, and Dirksen R (2001), Ca^{2+} release through ryanodine receptors regulates skeletal muscle L-type Ca^{2+} channel expression. *Journal of Biological Chemistry* 276:17732–8.

Balshaw D, Gao L, and Meissner G (1999), Luminal loop of the ryanodine receptor: A pore-forming segment. *Proceedings of the National Academy of Sciences* 96:3345–7.

Beam K, Knudson C, and Powell J (1986), A lethal mutation in mice eliminates the slow calcium current in skeletal muscle cells. *Nature* 320:168–70.

Benacquista B, Sharma M, Samso M, Zorzato F, Treves S, and Wagenknecht T (2000), Amino acid residues 4425-4621 localized on the three-dimensional structure of the skeletal muscle ryanodine receptor. *Biophysical Journal* 78:1349–58.

Berridge M (1993), Inositol trisphosphate and calcium signalling. *Nature* 361:315–25, review.

Bezprozvanny I and Ehrlich B (1994), Inositol (1,4,5)-trisphosphate ($InsP_3$)-gated Ca channels from cerebellum: Conduction properties for divalent cations and regulation by intraluminal calcium. *Journal of General Physiology* 104:821–56.

Bhat M, Zhao J, Takeshima H, and Ma J (1997), Functional calcium release channel formed by the carboxyl-terminal portion of ryanodine receptor. *Biophysical Journal* 73:1329–36.

Block B, Imagawa T, Campbell K, and Franzini-Armstrong C (1988), Structural evidence for direct interaction between the molecular components of the transverse tubule/sarcoplasmic reticulum junction in skeletal muscle. *Journal of Cell Biology* 107:2587–600.

Bootman M, Taylor C, and Berridge M (1992), The thiol reagent, thimerosal, evokes Ca^{2+} spikes in HeLa cells by sensitizing the inositol 1,4,5-trisphosphate receptor. *Journal of Biological Chemistry* 267:25113–9.

Buck E, Nguyen H, Pessah I, and Allen P (1997), Dyspedic mouse skeletal muscle expresses major elements of the triadic junction but lacks detectable ryanodine receptor protein and function. *Journal of Biological Chemistry* 272:7360–7.

Buck E, Zimanyi I, Abramson J, and Pessah I (1992), Ryanodine stabilizes multiple conformational states of the skeletal muscle calcium release channel. *Journal of Biological Chemistry* 267:23560–7.

Bull R and Marengo J (1993), Sarcoplasmic reticulum release channels from frog skeletal muscle display two types of calcium dependence. *FEBS Letters* 331:223–7.

Chen S, Airey J, and MacLennan D (1993), Positioning of major tryptic fragments in the Ca^{2+} release channel (ryanodine receptor) resulting from partial digestion of rabbit skeletal muscle sarcoplasmic reticulum. *Journal of Biological Chemistry* 268:22642–9.

Chen S, Ebisawa K, Li X, and Zhang L (1998), Molecular identification of the ryanodine receptor Ca^{2+} sensor. *Journal of Biological Chemistry* 273:14675–8.

Chen S, Leong P, Imredy J, Bartlett C, Zhang L, and MacLennan D (1997), Single-channel properties of the recombinant skeletal muscle Ca^{2+} release channel (ryanodine receptor). *Biophysical Journal* 73:1904–12.

Cooke R (1986), The mechanism of muscle contraction. *CRC Critical Reviews in Biochemistry* 21:53–118, review.

Dirksen R and Beam K (1996), Unitary behavior of skeletal, cardiac, and chimeric L-type Ca^{2+} channels expressed in dysgenic myotubes. *Journal of General Physiology* 107:731–42.

Dirksen R and Beam K (1999), Role of calcium permeation in dihydropyridine receptor function. Insights into channel gating and excitation-contraction coupling. *Journal of General Physiology* 114:393–403.

Du G and MacLennan D (1999), Ca^{2+} inactivation sites are located in the COOH-terminal quarter of recombinant rabbit skeletal muscle Ca^{2+} release channels (ryanodine receptors). *Journal of Biological Chemistry* 274:26120–6.

Dulhunty A, Laver D, Gallant E, Casarotto M, Pace S, and Curtis S (1999), Activation and inhibition of skeletal RYR channels by a part of the skeletal DHPR II-III loop: Effects of DHPR Ser687 and FKBP12. *Biophysical Journal* 77:189–203.

El Hayek R, Antoniu B, Wang J, Hamilton S, and Ikemoto N (1995), Identification of calcium release-triggering and blocking regions of the II-III loop of the skeletal muscle dihydropyridine receptor. *Journal of Biological Chemistry* 270:22116–8.

Fabiato A (1983), Calcium-induced release of calcium from the cardiac sarcoplasmic reticulum. *American Journal of Physiology* 245:C1–14, review.

Fabiato A (1985), Time and calcium dependence of activation and inactivation of calcium-induced release of calcium from the sarcoplasmic reticulum of a skinned canine cardiac Purkinje cell. *Journal of General Physiology* 85:247–89.

Feng W, Liu G, Allen P, and Pessah I (2000), Transmembrane redox sensor of ryanodine receptor complex. *Journal of Biological Chemistry* 275:35902–7.

Fessenden J, Chen L, Wang Y, Paolini C, and Franzini-Armstrong C (2001), Ryanodine receptor point mutant E4032A reveals an allosteric interaction with ryanodine. *Proceedings of the National Academy of Sciences* 98:2865–70.

Finch E, Turner T, and Goldin S (1991), Calcium as a coagonist of inositol 1,4,5-trisphosphate-induced calcium release. *Science* 252:443–6.

Flucher B, Conti A, Takeshima H, and Sorrentino V (1999), Type 3 and type 1 ryanodine receptors are localized in triads of the same mammalian skeletal muscle fibers. *Journal of Cell Biology* 146:621–9.

Fosset M, Jaimovich E, Delpont E, and Lazdunski M (1983), [3H]nitrendipine receptors in skeletal muscle. *Journal of Biological Chemistry* 258:6086–92.

Franzini-Armstrong C (1970), Natural variability in the length of thin and thick filaments in single fibres from a crab, *Portunus depurator*. *Journal of Cell Science* 6:559–92.

Franzini-Armstrong C and Nunzi G (1983), Junctional feet and particles in the triads of a fast-twitch muscle fibre. *Journal of Muscle Research and Cell Motility* 4:233–52.

Franzini-Armstrong C, Pincon-Raymond M, and Rieger F (1991), Muscle fibers from dysgenic mouse in vivo lack a surface component of peripheral couplings. *Developmental Biology* 146:364–76.

Furuichi T, Yoshikawa S, Miyawaki A, Wada K, Maeda N, and Mikoshiba K (1989), Primary structure and functional expression of the inositol 1,4,5-trisphosphate-binding protein P400. *Nature* 342:32–8.

Gao L, Balshaw D, Xu L, Tripathy A, Xin C, and Meissner G (2000), Evidence for a role of the lumenal M3-M4 loop in skeletal muscle Ca(2+) release channel (ryanodine receptor) activity and conductance. *Biophysical Journal* 79:828–40.

Gao L, Tripathy A, Lu X, and Meissner G (1997), Evidence for a role of C-terminal amino acid residues in skeletal muscle Ca^{2+} release channel (ryanodine receptor) function. *FEBS Letters* 412:223–6.

García J and Beam K (1994a), Measurement of calcium transients and slow calcium current in myotubes. *Journal of General Physiology* 103:107–23.

García J and Beam K (1994b), Physiological and molecular insights into excitation-contraction coupling in cardiac and skeletal muscle. In *Ion channels in the cardiovascular system: Function and dysfunction*, edited by P Spooner, R Joyner, and J Jalife, Futura Publishing Co., Inc., Armonk, NY, pages 355–67.

García J, Tanabe T, and Beam K (1994), Relationship of calcium transients to calcium currents and charge movements in myotubes expressing skeletal and cardiac dihydropyridine receptors. *Journal of General Physiology* 103:125–47.

Giannini G, Clementi E, Ceci R, Marziali G, and Sorrentino V (1992), Expression of a ryanodine receptor-Ca^{2+} channel that is regulated by TGF-beta. *Science* 257:91–4.

Giannini G, Conti A, Mammarella S, Scrobogna M, and Sorrentino V (1995), The ryanodine receptor/calcium channel genes are widely differentially expressed in murine brain and peripheral tissues. *Journal of Cell Biology* 128:893–904.

Godt R and Maughan D (1988), On the composition of the cytosol of relaxed skeletal muscle of the frog. *American Journal of Physiology* 254:C591–C604.

Gonzalez-Serratos H, Valle-Aguilera R, Lathrop D, and Garcia M (1982), Slow inward calcium currents have no obvious role in muscle excitation-contraction coupling. *Nature* 298:292–4.

Grabner M, Dirksen R, and Beam K (1998), Tagging with green fluorescent protein reveals a distinct subcellular distribution of L-type and non-L-type Ca^{2+} channels expressed in dysgenic myotubes. *Proceedings of the National Academy of Sciences* 95:1903–8.

Grabner M, Dirksen R, Suda N, and Beam K (1999), The II-III loop of the skeletal muscle dihydropyridine receptor is responsible for the bi-directional coupling with the ryanodine receptor. *Journal of Biological Chemistry* 274:21912–9.

Grunwald R and Meissner G (1995), Lumenal sites and C terminus accessibility of the skeletal muscle calcium release channel (ryanodine receptor). *Journal of Biological Chemistry* 270:11338–47.

Györke S and Fill M (1993), Ryanodine receptor adaptation: Control mechanism of Ca(2+)-induced Ca^{2+} release in heart. *Science* 260:807–9.

Hakamata Y, Nakai J, Takeshima H, Imoto K, and Erickson H (1992), Primary structure and distribution of a novel ryanodine receptor/calcium release channel from rabbit brain. *FEBS Letters* 312:229–35.

Hille B (2001), *Ion Channels of Excitable Membranes*. Sinauer Associates, Inc., Sunderland, MA, third edition.

Hilly M, Pietri-Rouxel F, Coquil J, Guy M, and Mauger J (1993), Thiol reagents increase the affinity of the inositol 1,4,5-trisphosphate receptor. *Journal of Biological Chemistry* 268:16488–94.

Ho S, Hunt H, Horton R, Pullen J, and Pease L (1989), Site-directed mutagenesis by overlap extension using the polymerase chain reaction. *Gene* 77:51–9.

Hurne A, Wingrove D, Allen P, and Pessah I (2002), Ryanodine receptor mutants C4958S and C4961S are incapable of orthograde signaling and enhance depolarization-induced Ca^{2+} entry in 1B5 myotubes. *Biophysical Journal* 82:76a, abstract.

Iino M (1990), Biphasic Ca^{2+} dependence of inositol 1,4,5-trisphosphate-induced Ca release in smooth muscle cells of the guinea pig taenia caeci. *Journal of General Physiology* 95:1103–22.

Imagawa T, Smith J, Coronado R, and Campbell K (1987), Purified ryanodine receptor from skeletal muscle sarcoplasmic reticulum is the Ca^{2+}-permeable pore of the calcium release channel. *Journal of Biological Chemistry* 262:16636–43.

Inui M, Saito A, and Fleischer S (1987a), Isolation of the ryanodine receptor from cardiac sarcoplasmic reticulum and identity with feet structures. *Journal of Biological Chemistry* 262:15637–42.

Inui M, Saito A, and Fleischer S (1987b), Purification of the ryanodine receptor and identity with feet structures of junctional terminal cisternae of sarcoplasmic reticulum from fast skeletal muscle. *Journal of Biological Chemistry* 262:1740–7.

Jurman M, Boland L, Liu Y, and Yellen G (1994), Visual identification of individual transfected cells for electrophysiology using antibody-coated beads. *Biotechniques* 17:876–81.

Knudson C, Chaudhari N, Sharp A, Powell J, Beam K, and Campbell K (1989), Specific absence of the alpha 1 subunit of the dihydropyridine receptor in mice with muscular dysgenesis. *Journal of Biological Chemistry* 264:1345–8.

Konishi M, Suda N, and Kurihara S (1993), Fluorescence signals from the Mg^{2+}/Ca^{2+} indicator furaptra in frog skeletal muscle fibers. *Biophysical Journal* 64:223–39.

Kuwajima G, Futatsugi A, Niinobe M, Nakanishi S, and Mikoshiba K (1992), Two types of ryanodine receptors in mouse brain: Skeletal muscle type exclusively in Purkinje cells and cardiac muscle type in various neurons. *Neuron* 9:1133–42.

Lai F, Erickson H, Rousseau E, Liu Q, and Meissner G (1988), Purification and reconstitution of the calcium release channel from skeletal muscle. *Nature* 331:315–9.

Lamb G, Cellini M, and Stephenson D (2001), Different Ca^{2+} releasing action of caffeine and depolarisation in skeletal muscle fibres of the rat. *Journal of Physiology* 531:715–28.

Lamb G and Stephenson D (1991), Effect of Mg^{2+} on the control of Ca^{2+} release in skeletal muscle fibres of the toad. *Journal of Physiology* 434:507–28.

Lamb G and Stephenson D (1994), Effects of intracellular pH and $[Mg^{2+}]$ on excitation-contraction coupling in skeletal muscle fibres of the rat. *Journal of Physiology* 478:331–9.

Laver D, Baynes T, and Dulhunty A (1997), Magnesium inhibition of ryanodine-receptor calcium channels: Evidence for two independent mechanisms. *J Membr Biol* 156:213–29.

Leong P and MacLennan D (1998), A 37-amino acid sequence in the skeletal muscle ryanodine receptor interacts with the cytoplasmic loop between domains II and III in the skeletal muscle dihydropyridine receptor. *Journal of Biological Chemistry* 273:7791–4.

Li P and Chen S (2001), Molecular basis of Ca(2)+ activation of the mouse cardiac Ca(2)+ release channel (ryanodine receptor). *Journal of General Physiology* 118:33–44.

Loke J and MacLennan D (1998), Malignant hyperthermia and central core disease: Disorders of Ca^{2+} release channels. *American Journal of Medicine* 104:470–86.

Lynch P, Tong J, Lehane M, Mallet A, Giblin L, Heffron J, Vaughan P, Zafra G, and MacLenna (1999), A mutation in the transmembrane/luminal domain of the ryanodine receptor is associated with abnormal Ca^{2+} release channel function and severe central core disease. *Proceedings of the National Academy of Sciences* 96:4164–9.

MacLennan D and Phillips M (1992), Malignant hyperthermia. *Science* 256:789–94.

Maeda N, Kawasaki T, Nakade S, Yokota N, Taguchi T, Kasai M, and Mikoshiba K (1991), Structural and functional characterization of inositol 1,4,5-trisphosphate receptor channel from mouse cerebellum. *Journal of Biological Chemistry* 266:1109–16.

Marty I, Robert M, Villaz M, De Jongh K, Lai Y, Catterall W, and Ronjat M (1994), Biochemical evidence for a complex involving dihydropyridine receptor and ryanodine receptor in triad junctions of skeletal muscle. *Proceedings of the National Academy of Sciences* 91:2270–4.

Meissner G (1994), Ryanodine receptor/Ca^{2+} release channels and their regulation by endogenous effectors. *Annual Review of Physiology* 56:485–508.

Meissner G, Darling E, and Eveleth J (1986), Kinetics of rapid Ca^{2+} release by sarcoplasmic reticulum. Effects of Ca^{2+}, Mg^{2+}, and adenine nucleotides. *Biochemistry* 25:236–44.

Meissner G, Rios E, Tripathy A, and Pasek D (1997), Regulation of skeletal muscle Ca^{2+} release channel (ryanodine receptor) by Ca^{2+} and monovalent cations and anions. *Journal of Biological Chemistry* 272:1628–38.

Meissner G, Rousseau E, and Lai F (1989), Structural and functional correlation of the trypsin-digested Ca^{2+} release channel of skeletal muscle sarcoplasmic reticulum. *Journal of Biological Chemistry* 264:1715–22.

Michikawa T, Hamanaka H, Otsu H, Yamamoto A, Miyawaki A, Furuichi T, Tashiro Y, and Mikoshiba K (1994), Transmembrane topology and sites of N-glycosylation of inositol 1,4,5-trisphosphate receptor. *Journal of Biological Chemistry* 269:9184–9.

Mignery G and Sudhof T (1990), The ligand binding site and transduction mechanism in the inositol-1,4,5-triphosphate receptor. *EMBO Journal* 9:3893–8.

Mignery G, Sudhof T, Takei K, and De Camilli P (1989), Putative receptor for inositol 1,4,5-trisphosphate similar to ryanodine receptor. *Nature* 342:192–5.

Miyakawa T, Mizushima A, Hirose K, Yamazawa T, Bezprozvanny I, Kurosaki T, and Iino M (2001), Ca(2+)-sensor region of IP(3) receptor controls intracellular Ca(2+) signaling. *EMBO Journal* 20:1674–80.

Miyawaki A, Furuichi T, Ryou Y, Yoshikawa S, Nakagawa T, Saitoh T, and Mikoshiba K (1991), Structure-function relationships of the mouse inositol 1,4,5-trisphosphate receptor. *Proceedings of the National Academy of Sciences* 88:4911–5.

Miyazaki S, Yuzaki M, Nakada K, Shirakawa H, Nakanishi S, Nakade S, and Mikoshiba K (1992), Block of Ca^{2+} wave and Ca^{2+} oscillation by antibody to the inositol 1,4,5-trisphosphate receptor in fertilized hamster eggs. *Science* 257:251–5.

Monkawa T, Miyawaki A, Sugiyama T, Yoneshima H, Yamamoto-Hino M, Furuichi T, Saruta T, and Hasegawa M (1995), Heterotetrameric complex formation of inositol 1,4,5-trisphosphate receptor subunits. *Journal of Biological Chemistry* 270:14700–4.

Moore R, Nguyen H, Galceran J, Pessah I, and Allen P (1998), A transgenic myogenic cell line lacking ryanodine receptor protein for homologous expression studies: Reconstitution of Ry1R protein and function. *Journal of Cell Biology* 140:843–51.

Murray B and Ohlendieck K (1997), Cross-linking analysis of the ryanodine receptor and alpha1-dihydropyridine receptor in rabbit skeletal muscle triads. *Biochemistry Journal* 324 (Pt 2):689–96.

Nabauer M, Callewaert G, Cleemann L, and Morad M (1989), Regulation of calcium release is gated by calcium current, not gating charge, in cardiac myocytes. *Science* 244:800–3.

Nakai J, Dirksen R, Nguyen H, Pessah I, Beam K, and Allen P (1996), Enhanced dihydropyridine receptor channel activity in the presence of ryanodine receptor. *Nature* 380:72–5.

Nakai J, Gao L, Xu L, Xin C, Pasek D, and Meissner G (1999), Evidence for a role of C-terminus in Ca^{2+} inactivation of skeletal muscle Ca^{2+} release channel (ryanodine receptor). *FEBS Letters* 459:154–8.

Nakai J, Imagawa T, Hakamat Y, Shigekawa M, Takeshima H, and Numa S (1990), Primary structure and functional expression from cDNA of the cardiac ryanodine receptor/calcium release channel. *FEBS Letters* 271:169–77.

Nakai J, Ogura T, Protasi F, Franzini-Armstrong C, Allen P, and Beam K (1997), Functional nonequality of the cardiac and skeletal ryanodine receptors. *Proceedings of the National Academy of Sciences* 94:1019–22.

Nakai J, Sekiguchi N, Rando T, Allen P, and Beam K (1998a), Two regions of the ryanodine receptor involved in coupling with L-type Ca^{2+} channels. *Journal of Biological Chemistry* 273:13403–406.

Nakai J, Tanabe T, Konno T, Adams B, and Beam K (1998b), Localization in the II-III loop of the dihydropyridine receptor of a sequence critical for excitation-contraction coupling. *Journal of Biological Chemistry* 273:24983–6.

Neely A, Olcese R, Wei X, Birnbaumer L, and Stefani E (1994), Ca(2+)-dependent inactivation of a cloned cardiac Ca^{2+} channel alpha 1 subunit (alpha 1C) expressed in Xenopus oocytes. *Biophysical Journal* 66:1895–903.

Penner R, Neher E, Takeshima H, Nishimura S, and Numa S (1989), Functional expression of the calcium release channel from skeletal muscle ryanodine receptor cDNA. *FEBS Letters* 259:217–21.

Peterson B, DeMaria C, Adelman J, and Yue D (1999), Calmodulin is the Ca^{2+} sensor for Ca^{2+} -dependent inactivation of L-type calcium channels. *Neuron* 22:549–58.

Phillips Jr G, Fillers J, and Cohen C (1986), Tropomyosin crystal structure and muscle regulation. *Journal of Molecular Biology* 192:111–31.

Porter Moore C, Zhang J, and Hamilton S (1999), A role for cysteine 3635 of RYR1 in redox modulation and calmodulin binding. *Journal of Biological Chemistry* 274:36831–4.

Proenza C (1999), *Yeast two-hybrid analysis of skeletal muscle triad junction proteins*. Ph.D. thesis, Colorado State University, Fort Collins, CO 80523.

Proenza C, Wilkens C, and Beam K (2000), Excitation-contraction coupling is not affected by scrambled sequence in residues 681-690 of the dihydropyridine receptor II-III loop. *Journal of Biological Chemistry* 275:29935–7.

Protasi F, Franzini-Armstrong C, and Allen P (1998), Role of ryanodine receptors in the assembly of calcium release units in skeletal muscle. *Journal of Cell Biology* 140:831–42.

Qin N, Olcese R, Bransby M, Lin T, and Birnbaumer L (1999), Ca^{2+}-induced inhibition of the cardiac Ca^{2+} channel depends on calmodulin. *Proceedings of the National Academy of Sciences* 96:2435–8.

Radermacher M, Rao V, Grassucci R, Frank J, Timmerman A, Fleischer S, and Wagenknecht T (1994), Cryo-electron microscopy and three-dimensional reconstruction of the calcium release channel/ryanodine receptor from skeletal muscle. *Journal of Cell Biology* 127:411–23.

Ramos-Franco J, Galvan D, Mignery G, and Fill M (1999), Location of the permeation pathway in the recombinant type 1 inositol 1,4,5-trisphosphate receptor. *Journal of General Physiology* 114:243–50.

Rando T and Blau H (1994), Primary mouse myoblast purification, characterization, and transplantation for cell-mediated gene therapy. *Journal of Cell Biology* 125:1275–87.

Rayment I, Holden H, Whittaker M, Yohn C, Lorenz M, Holmes K, and Milligan R (1993), Structure of the actin-myosin complex and its implications for muscle contraction. *Science* 261:58–65.

Rios E and Brum G (1987), Involvement of dihydropyridine receptors in excitation-contraction coupling in skeletal muscle. *Nature* 325:717–720.

Rios E and Pizarro G (1991), Voltage sensor of excitation-contraction coupling in skeletal muscle. *Physiology Reviews* 71:849–908.

Ross C, Danoff S, Schell M, Snyder S, and Ullrich A (1992), Three additional inositol 1,4,5-trisphosphate receptors: molecular cloning and differential localization in brain and peripheral tissues. *Proceedings of the National Academy of Sciences* 89:4265–9.

Sayers L, Miyawaki A, Muto A, Takeshita H, Yamamoto A, Michikawa T, Furuichi T, and Mikoshiba K (1997), Intracellular targeting and homotetramer formation of a truncated inositol 1,4,5-trisphosphate receptor-green fluorescent protein chimera in Xenopus laevis oocytes: Evidence for the involvement of the transmembrane spanning domain in endoplasmic reticulum targeting and homotetramer complex formation. *Biochemistry Journal* 323 (Pt 1):273–80.

Schneider M (1994), Control of calcium release in functioning skeletal muscle fibers. *Annual Review of Physiology* 56:463–84.

Schneider M and Chandler W (1973), Voltage dependent charge movement of skeletal muscle: A possible step in excitation-contraction coupling. *Nature* 242:244–6.

Serysheva I, Schatz M, van Heel M, Chiu W, and Hamilton S (1999), Structure of the skeletal muscle calcium release channel activated with Ca^{2+} and AMP-PCP. *Biophysical Journal* 77:1936–44.

Sharma M, Jeyakumar L, Fleischer S, and Wagenknecht T (2000), Three-dimensional structure of ryanodine receptor isoform three in two conformational states as visualized by cryo-electron microscopy. *Journal of Biological Chemistry* 275:9485–91.

Sharma M, Penczek P, Grassucci R, Xin H, Fleischer S, and Wagenknecht T (1998), Cryoelectron microscopy and image analysis of the cardiac ryanodine receptor. *Journal of Biological Chemistry* 273:18429–34.

Sharp A, McPherson P, Dawson T, Aoki C, Campbell K, and Snyder S (1993), Differential immunohistochemical localization of inositol 1,4,5-trisphosphate- and ryanodine-sensitive Ca^{2+} release channels in rat brain. *Journal of Neuroscience* 13:3051–63.

Smith J, Coronado R, and Meissner G (1985), Sarcoplasmic reticulum contains adenine nucleotide-activated calcium channels. *Nature* 316:446–9.

Smith J, Coronado R, and Meissner G (1986), Single channel measurements of the calcium release channel from skeletal muscle sarcoplasmic reticulum. activation by Ca^{2+} and ATP and modulation by Mg^{2+}. *Journal of General Physiology* 88:573–88.

Smith J, Imagawa T, Ma J, Fill M, Campbell K, and Coronado R (1988), Purified ryanodine receptor from rabbit skeletal muscle is the calcium-release channel of sarcoplasmic reticulum. *Journal of General Physiology* 92:1–26.

Sorrentino V and Volpe P (1993), Ryanodine receptors: How many, where and why? *Trends in Physiological Sciences* 14:98–103.

Stroffekova K and Beam K (2002), The CaM binding site (IQ motif) of α_{1S} may be involved in EC coupling. *Biophysical Journal* 82:79a, abstract.

Stroffekova K, Yue D, and Beam K (2001), The effect of calmodulin on cardiac and skeletal L-type Ca^{2+} currents in skeletal muscle myotubes. *Biophysical Journal* 80:619a, abstract.

Sun X, Protasi F, Takahashi M, Takeshima H, Ferguson D, and Franzini-Armstrong C (1995), Molecular architecture of membranes involved in excitation-contraction coupling of cardiac muscle. *Journal of Cell Biology* 129:659–71.

Takahashi M, Seagar M, Jones J, Reber B, and Catterall W (1987), Subunit structure of dihydropyridine-sensitive calcium channels from skeletal muscle. *Proceedings of the National Academy of Sciences* 84:5478–82.

Takekura H, Bennett L, Tanabe T, Beam K, and Franzini-Armstrong C (1994), Restoration of junctional tetrads in dysgenic myotubes by dihydropyridine receptor cDNA. *Biophysical Journal* 67:793–803.

Takekura H, Nishi M, Noda T, Takeshima H, and Franzini-Armstrong C (1995), Abnormal junctions between surface membrane and sarcoplasmic reticulum in skeletal muscle with a mutation targeted to the ryanodine receptor. *Proceedings of the National Academy of Sciences* 92:3381–5.

Takeshima H, Iino M, Takekura H, Nishi M, Kuno J, Minowa O, Takano H, and Noda T (1994), Excitation-contraction uncoupling and muscular degeneration in mice lacking functional skeletal muscle ryanodine-receptor gene. *Nature* 369:556–9.

Takeshima H, Nishimura S, Matsumoto T, Ishida H, Kangawa M, Minamino N, Matsuo H, Ueda M, Hanaoka M, Hirose T, and Numa S (1989), Primary structure and expression from complementary DNA of skeletal muscle ryanodine receptor. *Nature* 339:439–45.

Tanabe T, Adams B, Numa S, and Beam K (1991), Repeat I of the dihydropyridine receptor is critical in determining calcium channel activation kinetics. *Nature* 352:800–3.

Tanabe T, Beam K, Adams B, Niidome T, and Numa S (1990a), Regions of the skeletal muscle dihydropyridine receptor critical for excitation-contraction coupling. *Nature* 346:567–9.

Tanabe T, Beam K, Powell J, and Numa S (1988), Restoration of excitation-contraction coupling and slow calcium current in dysgenic muscle by dihydropyridine receptor complementary DNA. *Nature* 336:134–9.

Tanabe T, Mikami A, Numa S, and Beam K (1990b), Cardiac-type excitation-contraction coupling in dysgenic skeletal muscle injected with cardiac dihydropyridine receptor cDNA. *Nature* 344:451–3.

Tanabe T, Takeshima H, Mikami A, Flockerzi V, Takahashi H, Kangawa K, and Kojim (1987), Primary structure of the receptor for calcium channel blockers from skeletal muscle. *Nature* 328:313–8.

Tunwell R, Wickenden C, Bertrand B, Shevchenko V, Walsh M, Allen P, and Lai F (1996), The human cardiac muscle ryanodine receptor-calcium release channel: Identification, primary structure and topological analysis. *Biochemistry Journal* 318 (Pt 2):477–87.

Wagenknecht T, Berkowitz J, Grassucci R, Timerman A, and Fleischer S (1994), Localization of calmodulin binding sites on the ryanodine receptor from skeletal muscle by electron microscopy. *Biophysical Journal* 67:2286–95.

Wang Y, Fraefel C, Protasi F, Moore R, Fessenden J, Pessah I, and DiFrancesco A (2000), HSV-1 amplicon vectors are a highly efficient gene delivery system for skeletal muscle myoblasts and myotubes. *American Journal of Physiology* 278:C619–26.

Westerblad H and Allen D (1992), Myoplasmic free Mg^{2+} concentration during repetitive stimulation of single fibres from mouse skeletal muscle. *Journal of Physiology* 453:413–34.

Wilkens C, Kasielke N, Flucher B, Beam K, and Grabner M (2001), Excitation-contraction coupling is unaffected by drastic alteration of the sequence surrounding residues L720-L764 of the alpha 1S II-III loop. *Proceedings of the National Academy of Sciences* 98:5892–7.

Wu Y, Aghdasi B, Dou S, Zhang J, Liu S, and Hamilton S (1997), Functional interactions between cytoplasmic domains of the skeletal muscle Ca^{2+} release channel. *Journal of Biological Chemistry* 272:25051–61.

Yamazawa T, Takeshima H, Shimuta M, and Iino M (1997), A region of the ryanodine receptor critical for excitation-contraction coupling in skeletal muscle. *Journal of Biological Chemistry* 272:8161–4.

Yoshida Y and Imai S (1997), Structure and function of inositol 1,4,5-trisphosphate receptor. *Japanese Journal of Pharmacology* 74:125–37, review.

Zhao M, Li P, Li X, Zhang L, Winkfein R, and Chen S (1999), Molecular identification of the ryanodine receptor pore-forming segment. *Journal of Biological Chemistry* 274:25971–4.

Zimanyi I and Pessah I (1991), Comparison of [3H]ryanodine receptors and Ca^{++} release from rat cardiac and rabbit skeletal muscle sarcoplasmic reticulum. *Journal of Pharmacology and Experimental Therapeutics* 256:938–46.

Zorzato F, Fujii J, Otsu K, Phillips M, Green N, Lai F, Meissner G, and MacLennan D (1990), Molecular cloning of cDNA encoding human and rabbit forms of the Ca^{2+} release channel (ryanodine receptor) of skeletal muscle sarcoplasmic reticulum. *Journal of Biological Chemistry* 265:2244–56.

Zühlke R, Pitt G, Deisseroth K, Tsien R, and Reuter H (1999), Calmodulin supports both inactivation and facilitation of L-type calcium channels. *Nature* 399:159–62.